THE ICELAND MICROCONTINENT AND A CONTINENTAL GREENLAND-ICELAND-FAROE RIDGE

Gillian R. Foulger¹, Tony Doré², C. Henry Emeleus^{1,§}, Dieter Franke³, Laurent Geoffroy⁴, Laurent Gernigon⁵, Richard Hey⁶, Robert E. Holdsworth¹, Malcolm Hole⁷, Ármann Höskuldsson⁸, Bruce Julian¹, Nick Kusznir⁹, Fernando Martinez¹⁰, Ken J.W. McCaffrey¹, James H. Natland¹¹, Alex Peace¹², Kenni Petersen¹³, Christian Schiffer¹, Randell Stephenson¹⁴ & Martyn Stoker¹⁵.

¹ Department of Earth Sciences, Durham University, Science Laboratories, South Rd. DH1 3LE, UK

² Statoil UK Ltd., Statoil House, 11a Regent Street, London SW1Y 4ST, UK

³ Bundesanstalt für Geowissenschaften und Rohstoffe (Federal Institute for Geosciences and Natural Resources), Germany

⁴ Université de Bretagne Occidentale, Brest, 29238 Brest, CNRS, UMR 6538, Laboratoire Domaines Océaniques, 29280 Plouzané, France

⁵ Norges Geologiske Undersøkelse (NGU), Geological Survey of Norway, Leiv Erikssons vei 39, N-7491 Trondheim, Norway

⁶ Hawaii Institute of Geophysics and Planetology, School of Ocean and Earth Science and Technology, University of Hawaii, Honolulu, HI 96822 USA

⁷ Department of Geology & Petroleum Geology, University of Aberdeen, Aberdeen AB243UE, UK.

⁸ Háskóli Íslands (University of Iceland), Sturlugötu 7, 101 Reykjavík, Iceland

⁹ School of Environmental Sciences, University of Liverpool, Jane Herdman Building, Liverpool L69 3GP, UK

 $^{^{10}\,\}mathrm{Hawaii}$ Institute of Geophysics and Planetology, School of Ocean and Earth Science and Technology, University of Hawaii, Honolulu, HI 96822 USA

¹¹ Rosenstiel School of Marine and Atmospheric Science, University of Miami, Miami FL 33149, USA

¹² Department of Earth Sciences, Memorial University of Newfoundland, St. Johns, Newfoundland, Canada, A1B 3X5; currently at School of Geography and Earth Sciences, McMaster University, 1280 Main Street West, Hamilton, Ontario, Canada L8S 4K1

¹³ Department of Geoscience, Aarhus University, Høegh-Guldbergs Gade 2, DK-8000 Aarhus C., Denmark

¹⁴ School of Geosciences, Geology and Petroleum Geology, Meston Building, King's College, University of Aberdeen, Aberdeen AB24 3UE, UK

¹⁵ Australian School of Petroleum, University of Adelaide, Adelaide, South Australia 5005 Australia

[§] deceased

1 Abstract

- 2 The breakup of Laurasia to form the Northeast Atlantic Realm disintegrated an
- 3 inhomogeneous collage of cratons sutured by cross-cutting orogens. Volcanic rifted margins
- 4 formed that are underlain by magma-inflated, extended continental crust. North of the
- 5 Greenland-Iceland-Faroe Ridge a new rift—the Aegir Ridge—propagated south along the
- 6 Caledonian suture. South of the Greenland-Iceland-Faroe Ridge the proto-Reykjanes Ridge
- 7 propagated north through the North Atlantic Craton along an axis displaced ~150 km to the
- 8 west of the rift to the north. Both propagators stalled where the confluence of the
- 9 Nagssugtoqidian and Caledonian orogens formed an ~300-km-wide transverse barrier.
- 10 Thereafter, the ~150 x 300-km block of continental crust between the rift tips—the Iceland
- 11 Microcontinent–extended in a distributed, unstable manner along multiple axes of extension.
- 12 These axes repeatedly migrated or jumped laterally with shearing occurring between them in
- diffuse transfer zones. This style of deformation continues to the present day in Iceland. It is
- 14 the surface expression of underlying magma-assisted stretching of ductile continental crust
- that has flowed from the Iceland Microplate and flanking continental areas to form the lower
- crust of the Greenland-Iceland-Faroe Ridge. Icelandic-type crust which underlies the
- 17 Greenland-Iceland-Faroe Ridge is thus not anomalously thick oceanic crust as is often
- assumed. Upper Icelandic-type crust comprises magma flows and dykes. Lower Icelandic-
- 19 type crust comprises magma-inflated continental mid- and lower crust. Contemporary magma
- production in Iceland, equivalent to oceanic layers 2-3, corresponds to Icelandic-type upper
- 21 crust plus intrusions in the lower crust, and has a total thickness of only 10-15 km. This is
- 22 much less than the total maximum thickness of 42 km for Icelandic-type crust measured
- 23 seismically in Iceland. The feasibility of the structure we propose is confirmed by numerical
- 24 modeling that shows extension of the continental crust can continue for many tens of millions
- of years by lower-crustal ductile flow. A composition of Icelandic-type lower crust that is
- 26 largely continental can account for multiple seismic observations along with gravity,
- bathymetric, topographic, petrological and geochemical data that are inconsistent with a
- 28 gabbroic composition for Icelandic-type lower crust. It also offers a solution to difficulties in
- 29 numerical models for melt-production by downward-revising the amount of melt needed.
- 30 Unstable tectonics on the Greenland-Iceland-Faroe Ridge can account for long-term tectonic
- 31 disequilibrium on the adjacent rifted margins, the southerly migrating rift propagators that
- 32 build diachronous chevron ridges of thick crust about the Reykjanes Ridge, and the tectonic
- decoupling of the oceans to the north and south. A model of complex, discontinuous
- 34 continental breakup influenced by crustal inhomogeneity that distributes continental material
- 35 in growing oceans fits other regions including the Davis Strait, the South Atlantic and the
- 36 West Indian Ocean.

37	1 Introduction	5			
38	2 Continental breakup forming the Northeast Atlantic Realm	6			
39	2.1 High-velocity lower crust	8			
40	2.2 Seafloor spreading north and south of the Greenland-Iceland-Faroe Ridge.				
41	2.2.1 North of the Greenland-Iceland-Faroe Ridge	11			
42	2.2.2 South of the Greenland-Iceland-Faroe Ridge	11			
43	3 The Greenland-Iceland-Faroe Ridge	12			
44	3.1 Crustal structure	13			
45	3.2 The Faroe-Shetland basin—a bellwether of GIFR tectonic instability	15			
46	4 A new model for the Greenland-Iceland-Faroe Ridge	16			
47	4.1 Mass balance	18			
48	4.2 Problems and paradoxes solved	19			
49	5 Thermo-mechanical modeling	21			
50	-				
51	6.1 Composition of the melt source	24			
52	6.2 Temperature of the melt source	25			
53	6.3 ³ He/ ⁴ He	26			
54	7 Discussion	27			
55	7.1 The Greenland-Iceland-Faroe Ridge	27			
56	7.2 Crustal flow	28			
57	7.3 Magmatism	28			
58	7.3.1 The concept of the North Atlantic Igneous Province	28			
59	7.3.2 Magma volume	29			
60	7.3.3 The chevron ridges	30			
61	7.3.4 The North Atlantic geoid high	31			
62	7.3.5 Regions analogous to the GIFR	31			
63	7.3.6 Regions analogous to the NE Atlantic Realm	32			
64	8 Conclusions				
65					

67 List of acronyms. See also Table 2. 68 69 **GIFR** Greenland-Iceland-Faroe Ridge 70 **JMMC** Jan Mayen Microplate Complex Seaward-dipping reflector 71 SDR 72 NVZ Northern Volcanic Zone 73 Eastern Volcanic Zone EVZ 74 WVZ Western Volcanic Zone 75 **HVLC** High-velocity lower crust 76 T_P potential temperature 77 V_P compressional (P-) wave velocity 78 REE rare-Earth element 79 **SCLM** sub-continental lithospheric mantle 80 81 Keywords: Atlantic; Iceland; continental breakup; tectonics; Icelandic-type crust; SDRs; 82 geochemistry; geophysics.

1 Introduction

- 86 The NE Atlantic Realm, the region north of the Charlie Gibbs Fracture Zone, including the
- 87 seas and seaboards west of Greenland, has persistently resisted attempts to account for many
- 88 of its features in terms of conventional plate tectonics. Although the region figured
- 89 prominently in the development of the spectacularly successful continental drift and plate
- 90 tectonic theories, e.g., with the discovery of symmetrical magnetic anomalies across the
- Reykjanes Ridge, it has also defied predictions made by this theory that are successful in
- 92 most other areas. This is particularly true along the Greenland-Iceland-Faroe Ridge (GIFR)
- 93 where the crust is typically 30 km thick and the bathymetry a full kilometer shallower than is
- expected by cooling and subsidence models for oceanic-crust [Detrick et al., 1977]. These
- 95 observations cannot be satisfactorily explained simply as conventional sea-floor-spreading
- 96 with a larger-than-typical magmatic rate at Iceland (Figure 1).
- 97 It is ironic that, despite the GIFR region not fitting the simple plate tectonic theory, it played
- an important role in development of that theory. In the early 20th century Iceland attracted the
- attention of Alfred Wegener who, as part of his theory of continental drift [Wegener, 1915],
- predicted that Greenland and Scandinavia were separating at 2.5 m/a. Although his estimate
- of rate was two orders of magnitude too large, his general theory was correct. Wegener was
- influenced by arguments that a land bridge, postulated on biogeographical grounds to have
- 103 connected Europe and America, was inconsistent with isostasy. At the time, such land
- bridges were widely invoked to explain the similarity, at some times in geological history,
- between biota on opposite sides of wide oceans. Wegener recognized that biogeographical
- observations worldwide could be explained by continental drift without land bridges.
- Following acceptance of continental drift, the land bridge theory was essentially dropped.
- Ironically, the NE Atlantic is perhaps the only place in the world where a long, ocean-
- spanning land bridge did actually exist [Ellis & Stoker, 2014] (Section 3). The reason why
- such a bridge existed, even when the ocean had attained a width of over 1000 km, is one
- feature of many of the NE Atlantic that has, to date, not been satisfactorily explained.
- A model for development of the NE Atlantic Realm that can account for these and all other
- observations in a holistic way is required. Models that involve simple palinspastic
- reconstructions of Laurasian super-continent breakup, and assume a bimodal crustal
- composition (continental or oceanic) with sharp boundaries, are insufficient [Barnett-Moore
- et al., 2018; Nirrengarten et al., 2018]. Models that explain the quantity, distribution and
- petrology of igneous rocks in an *ad hoc* fashion are not forward-predictive and cannot
- account for observations such as the close juxtaposition of volcanic and non-volcanic
- margins, high-velocity lower crust (HVLC), frequent ridge jumps, and southward-
- propagating rifts on the Reykjanes Ridge [Hey et al., 2010; Peron-Pinvidic & Manatschal,
- 121 2010]. Nor can such models, a century after Wegener's work, explain why a land bridge
- spanned the NE Atlantic Ocean until it had attained a width of ~1,000 km, and why 40% of
- its length remains subaerial to the present day as the island of Iceland.
- In this paper we develop such a model. We propose that the currently ~1,200 km wide
- Greenland-Iceland-Faroe Ridge (GIFR) formed by magma-assisted continental extension
- facilitated by ductile crustal flow, in a similar fashion to magmatic passive margins. The
- extraordinary width of the GIFR was enabled by the inclusion of a ~45,000 km² block of
- 128 continental crust which we term the Iceland Microcontinent. The lower part of the ~30 km
- thick GIFR crust is magma-dilated continental mid- and lower crust. Surface extension has

- been taken up on the GIFR by distributed, migrating rifts with shear between them
- accommodated diffusely. Continental material is dispersed throughout the GIFR and sea-
- floor spreading has not yet been established on a single, stable rift. Complete continental
- breakup has thus still not fully occurred at this latitude.
- Our paper is structured in the following way. First, we describe the unusual setting and
- complex history of breakup of the NE Atlantic Realm that predicated the subsequent
- complexities (Section 2). We then summarize structural and tectonic observations from the
- GIFR and the adjacent Faroe-Shetland basin (Section 3). In Section 4 we present our new
- model for the structure and evolution of the GIFR. Section 5 presents a numerical thermo-
- mechanical simulation that illustrates the model is physically viable given reasonable
- geological assumptions and Section 6 shows that it is consistent with the petrology,
- geochemistry and source potential temperatures of NE Atlantic igneous rocks. Finally, in
- Section 7, we discuss wider implications and analogous regions elsewhere in the oceans.

2 Continental breakup forming the Northeast Atlantic Realm

- Opening of the NE Atlantic Realm in the early Cenozoic was not a simple, abrupt, isolated
- event. It was the latest event in a >300 Myr period of episodic rifting and cooling that lasted
- from the Late Palaeozoic through the Mesozoic. It affected a region extending some half the
- circumference of the Earth and disassembled a heterogeneous patchwork of cratonic blocks
- and orogens [Bingen & Viola, 2018; Gasser, 2014; Gee et al., 2008b; Peace et al., this
- volume; Wilkinson et al., 2017].

- Final breakup occurred by magma-assisted continental extension [Gernigon et al., this
- volume; Lundin & Doré, 2005; Peace et al., this volume; Roberts, 2003; Roberts et al., 1999;
- Skogseid et al., 2000; Soper et al., 1992]. The crust extended by tens or hundreds of
- kilometers from the Rockall Trough to the Barents Sea [Funck et al., 2017; Gaina et al.,
- 2017; Skogseid et al., 2000; Stoker et al., 2017]. Pre-breakup magmatism occurred
- throughout the region including in Britain, the Rockall Trough, East Greenland, the Faroe
- 156 Islands and small-volume, small-fraction, scattered fields found in west Greenland and
- Newfoundland [Larsen et al., 2009; Peace et al., 2016; Wilkinson et al., 2017]. Final
- development of the axes of breakup in the NE Atlantic was influenced by both the direction
- of extensional stress, pre-existing structure, and magmatism [Peace et al., 2018; Peace et al.,
- submitted; Schiffer *et al.*, this volume].
- Greenland is cross-cut by several orogens that continue across formerly adjacent landmasses.
- Easterly orientated orogens include the Inglefield mobile belt in the north
- 163 (Paleoproterozoic—ca. 1.96 1.91 Ga), the central Greenland Nagssugtogidian orogen
- bounded to the north by the Disko Bugt suture and to the south by the Nagssugtogidian front
- 165 (Paleoproterozoic—ca. 1.86 1.84 Ga), and the south Greenland Ketilidian orogen
- 166 (Paleoproterozoic—ca. 1.89 1.80 Ga) (Figure 2) [Garde et al., 2002; van Gool et al., 2002].
- On the Eurasian continent the Nagssugtoqidian orogen is represented in Scotland as the
- Lewisian gneiss (Laxfordian) and the Ketilidian orogen is represented in NW Ireland as the
- 169 Rhinns Complex (Figure 3).
- 170 The much younger Caledonian suture formed in the Ordovician-Devonian and closed the
- 171 Tornquist Sea and Iapetus Ocean to unite Laurentia, Baltica and Avalonia [Pharaoh, 1999;
- 172 Schiffer et al., this volume; Soper et al., 1992]. The Scottish Caledonides lie orthogonal to
- the eastward continuation of the Nagssugtoqidian and Ketilidian orogens [Holdsworth et al.,

- 174 2018]. The western frontal thrust of this suture runs down east Greenland \sim 100 300 km
- from the coast [Gee et al., 2008a; Haller, 1971; Henriksen, 1999; Henriksen & Higgins,
- 176 1976]. A dipping feature imaged seismically using receiver functions at ~40 100 km
- beneath east Greenland is interpreted as a subducted slab, trapped in the continental
- lithosphere, when the Caledonian suture finally closed (Figure 4) [Schiffer et al., 2014].
- Residual Caledonian slabs beneath the region were predicted earlier by plate models for the
- geochemistry of Icelandic volcanics [Foulger & Anderson, 2005; Foulger et al., 2005]. A
- congruent structure—the Flannan reflector—has been imaged seismically beneath north
- 182 Scotland [Schiffer et al., 2015; Smythe et al., 1982].
- The breakup phases that formed the oceans west and east of Greenland are described in detail
- by Peace et al. [this volume], Gernigon et al. [this volume] and Martinez and Hey [this
- volume]. It is summarized here and a brief chronology of the most significant events is given
- in Table 1. The north-propagating mid-Atlantic Ridge reached the latitude of the future
- 187 Charlie Gibbs Fracture Zone in the Late Cretaceous (~86.3 83.6 Ma) and the Rockall
- 188 Trough formed (Figure 1). The rift then propagated west of present-day Greenland at ~63 Ma
- 189 forming magma-poor margins and opening the Labrador Sea [Abdelmalak et al., 2018; Keen
- 190 et al., 2018; Nirrengarten et al., 2018; Oakey & Chalmers, 2012; Roest & Srivastava, 1989].
- 191 Propagation proceeded unhindered across the Grenville and Ketilidian orogens and the North
- 192 Atlantic craton but stalled at the junction of the Nagssugtoqidian and Rinkian orogens
- 193 [Connelly et al., 2006; Grocott & McCaffrey, 2017; Peace et al., 2018; Peace et al.,
- submitted]. There, the crust was locally thick [Clarke & Beutel, 2019; Funck et al., 2007;
- Funck et al., 2012; Peace et al., 2017; St-Onge et al., 2009] and pre-existing subducted slabs
- may also have been preserved in the lithosphere [Heron et al., 2019]. Rift propagation stalled
- and the Davis Strait NNE-SSW sinistral, right-stepping transfersional accommodation zone
- 198 formed. This subsequently opened by magma-assisted continental transtension and
- transpression. Further north Baffin Bay opened by a combination of continental extension
- and possibly some subsidiary sea-floor spreading [Chalmers & Laursen, 1995; Chauvet et al.,
- 201 2019; Oakey & Chalmers, 2012; Suckro et al., 2012; Welford et al., 2018]. The Davis Strait
- 202 today is a 550-km wide shallow ridge of extended, magma-inflated, continental crust that
- spans the ocean from Baffin Island to West Greenland [Dalhoff et al., 2006; Heron et al.,
- 204 2019; Schiffer et al., 2017].
- 205 At ~56 52 Ma rifting began to propagate east of Greenland forming the proto-Reykjanes
- Ridge and a ridge-ridge triple junction at the location of the current Bight fracture zone
- 207 (Figure 1). Shortly thereafter, at ~50 48 Ma, the pole of rotation for Labrador Sea/Baffin
- 208 Bay opening migrated south by ~1000 km resulting in clockwise rotation of ~30 40 of the
- direction of motion of Greenland relative to Laurentia [Oakey & Chalmers, 2012; Srivastava,
- 210 1978]. As a consequence the Labrador Sea/Baffin Bay plate boundary west of Greenland
- became less favorable to extension [Gaina et al., 2017] and motion was progressively
- 212 transferred to the axis east of Greenland. From ~36 Ma, opening was taken up entirely in the
- 213 NE Atlantic [Chalmers & Pulvertaft, 2001; Gaina et al., 2017].
- As was the case for breakup west of Greenland, development of the mid-Atlantic Ridge in the
- NE Atlantic was strongly influenced by pre-existing structure [Schiffer *et al.*, this volume].
- The classic "Wilson Cycle" model suggests that continental breakup occurs along older
- sutures [Ady & Whittaker, 2018; Buiter & Torsvik, 2014; Chenin et al., 2015; Krabbendam,
- 218 2001; Petersen & Schiffer, 2016; Vauchez et al., 1997]. The collage of cratons and cross-

- 219 cutting orogens that comprised the disintegrating Laurasian supercontinent had several
- sutures that influenced breakup.
- Development of the oceanic regions north and south of the GIFR described in more detail in
- Sections 2.2.1 and 2.2.2 is summarized here. North of the present GIFR, the axis of extension
- opened by southerly propagation within the Caledonian orogen. That orogen consists of
- overthrust stacks of nappes and sinistral shear zones including the Møre-Trøndelag Fault
- Zone (Norway) and the Walls Boundary-Great Glen Fault and Highland Boundary Fault
- 226 (Scotland). These features may have controlled the structures that opened [Dewey & Strachan,
- 227 2003; Doré et al., 1997; Fossen, 2010; Peace et al., this volume]. The new mid-Atlantic
- Ridge formed obliquely along the orogen, however, so the propagating rift tip eventually
- intersected its edge at the Caledonian Western Frontal Thrust [Schiffer et al., this volume].
- There, it stalled.
- South of the present GIFR the proto-Reykjanes Ridge propagated north from the Bight
- Fracture Zone, cut unhindered across the Ketilidian orogen as did the Labrador Sea rift, and
- split the North Atlantic craton. It arrived at the confluence of the transverse Nagssugtoqidian
- and Caledonian orogens at ~C21 (50 48 Ma) [Elliott & Parson, 2008] and stopped at a
- 235 location ~300 km to the south and ~150 km to the west of the stalled, south-propagating ridge
- 236 tip to the north. It was between and around these two stalled ridge tips that the GIFR formed,
- by magma-assisted deformation of the continental region between them.
- 238 2.1 High-velocity lower crust
- High velocity lower crust (HVLC) is widespread beneath the margins of the NE Atlantic and
- 240 has very similar geophysical properties to the lower part of the Icelandic-type crust that
- underlies the GIFR [Bott, 1974; Foulger et al., 2003]. Because of this, understanding the
- origin and composition of HVLC is key to unraveling the development and current structure
- of the NE Atlantic. In this section, we discuss in detail its geophysical characteristics and
- possible origins.
- 245 Before oceanic crust began to form in the NE Atlantic Realm, wide rifted margins of
- stretched continental crust developed and in some areas were blanketed by thick sequences of
- seaward-dipping basalt flows (seaward-dipping reflectors—SDRs) [Á Horni et al., 2016;
- Talwani & Eldholm, 1977]. Lithospheric necking occurred by normal faulting in the upper
- crust and distributed magma inflation and ductile flow in the mid- and lower crust (Figure 5).
- 250 Multiple changes in extension direction complicated the final structure [Barnett-Moore et al.,
- 251 2018].
- 252 The volcanic rifted margins may be divided into Inner-SDR and Outer-SDR regions [Planke
- et al., 2000]. The Inner-SDRs comprise lavas up to 5 10 km thick that blanket heavily dyke-
- 254 injected continental upper crust formed during the continental extensional necking phase
- 255 [e.g., Benson, 2003; Geoffroy, 2005; Geoffroy et al., 2015]. Beneath this the sill-injected
- lower crust exhibits high seismic velocities. Outer-SDRs sometimes lie seaward of these and
- 257 directly overlie thinner HVLC, with seismic properties identical to the HVLC beneath the
- 258 necked continental crust [Geoffroy et al., 2015]. HVLC may also extend for up to 100 km
- beneath both the adjacent oceanic and continental domains [Funck et al., 2016 and references
- 260 therein; Rudnick & Fountain, 1995; Thybo & Artemieva, 2013].

- 261 HVLC typically has seismic velocities intermediate between those expected for crust and
- 262 mantle. Constraints on its density are poor because the densities of the SDRs and underlying
- lower crust are not well known. Geoffroy et al. [2015] define two kinds of HVLC LC1 and
- LC2. Typical working values for velocity and density are, for LC1 $V_P \sim 7.2 7.3$ km/s and
- 265 density 3000 3100 kg/m³, and for LC2 $V_P \sim 7.6$ to 7.8 km/s and density 3200 3300 kg/m³
- 266 (Figure 5) [Bauer et al., 2000; Geoffroy et al., 2015; Schiffer et al., 2016].

- These geophysical properties are ambiguous regarding the composition, origin, and tectonic significance of HVLC. Possible lithologies include:
 - Ultra-high-pressure granulite/eclogite crystalline basement representing exhumed continental mid- and lower crust [Abdelmalak et al., 2017; Ebbing et al., 2006; Gernigon et al., 2004; Gernigon et al., this volume; Mjelde et al., 2013]. Such material can have both high V_P (7.2 8.5 km/s) and high density [2.8-3.6 g/cm3; Fountain et al., 1994]. It outcrops in the Norwegian Western Gneiss Region which continues beneath the North Sea and the platform east of the Møre basin. Its top surface may comprise old suture accommodation zones that controlled deformation prior to breakup;
 - Syn-extension sill-intruded mid-to-lower continental crust. In wide-angle seismic lines most HVLC beneath Inner-SDRs present high-amplitude, folded reflectors disconnected from the deepest layered lower crust [Clerc et al., 2015; Geoffroy, 2005; Geoffroy et al., 2015]. Such deformation fits with seaward ductile flow of this layer;
 - Exhumed and syn-rift serpentinized mantle. The HVLC beneath the mid-Norwegian early Cretaceous basins, the Labrador Sea, Baffin Bay, Rockall Trough and the Porcupine basin may be partially syn-rift serpentinized mantle exhumed beneath the axes of maximum extension [Keen et al., 2018; Lundin & Doré, 2011; O'Reilly et al., 1996; Peron-Pinvidic et al., 2013; Reston et al., 2001; Reynisson et al., 2011]. It is directly observed at amagmatic margins, e.g., the Iberian margin, where the serpentinization is thought to be caused by seawater infiltrating down crustal faults and reacting with exhumed mantle at shallow depths. The HVLC beneath the NE Atlantic SDRs lies under several kilometers of sediments and crust and it is unlikely that seawater can penetrate sufficiently deep to cause pervasive serpentinization beneath the basalt [Abdelmalak et al., 2017; Gernigon et al., 2004; Zastrozhnov et al., 2018];
 - Inherited serpentinized material. Water could have been sourced from inherited Caledonian or Sveconorwegian-Grenvillian mantle wedge material [Fichler *et al.*, 2011; Petersen & Schiffer, 2016; Schiffer *et al.*, 2016; Slagstad *et al.*, 2017]. The source of NE Atlantic basalts is known to be wet [Jamtveit *et al.*, 2001; Nichols *et al.*, 2002]. Pressure conditions corresponding to deep crust/shallow upper mantle depths and temperatures of 500 700°C should not be exceeded for serpentinite to exist [*e.g.*, Petersen & Schiffer, 2016; Ulmer & Trommsdorff, 1995]. Numerical modeling confirms that such material can be preserved in rifted margins [Petersen & Schiffer, 2016] and that its strength would be less than half that of dry peridotite [Escartin *et al.*, 2001];
 - Mantle infiltrated with gabbroic melt. Such material has been observed at magmapoor margins [Lundin & Doré, 2018; Müntener *et al.*, 2010] and would have an average seismic velocity midway between that of mantle and gabbro ($V_P \sim 7 \text{ km/s}$);

• Hybrid material comprising a mixture of some or all of the above on various scales. For example, Schiffer *et al.* [2015] interpret HVLC bodies beneath east Greenland as Caledonian subduction material including eclogitized mafic crust. What appears geophysically to be a continuous layer might also vary laterally in composition—a classic example of geophysical ambiguity [Mjelde *et al.*, 2002].

310 311

306

307

308

- An interpretation of HVLC as underplated material, i.e., high-temperature melt that
- 313 accumulated during initial opening of the NE Atlantic [Eldholm & Grue, 1994b; Mjelde et
- 314 al., 1997; Mjelde et al., 2002; Mjelde et al., 1998; Thybo & Artemieva, 2013] is challenged
- by key geophysical and structural observations from the outer Vøring basin. There,
- 316 Cretaceous deformation was partly controlled by the top of a HVLC dome before the main
- 317 magmatic event in the Late Paleocene-Early Eocene, suggesting that the dome may predate
- breakup magmatism by at least 15 25 Myr [Abdelmalak et al., 2017; Gernigon et al., 2004;
- 319 Gernigon et al., 2006].
- 320 In summary, the provenance of the HVLC underlying the Outer SDRs is ambiguous but it
- 321 likely includes a large proportion of continental crust. As a consequence the exact locations
- of the outer limits of continuous offshore continental material (the continent-ocean boundary)
- is poorly known in some areas [Bronner et al., 2011; Eagles et al., 2015; Gernigon et al.,
- 324 2015; Lundin & Doré, 2018; Schiffer et al., 2018]. Continental crust may grade into thick
- 325 oceanic crust via a magmatic transition zone tens of kilometers wide of stretched, intruded
- 326 continental crust—the continent-ocean transition [Eagles et al., 2015; Eldholm et al., 1989;
- Gernigon et al., this volume; Meyer et al., 2009]. The width of the continent-ocean transition
- may be partly controlled by the degree of stretching with narrow extensional zones forming
- where new rifts follow pre-existing fabric, and wide zones where rifts cross-cut tectonic
- fabric [Buck, 1991; Dunbar & Sawyer, 1988; Harry et al., 1993; Schiffer et al., this volume].
- Full rupture of the crust leading to region-wide sea-floor spreading may be discontinuous,
- diachronous and segmented [Elliott & Parson, 2008; Guan et al., 2019; Manton et al., 2018;
- 333 Schiffer et al., this volume; Theissen-Krah et al., 2017]. Continental fragments trapped
- between pairs of volcanic rifted margins and transported into the new ocean to form "C-
- blocks" may be widespread (Figure 5; Section 4) [Geoffroy et al., 2015; Geoffroy et al.,
- submitted]. Continental crust may also be distributed by igneous mullioning as seen in the
- southern Jan Mayen Microplate Complex (JMMC; Section 2.2.1), and by small-scale lateral
- rift migrations [Bonatti, 1985; Gernigon et al., 2012; Gillard et al., 2017]. Continental
- fragments may range in size from the 100-km scale down. Geophysical ambiguity and
- 340 blanketing of microcontinents with lavas hinder mapping the full distribution of continental
- crust in the oceans. The eastern margin of the JMMC, for example, is overlain by SDRs and
- 342 the subaerial part of the GIFR (i.e. Iceland) is blanketed with lavas younger than ~17 Ma
- 343 [Breivik et al., 2012; Gudlaugsson et al., 1988]. Geochemistry can be used to complement
- geophysics by testing the viability of proposed HVLC petrologies (Section 6).
- 345 2.2 Seafloor spreading north and south of the Greenland-Iceland-Faroe Ridge
- 346 Clear, well-mapped, linear magnetic anomalies reveal the contrasting histories of ocean
- opening north and south of the GIFR (Figure 6). Breakup did not occur simultaneously along
- 348 the entire seaboard, as often assumed, but involved several isolated propagators and
- intermediate continental blocks [Elliott & Parson, 2008; Gernigon et al., this volume].

2.2.1 North of the Greenland-Iceland-Faroe Ridge

- 351 The earliest anomalies are likely associated with magma injection into extended continental
- 352 crust. True sea-floor spreading on the Aegir Ridge began at ~54 Ma (C24r). It started at its
- northern end and propagated south to reach its full extent by ~52 Ma (Chron C23). Tectonic
- reorganization and fan-shaped spreading occurred about this ridge C22-C21 (~48 Ma) with
- spreading slower in the south than in the north (Table 1) [Gernigon et al., 2015].
- 356 Much if not all of the southern extension deficit was accommodated by diffuse, dyke-assisted
- 357 crustal dilation in the continental crust immediately to the west. This region later became the
- 358 southern JMMC [Brandsdóttir et al., 2015]. Crustal extension of up to 500% occurred
- forming mullioned crust [Gernigon et al., 2015; Schiffer et al., 2018]. Extension ultimately
- 360 concentrated on the most westerly axis of dilation which developed into the Kolbeinsey
- Ridge. The first unambiguous magnetic anomaly formed there at ~24 Ma [C6/7; Blischke et
- 362 al., 2017; Vogt et al., 1980].

350

- 363 The Aegir Ridge dwindled and became extinct a little after ~31 28 Ma [C12-C10; Gernigon
- et al., 2015] after which all spreading north of the GIFR was taken up on the proto-
- 365 Kolbeinsey Ridge. This migration of the locus of extension likely occurred as a result of a
- 366 tectonic reorganization that rotated the local direction of motion counter-clockwise [Gaina et
- 367 al., 2017]. This would have rendered the southern part of the Aegir Ridge less favorable for
- spreading and encouraged extension on the proto-Kolbeinsey Ridge. That extension
- progressively detached the continental block and adjacent mullioned crust between the proto-
- 370 Kolbeinsey Ridge and the Aegir Ridge to form the JMMC [Schiffer et al., 2018]. Opening of
- 371 the Atlantic north of the GIFR (e.g. the Norwegian-Greenland Sea) thus occurred on a series
- of unconnected, sub-parallel, migrating, propagating rifts.
- 373 The northern part of the JMMC is a coherent microcontinent on the 100-km scale [Peron-
- Pinvidic et al., 2012]. SDRs formed on its eastern margin [Kodaira et al., 1998]. The crust
- that makes up its southern part is severely intruded continental crust with clear rift zones
- 376 [Brandsdóttir *et al.*, 2015]. The nature of its transition into Iceland is, however, unknown.
- 377 Despite developing in the highly magmatically productive environment of the early NE
- 378 Atlantic the late Aegir Ridge was magma-starved and formed oceanic crust only 4 7 km
- 379 thick [Breivik et al., 2006; Greenhalgh & Kusznir, 2007]. This contrasts with both the
- 380 Kolbeinsey Ridge and the Reykjanes Ridge which are underlain by oceanic crust ~10 km
- thick. Extreme variations in magmatic rate over short distances are inconsistent with
- mechanisms of melt production that envisage extensive, coherent regions of influence and
- suggest, instead, local dependency on melt productivity [Lundin et al., 2018; Simon et al.,
- 384 2009].

385 2.2.2 South of the Greenland-Iceland-Faroe Ridge

- 386 South of the GIFR, on the European side, poorly constrained, complicated magnetic
- anomalies SW of the Faroe Islands suggest early disaggregated sea-floor spreading. The first
- unambiguous and continuous spreading anomaly south of the Faroe Plateau formed at ~47
- 389 Ma (C21) [Elliott & Parson, 2008; Ellis & Stoker, 2014; Stoker et al., 2012]. On the
- 390 Greenland side, the oldest linear magnetic anomalies produced by the proto-Reykjanes Ridge
- date from C24-22 (56 52 Ma), but they may represent rift-related basalt extrusion in the
- 392 Outer-SDR region and not true oceanic spreading. Linear magnetic anomalies terminate

- along the SE Greenland margin, unlike the European side where they are continuous along
- 394 the margin. This is consistent with early westward migration of the spreading axis. It finally
- 395 stabilized along a zone ~150 km west of the Aegir Ridge.
- 396 Extension proceeded normal to the strike of the Reykjanes Ridge and the continental edges
- until ~37 38 Ma (C17) when an abrupt counter-clockwise rotation of the direction of plate
- motion occurred. Spreading in the Labrador Sea then rapidly ceased (Table 1) [Gaina et al.,
- 399 2017; Jones, 2003; Martinez & Hey, this volume]. The Bight ridge-ridge-ridge triple junction
- 400 ceased to exist and the linear Reykjanes Ridge reconfigured to a right-stepping ridge-
- 401 transform array such that the new ridge segments were normal to the new direction of plate
- 402 motion.

- Subsequently, and up to the present day, the Reykjanes Ridge has been slowly migrated east
- by a series of small-offset, right-stepping propagators within the plate boundary zone that
- 405 have eliminated the transforms [Benediktsdóttir et al., 2012; Hey et al., 2010; Martinez &
- Hey, this volume]. They originate at the GIFR and migrate south at rates of 10 25 cm/a,
- 407 each slicing a few kilometers off the Eurasian plate and transferring it to the North American
- 408 plate [Hey et al., 2016]. At least five and possibly as many as seven propagators [Jones et al.,
- 409 2002] have now transferred a swathe of the Eurasian plate ~30 km wide to the North
- American plate between the GIFR and the Bight Fracture Zone [Benediktsdóttir et al., 2012].
- Progression of each propagator tip is associated with transient changes in thickness of $\sim 2 \pm 1$
- 412 km in the oceanic crust formed. This has the curious consequence that the Reykjanes Ridge is
- 413 flanked by diachronous "chevrons" (also called "V-shaped ridges") of alternating thick and
- 414 thin crust that are most clearly seen in the gravity field (Figure 7) [Vogt, 1971].

3 The Greenland-Iceland-Faroe Ridge

- 416 The GIFR comprises a ~1,200-km-long, shallow, trans-oceanic aseismic ridge up to 450 km
- wide in the northerly direction (Figure 1). At present, 40% of it is exposed above sea level in
- 418 Iceland. It is shallower than 600 m and 500 m deep offshore west and east Iceland
- respectively, ~1000 m shallower than the ocean basins to the north and south (Figure 8).
- 420 The GIFR was subaerial along its entire length for most of the history of the NE Atlantic.
- 421 Biogeographical evidence for plant and animal dispersal [Denk et al., 2011] and dating of the
- onset of overflow of intermediate- and deep waters between the Norway and Iceland basins
- 423 [Ellis & Stoker, 2014; Stoker et al., 2005b] suggest that it formed a largely intact, trans-
- 424 Atlantic land bridge (the Thulean land bridge) until ~10 15 Ma and that much survived
- above sea level longer than this. This leads to the surprising conclusion that the Thulean land
- bridge survived intact until the NE Atlantic Ocean had attained a width of ~1000 km.
- 427 Magnetic anomalies on the GIFR are poorly defined, broader than classical oceanic spreading
- anomalies, and resemble more closely anomalies on the outer SDRs (Figure 6) [e.g., Gaina et
- 429 al., 2017]. Very few can be clearly traced across the GIFR so the detailed history of breakup
- in this region cannot be deduced reliably. Previous interpretations have relied largely on
- extrapolation of anomalies to the north and south that are clear, assuming simple oceanic
- crustal accretion in the region between.
- 433 Prior explanations for the poorly developed magnetic anomalies include repeated dyke
- intrusion into the same zone during more than one magnetic chron, re-magnetization by later
- intrusions, weathering, lateral migration of spreading centers and magmatism at multiple

- spreading centers [Bott, 1974]. Unclear anomalies are also expected because basalt extrusion
- was subaerial and flooded older lavas, and because the legacy magnetic data available are
- poor quality, limited, and poorly levelled.
- We concur with these suggestions but go further and propose that distinct, oceanic-type linear
- magnetic anomalies do not exist on the GIFR because it does not comprise oceanic crust
- formed by classical sea-floor spreading. Instead, much of it may consist of magma-dilated,
- ductile continental crust. Upper Icelandic-type crust [Bott, 1974; Foulger et al., 2003]
- corresponds to current basaltic production. Lower Icelandic-type crust corresponds to
- magma-inflated mid- and lower continental crust, the most likely lithology for the HVLC that
- is widespread beneath the NE Atlantic passive margins (Section 2.1).

446 3.1 Crustal structure

- The GIFR has been the target of numerous refraction, wide-angle reflection, and passive
- seismic experiments [Foulger et al., 2003] as well as gravity, magnetic and magnetotelluric
- 449 work [Beblo & Bjornsson, 1978; 1980; Beblo et al., 1983; Eysteinsson & Hermance, 1985;
- 450 Hermance & Grillot, 1974; Thorbergsson et al., 1990]. It was the anomalous seismic nature
- of its crust that led to it being termed "Icelandic-type" [Bott, 1974; Foulger et al., 2003]. It
- 452 features an upper crust with a thickness of ~3 10 km with high vertical velocity gradients,
- and a lower crust ~10 30 km thick with low vertical velocity gradients (Figure 9 and Figure
- 454 10) [Darbyshire *et al.*, 1998a; Foulger *et al.*, 2003; Holbrook *et al.*, 2001; Hopper *et al.*,
- 455 2003]. The lower crust has a V_P of 7.0 7.3 km/s. Icelandic-type crust has, in recent years,
- 456 usually been assumed to be anomalously thick oceanic crust with the lower crust equivalent
- 457 to oceanic layer 3. That model became the default assumption after Bjarnason *et al.* [1993]
- 458 reported a deep reflecting horizon at ~ 20 24 km depth beneath SW Iceland. It replaced an
- earlier model that interpreted the layer beneath the upper crust as anomalously hot mantle
- 460 [Angenheister et al., 1980; Gebrande et al., 1980; Palmason, 1971; Tryggvason, 1962].
- The model that Icelandic-type lower crust is oceanic is inconsistent with other observations.
- 462 Isostatic studies reveal the density of the lower crust to be ~3150 kg/m³, which is too high for
- it to be oceanic [Gudmundsson, 2003; Menke, 1999]. At the same time, its seismic velocity is
- 464 too low for normal mantle peridotite. Models involving partial melt are ruled out by the low
- attenuation of seismic shear waves which suggests that Icelandic-type lower crust is no hotter
- 466 than 800 900 C if it is peridotite [Sato *et al.*, 1989] and 875 950 C if it is gabbroic [Menke
- 467 & Levin, 1994; Menke *et al.*, 1995].
- The theory that Icelandic lower crust is oceanic is largely based on interpreting deep seismic
- reflections as the Moho. However, such reflections can also be interpreted as sills intruded
- into continental lower crust. Refracted head waves are almost never observed in Iceland and
- 471 the large amplitudes of reflections expected from a Moho are not observed in receiver
- 472 functions [Du & Foulger, 1999; Du et al., 2002; Du & Foulger, 2001]. These properties are
- similar to those of HVLC beneath the Inner- and Outer SDRs of the continental margins
- [Mjelde et al., 2001]. The possible compositions and provenances of that material, discussed
- in Section 2.1, thus provide candidates for Icelandic-type lower crust.
- 476 A serpentinized mantle origin for Icelandic-type lower crust is unlikely. If it were
- 477 serpentinized mantle, ~20% of serpentinization of peridotite at ~1 GPa (~30 km depth) is
- 478 required [Christensen, 2004]. Serpentinization in a rifting environment occurs from the top
- down and water is unlikely to be able to reach the mantle at the active rift zones of Iceland. If

- 480 it did, it would only be stable at temperatures < 700 °C or possibly < 500 °C [Tuttle &
- Bowen, 1958] and the Icelandic lower crust is hotter than this [Menke & Levin, 1994; Menke
- 482 et al., 1995; Sato et al., 1989]. The only other possible way of serpentinizing the mantle is via
- 483 fluxing from beneath. In the NE Atlantic such serpentinization could have occurred in the
- Caledonian suture [Fichler et al., 2011] and water is present in the source of basalts erupted
- in Iceland [Jamtveit et al., 2001; Nichols et al., 2002]. However, no peridotite xenoliths have
- been found in Iceland despite a century of extensive geological mapping and drilling,
- suggesting that, whereas serpentinite may exist beneath some rifted margins, it probably does
- 488 not comprise lower Icelandic-type crust or HVLC beneath the adjacent volcanic margins.
- 489 Transitional crust comprising massively dyke- and sill-intruded, hyper-extended mid- and
- lower continental crust is the most likely composition for Icelandic-type lower crust, as it is
- for much of the HVLC beneath the volcanic margins. There is considerable support for this:

- The seismic velocity and density of continental lower crust match those of Icelandic-type lower crust. Continental lower crust is thought to comprise predominately mafic garnet-bearing granulites which have V_P ~7.1 7.3 km/s and densities of 3000 3150 kg/m³ [Rudnick & Fountain, 1995]. It may also contain minor components of metapelite, intermediate and felsic granulites and mafic melts that would reduce V_P and density.
- The thickness of the brittle surface layer in Iceland and the viscosity of the underlying material have been constrained by geodetic studies of post-diking stress relaxation [Foulger *et al.*, 1992; Heki *et al.*, 1993; Hofton & Foulger, 1996a; b; Pollitz & Sacks, 1996] and post-glacial rebound [Sigmundsson, 1991]. The brittle surface layer is ~10 km thick, a value that is consistent with the maximum depth of earthquakes [Einarsson, 1991] and corresponds roughly to the upper crust from explosion seismology and receiver functions (Figure 9). The lower crust beneath has a viscosity of ~10¹⁹ Pa s and is thus ductile.
- The Faroe Islands are underlain by continental crust topped by > 6 km of basalt [Bott et al., 1974; Ólavsdóttir et al., 2017]. Seismic data from the eastern part of the Iceland-Faroe Ridge detect stretched continental crust similar to that underlying the Rockall Bank where HVLC has been interpreted as inherited continental crust of Palaeo-European affinity [Bohnhoff & Makris, 2004].
- Palinspastic reconstructions of Iceland require up to 150 km of crust older than the surface lavas to underlie the island—the extreme westerly and easterly ~15-Ma palaeo-rift products are separated by ~450 km whereas only ~300 km of widening could have occurred at the ambient rate of 1.8 cm/a. Reassembly of the NE Atlantic Ocean also requires up to 150 km of continental crust (original unstretched width) to lie in the ocean [Blischke et al., 2017; Bott, 1985; Foulger, 2006; Gaina et al., 2009; Gaina et al., 2017; Gernigon et al., 2015]. A similar width is required by the original lateral offset of the tips of the Aegir Ridge and proto-Reykjanes Ridge. A southerly continuation of the JMMC beneath the GIFR would be a simple source of this material [Bott, 1985; Foulger & Anderson, 2005; Schiffer et al., 2018]. Icelandic-type crust also underlies the transitional region between the NE Icelandic shelf and the JMMC [Brandsdóttir et al., 2015].
- Magma-assisted extension at the far western and eastern ends of the proto-GIFR, outside of the axes of breakup, is predicted by stress modeling and may have fed additional continental crust into the developing GIFR.

- There are multiple lines of petrological and geochemical evidence for a component of continental crust in Icelandic lavas, including Proterozoic and Mesozoic zircons
 [Amundsen *et al.*, 2002; Foulger, 2006; Paquette *et al.*, 2006; Schaltegger *et al.*,
 2002] elevated ⁸⁷Sr/⁸⁶Sr and Pb isotope ratios [Prestvik *et al.*, 2001] and extensive silicic and intermediate rocks including rhyolite and icelandite—an Fe-rich form of andesite (Section 6).
- 532 3.2 The Faroe-Shetland basin—a bellwether of GIFR tectonic instability
- 533 The Faroe-Shetland basin comprises the eastern extension of the GIFR, is thus sensitive to
- tectonic activity in that zone, and has been unstable throughout the Palaeogene-early
- Neogene [Stoker et al., 2018; Stoker et al., 2005b]. Key phases are summarized in Figure 11
- and include the following.

- Paleocene (~63 56 Ma): The pre-breakup rifting phase (late Danian—Thanetian) was characterized by formation of a series of sag and fault-controlled sub-basins [Dean et al., 1999; Lamers & Carmichael, 1999], coeval borderland uplift events (rift pulses) [Ebdon et al., 1995; Goodwin et al., 2009; Mudge, 2015] and rifting and extension accompanied by volcanism [Mudge, 2015; Ólavsdóttir et al., 2017].
 - Latest Paleocene (~56 55 Ma): Uplift [Ebdon *et al.*, 1995] and extrusion of synbreakup flood basalts and tuffs [Mudge, 2015] probably mark the onset of local, discontinuous sea-floor spreading [Passey & Jolley, 2009].
 - Early-Mid-Eocene (~54 46 Ma): The syn-breakup rift-to-drift transition continued during the early/mid-Ypresian-early Lutetian [Stoker *et al.*, 2018]. Cyclical coastal plain, deltaic and shallow-marine deposits attest to tectonic instability linked to episodic uplift of the Munkagrunnur and Wyville Thomson ridges on the south flank of the basin [Ólavsdóttir *et al.*, 2010; Ólavsdóttir *et al.*, 2013b; Stoker *et al.*, 2013]. Onset of continuous sea-floor spreading in the Norway basin (chron C21) was accompanied by uplift events, continued growth of the Wyville Thomson and Munkagrunnur ridges, and formation of inversion domes in the basin [Ólavsdóttir *et al.*, 2010; Ólavsdóttir *et al.*, 2013b; Ritchie *et al.*, 2008; Stoker *et al.*, 2013; Stoker *et al.*, 2018].
 - Late Paleogene-early Neogene (~35 15 Ma): The present-day basin physiography was initiated in the latest Eocene/Early Oligocene with sagging leading to basin-ward collapse of the margin west of Shetland [Stoker *et al.*, 2013]. Onlapping Oligocene and Lower Miocene basinal sequences were deformed by compressional stresses and widespread inversion and fold growth culminated in the early Mid-Miocene [Johnson *et al.*, 2005; Ritchie *et al.*, 2008; Stoker *et al.*, 2005c].
 - Mid-Miocene—Pleistocene (16/15 Ma present): Basinal sedimentation was dominated by deep-water deposits [Stoker et al., 2005b] with Early Pliocene uplift and tilting of the West Shetland and East Faroe margins accompanied by basinal subsidence and reorganization of bottom current patterns [Andersen et al., 2000; Ólavsdóttir et al., 2013b; Stoker et al., 2005a; Stoker et al., 2005b]. Mid-and Late Pleistocene sedimentation was dominated by shelf-wide glaciations [Stoker et al., 2005a].

In summary, the Faroe-Shetland basin has experienced persistent tectonic unrest from the Paleocene to the Early Miocene (~63 - 15 Ma). This is reflected onland in the Faroe Islands in Paleogene and younger faults and dykes that show progressive changes in the direction of

- extension prior to and following NE Atlantic break-up [Walker et al., 2011]. This chronic
- unrest likely reflects both instability on the GIFR to the west and the protracted breakup of
- 573 the wider NE Atlantic region.

4 A new model for the Greenland-Iceland-Faroe Ridge

- In this section, we build on the background given above and propose a new working
- 576 hypothesis for development of the GIFR and how this affected the rest of the NE Atlantic
- Realm. Numerical modeling of the processes we propose, and model fit with petrology and
- geochemistry, are discussed in Sections 5 and 6.
- As described above, the NE Atlantic Realm formed in a disorderly way as a consequence of
- inherited strength anisotropy, coupled with frequent changes in the poles of rotation of sub-
- regions [Hansen et al., 2009; Schiffer et al., 2018]. North of the GIFR, the Aegir rift opened
- by southward propagation obliquely along the Caledonian orogen. It stalled at the western
- frontal thrust and hooked around to the west (Figure 1). The Reykjanes Ridge to the south
- stalled at the Nagssugtoqidian orogen, ~300 km south of the Caledonian frontal thrust and
- ~150 km west of the Aegir Ridge (Section 2.2). The Reykjanes Ridge and Aegir Ridge thus
- formed a pair of propagating, approaching, laterally offset rifts. The broad barrier formed by
- 587 the Nagssugtoqidian and Caledonian orogens prevented them from propagating further and
- conceivably eventually forming a continuous, conventional oceanic plate boundary.
- As a consequence, the continental region between their tips, the ~300 x 150 km Iceland
- Microcontinent, deformed by magma-assisted, distributed continental transtension and
- developed into the GIFR as the ocean widened (Figure 12). The crust beneath the Iceland
- Microcontinent and flanking areas thinned by ductile flow in its deeper parts. Extensive
- magmatism built SDRs of the kind observed on the eastern margin of the JMMC and the NE
- Atlantic rifted margins. Initially, the GIFR may have comprised an array of four passive
- margins—one on each of the east Greenland and west Faroe margins, and one on either side of
- 596 the Iceland Microcontinent.
- As the GIFR lengthened, and up to the present day, deformation persisted in a distributed
- style along a series of ephemeral extensional rifts and diffuse, intermediate, poorly developed
- shear transfer zones [Gerya, 2011]. The loci of extension repeatedly reorganized by migrating
- 600 laterally to positions that were stress-optimal and likely also influenced by pre-existing
- structures in the underlying continental crust. Rifts that became extinct were transported
- laterally out of the actively extending, central part. As it formed the GIFR was blanketed by
- lavas in the style of volcanic-rifted-margins. Similar rift migrations also occurred in the
- eastern Norway basin where the oceanic crust is thickest [Gernigon et al., 2012]. After ~48
- Ma (C22) it seems that this style of extension persisted only on the GIFR. The permanent
- disconnect between the Aegir Ridge and the Reykjanes Ridge and the low spreading rate in
- the NE Atlantic (1 2 cm/a) would have further encouraged long-term diffuse deformation.
- Figure 13 shows palinspastic reconstructions of the observed positions of active and extinct
- rifts in the NE Atlantic Realm at various times. Swathes of extinct, short, NE-orientated
- 610 ridges similar to those that are currently active onland in Iceland are observed also in
- submarine parts of the GIFR [Hjartarson et al., 2017]. There is insufficient observational data
- at present to fully reconstruct the sequence of deformation on the GIFR because of the
- blanketing lava flows and insufficient geophysical and geological research to date.

- Nevertheless, in Figure 14 we attempt such a reconstruction by extrapolating in time from
- known active and extinct rifts [Hjartarson et al., 2017; Johannesson & Saemundsson, 1998].
- A large block of crust older than the surface lavas is required by palinspastic reconstructions
- to lie beneath Iceland [Foulger, 2006]. Thus, much of the Iceland Microcontinent may still
- exist beneath Iceland and comprise a C-block [Geoffroy et al., 2015; Geoffroy et al.,
- submitted]. C-blocks are expected to be flanked by Outer-SDRs and the geometry of some
- dykes and lava flows in Iceland resemble these [Bourgeois et al., 2005; Hjartarson et al.,
- 621 2017]. It has long been speculated that the continental crust required by geochemistry to
- underlie Iceland (Section 6) comprises a southerly extension of the magma-dilated southern
- JMMC. Give the extent of continental crust that is required to underlie the GIFR it may be
- more appropriate to view the JMMC as an offshore extension of the Iceland Microcontinent.
- Deformation on the GIFR cannot be described by traditional rigid plate tectonics and
- 626 corresponding reconstructions. It corresponds to the case of multiple overlapping ridges, the
- 627 limit of an extensional zone [Engeln et al., 1988]. It may be likened to a lateral array of
- 628 hyper-extended SDRs underlain by HVLC comprising heavily intruded, stretched, ductile
- 629 continental crust. Repeated rejuvenation of the rift axes by lateral migration may have
- boosted volcanism. Westerly migrations may have induced extension to the north to
- concentrate in the westernmost axis of extension in the southern JMMC, leading to extinction
- of the Aegir Ridge and formation of the Kolbeinsey Ridge at ~24 Ma. That migration
- switched the sense of the ridges north and south of the GIFR from right-stepping to left-
- 634 stepping.
- 635 Iceland is ~450 km wide in an EW direction and exposes ~40% of the GIFR (Figure 1). The
- oldest rocks found there to date are 17 Ma. There is no evidence, or reason to think, that the
- 637 tectonic style on the GIFR was fundamentally different in the past from present-day Iceland.
- On the contrary, the similarity of the submarine GIFR synclines to structure on land in
- 639 Iceland suggests that it was the same [Hjartarson *et al.*, 2017].
- 640 Onland in Iceland extension over the last ~15 Ma has occurred via multiple unstable,
- migrating, overlapping spreading segments connected by complex, immature shear transfer
- zones that reorganize every few Myr (Figure 15). These include the South Iceland Seismic
- Zone [Einarsson, 1988; 2008] and the Tjörnes Fracture Zone [e.g., Rognvaldsson et al.,
- 644 1998]. Both are broad, diffuse seismic zones that deform in a bookshelf-faulting manner and
- have not developed the clear topographic expression of faults that experience long-term
- 646 repeated slip.
- There is geological evidence in Iceland for at least 12 spreading zones (Table 2) of which
- seven are currently active, two highly oblique to the direction of plate motion, one waning,
- one propagating, two non-extensional and five extinct. At least five lateral rift jumps are
- known and a sixth is currently underway via transfer of extension from the Western Volcanic
- Zone (WVZ) to the Eastern Volcanic Zone (EVZ). Extension has always been concentrated
- in a small number of active, ephemeral rift zones at any one time (Figure 15).
- There is no evidence that mature sea-floor spreading has yet begun anywhere along the
- 654 GIFR. If such were the case it would be expected that all extension would be rapidly
- 655 transferred to that zone and normal-thickness oceanic crust (i.e., ~6 7 km) would begin to
- 656 form. Indeed, the fact that rift-zone migrations are still ongoing in Iceland suggest that this is
- not the case. There may be some narrow zones where embryonic sea-floor spreading began

- but was abandoned due to subsequent lateral rift jumps, e.g., immediately east of the east
- 659 Icelandic shelf, and in the deep channel in the Denmark Strait. Until this can be confirmed,
- however, it remains a possibility that full continental breakup has not yet occurred in the
- latitude band of the GIFR. This fundamentally challenges the concept that continental
- breakup has yet occurred in this part of the NE Atlantic.
- 663 4.1 Mass balance
- The GIFR today is 1,200 km long with a lower crust generally ~20 km thick and maximally
- ~30 km beneath central Iceland (Figure 9). If a substantial part of this is continental, a large
- volume thus needs to be accounted for. Taking a present-day average breadth for the GIFR of
- ~ 200 km, the surface area is $\sim 0.24 \times 10^6$ km². If an average thickness of 15 km of continental
- material lies beneath, a volume of $\sim 3.6 \times 10^6 \text{ km}^3$ is required.
- We propose that this material was sourced from the Iceland Microcontinent and flanking
- 670 continental regions by ductile flow of mid- and lower crust. Ductile flow can stretch such
- crust to many times its original length (necking), draw in material from great distances, and
- 672 maintain large crustal thicknesses. Numerical thermo-mechanical modeling (Section 5)
- 673 confirms that these processes can account for the lower-crustal thicknesses proposed and
- even increase crustal thickness as material rises to fill the void created by rupture of the upper
- 675 crust.
- Flow is enabled by the low viscosity of the lower crust beneath Iceland. This has been shown
- to be 10^{18} 10^{19} Pa s by GPS measurements of post-diking stress relaxation following a
- 678 regional, 10-m-wide dyke injection episode in the Northern Volcanic Zone (NVZ) 1975 -
- 679 1995 [Bjornsson et al., 1979; Foulger et al., 1992; Heki et al., 1993; Hofton & Foulger,
- 680 1996a; b]. Numerical modeling of those data also showed that the surface, brittle layer was
- approximately 10 km thick. The low viscosity found for the lower crust was confirmed by
- measurements and modeling of the rapid isostatic rebound from retreat of the Weichselian ice
- cap in Iceland and melting of the Vatnajökull glacier in south Iceland [Sigmundsson, 1991].
- 684 [Sigmundsson, 1991].
- As a prelude to numerical thermo-mechanical modeling we present here a simple mass-
- balance calculation. Inland in Greenland, receiver function studies indicate a Moho depth of
- ~40 km [Kumar *et al.*, 2007]. The Caledonian crust of east Greenland is currently up to ~50
- km thick [Darbyshire et al., 2018; Schiffer et al., 2016; Schmidt-Aursch & Jokat, 2005;
- Steffen et al., 2017]. A pre-breakup Caledonian crustal thickness of about 60 km and a post-
- breakup thickness of 30 km [Holbrook et al., 2001] is not unrealistic.
- Beneath the Faroe-Shetland basin, crustal thinning left only a 10-km-thick crust while below
- the Faroe shelf and islands seismic data indicate basement modified by weathering, igneous
- intrusions and tuffs with a thickness of about 25 35 km [Richard *et al.*, 1999]. Beneath the
- banks to the SW of the Faroe Islands the thickness of the subvolcanic crust is up to 25 km but
- it is as little as 8 km beneath the channels between them [Funck et al., 2008]. In the Faroe
- Bank Channel and the channel between George Bligh and Lousy Bank, in prolongation of the
- 697 GIFR, the continental middle crust is almost completely gone and the lower crust is
- dramatically thinned. Initial and final thicknesses of 60 km and 15 km are reasonable.
- Thinning of the mid- and lower crust of 30 km (Greenland) and 45 km (Faroe region)
- extending ~200 km along the margins and ~100 km inland could provide ~1.5 x 10^6 km³ of

- 701 material. Assuming original northerly and easterly dimensions for the Iceland Microcontinent
- of 300 km and 150 km respectively, and thinning from an original 60 km to 15 km, an
- additional $\sim 2 \times 10^6 \text{ km}^3$ of material is accounted for. Together, this totals $\sim 3.5 \times 10^6 \text{ km}^3$ of
- material, very close to the $\sim 3.6 \times 10^3 \text{ km}^3$ required.
- 705 This mass balance calculation illustrates simply that our model is reasonable. It also shows
- that the Iceland Microcontinent can provide over half of the continental material required.
- 707 This suggests that the formation of such an unusually large microcontinent was likely a key
- 708 element in the development of this unique region.
- 709 4.2 Problems and paradoxes solved

- 710 The model we propose can account naturally for many hitherto unexplained observations
- 711 from the GIFR and surrounding regions, and it is supported by multiple lines of evidence. In
- 712 particular, it offers a solution to the decades-old problems of why the Thulean land bridge
- existed, and the nature of Icelandic-type crust. Thus:
 - A composition of Icelandic-type crust comprising magma-inflated continental crust blanketed with lavas can explain the high topography and bathymetry of the GIFR and its prolonged persistence above sea level.
 - The assumption that the full thickness of Icelandic-type crust corresponds to melt has been widely accepted ever since Bjarnason *et al.* [1993] reported a reflective horizon at ~20 24 km depth beneath south Iceland which they interpreted as the Moho. That model cannot, however, account for the absence of refracted seismic phases (Section 3.1) which is inconsistent with gabbroic crust overlying mantle with a step-like interface velocity increase. The lack of such refractions is, however, consistent with the reflective horizon being a sill-like structure within or near the base of magmainflated continental crust.
 - Icelandic-type lower crust has a seismic velocity V_P of 7.0 7.3 km/s and a density of ~3150 kg/m³. No reasonable basaltic petrology is consistent with this [Gudmundsson, 2003; Menke, 1999], but these values fit a composition of magma-inflated continental crust.
 - A lower crust containing significant continental material solves the paradox of
 magmatic production on the GIFR. Icelandic-type lower crust cannot be gabbroic
 because a melt layer up to 40 km thick cannot be explained with any reasonable
 petrology and temperatures (Section 6) [Hole & Natland, this volume]. If the melt
 layer corresponds only to Icelandic-type upper crust plus magma inflating the lower
 crust—possibly a total thickness of up to ~15 km—much less melt needs to be
 explained.
 - A substantial volume of continental material in the lower crust can explain why the thicknesses of the upper and lower crustal layers on the GIFR are de-correlated (Figure 9) [Foulger et al., 2003; Korenaga et al., 2002]. In particular, the lower crust is thick throughout a NW-SE swathe across central Iceland where the upper crust is of average thickness. In the far south, the upper crust has its maximum thickness but the lower crust is unusually thin (Figure 9).
 - MORB melt formed in the mantle below the crust passes through the latter, melting
 fusible components to a high degree, boosting melt volume, and acquiring the
 continental signature observed in Icelandic rocks including the geochemistry,

- Proterozoic and Mesozoic zircons, and voluminous felsic and intermediate petrologies (Section 6).
 - The numerous, northerly trending synclines detected by seismology throughout submarine parts of the GIFR are readily explained as volcanically active extensional zones that were abandoned by lateral jumps and subsequently became extinct [Hjartarson *et al.*, 2017] (Figure 8).
 - If the JMMC is a northerly extension of the Iceland Microcontinent, the former may have shared the tectonic instability of the GIFR, providing an explanation for why the JMMC broke off east Greenland.
- Our new model for the GIFR can account for the many unusual extensional, transtensional
- and shear tectonic elements in the region. These include the curious distributed, bookshelf
- mode in which shear deformation is taken up in Iceland in the South Iceland Seismic Zone
- and the Tjörnes Fracture Zone [Bergerat & Angelier, 2000; Einarsson, 1988; Taylor et al.,
- 758 1994].

748

749

750

751

752

- 759 It can also account for the widespread hook-like tectonic morphology that resembles the tips
- of overlapping propagating cracks (Figure 16). These suggest that short extensional elements
- are abundant. The southernmost Aegir Ridge is hooked westward, mirroring the shape of the
- 762 Blosseville coast of Greenland and curving into the transverse Caledonian frontal thrust
- [Brooks, 2011]. The extensional NVZ of Iceland curves westward at its northern end where it
- links with the Kolbeinsey Ridge via the Tjörnes Fracture Zone. At its north end, the
- Reykjanes Ridge hooks to the east where it runs onshore to form the Reykjanes Peninsula
- extensional transform zone [Taylor et al., 1994]. The direction of extension in the EVZ is
- 767 rotated ~35° clockwise compared with the NVZ as shown by both the strike of dyke- and
- 768 fissure swarms and current measurements of surface deformation made using GPS [e.g., Perlt
- 769 et al., 2008]. The southernmost tip of this propagating rift, the Vestmannaeyjar archipelago,
- hooks to the west, complementing the east-hooking northern Reykjanes Ridge and Reykjanes
- 771 Peninsula Zone (Figure 16).
- The contrasting tectonic morphology and behavior north and south of the GIFR are naturally
- explained by tectonic decoupling by the GIFR that separates them. North of the GIFR the
- boundary is dominated by spreading ridges orthogonal to the direction of extension, separated
- by classic transform faults. To the south, the Reykjanes Ridge as a whole is oblique to the
- spreading direction and devoid of transform faults. Numerous tectonic events occurred north
- or south of the GIFR but not in both regions simultaneously [Gernigon et al., this volume;
- Martinez & Hey, this volume]. In Iceland, tectonic decoupling can explain the north-south
- contrast in geometry, morphology and history of the rift zones and the north-south
- asymmetry in geochemistry [e.g., Shorttle et al., 2013]. The latter may be important in
- mapping the distribution of continental material beneath Iceland.
- 782 Unstable tectonics on the GIFR can further explain the diachronous chevrons of alternating
- thick and thin crust that form at the tips of propagators within the Reykjanes Ridge plate
- boundary zone (Figure 7; Sections 2.2.2 and 7.3.3). The onset times of several of the most
- recent of these propagators at the GIFR coincide with major ridge jumps in Iceland (Table 1).
- 786 These observations are consistent with the propagators being triggered by major tectonic
- 787 reorganizations on the GIFR. Several similar ridges are observed in the oceanic crust east of
- the Kolbeinsey Ridge [Jones et al., 2002]. The chronic instability of the mid-Norwegian shelf
- and the adjacent Faroe-Shetland basin throughout the Palaeogene-earliest Neogene is also

- accounted for [Ellis & Stoker, 2014; Gernigon et al., 2012; Stoker et al., 2018] (Figure 11)
- 791 (Section 3.2).

792 5 Thermo-mechanical modeling

- We tested the plausibility of unusually prolonged survival of intact continental crust beneath
- the GIFR by modeling numerically the behavior under extension of structures characteristic
- of an ancient orogen such as the Caledonian and surrounding regions. The crust is required to
- have stretched to over twice its original width, retained a typical thickness of ~20 km, and
- persistently extended along more than one axis even up to the present day i.e. it underwent
- 798 long-term, diffuse extension.
- We used a two-dimensional thermo-mechanical modeling approach [Petersen & Schiffer,
- 800 2016] to calculate the visco-elastic-plastic response of an ancient orogen under simple
- extension. Full details of our methodological approach along with petrologic,
- thermodynamic, rheological, thermal conductivity, radiogenic heat productivity, initial model
- state, boundary conditions and melt productivity are described in detail by Petersen *et al.*
- 804 [2018]. The initial state for the model we use here differs from that used by Petersen *et al.*
- 805 [2018] only in that a) a uniform adiabatic temperature with potential temperature $T_P = 1325$ C
- is assumed for the entire mantle, and b) there is no MORB layer at the upper/lower mantle
- 807 boundary.
- Prior to continental breakup, crustal thickness and structure likely varied throughout the
- region, but precise details of the pre-rift conditions are not well known. Insights may be
- gained from well-studied, currently intact orogens. The Himalaya orogen, a heterogeneous
- stack of multiple terranes, entrained subduction zones, and continental material, is underlain
- by one or more fossil slabs trapped in the lithosphere. These locally thicken the crust and
- their lower parts are in the dense eclogite facies (Figure 17) [Tapponnier et al., 2001]. The
- Palaeozoic Ural Mountains preserve a crustal thickness of 50 55 km [Berzin et al., 1996].
- 815 The Caledonian crust is up to ~50 km thick under east Greenland [Darbyshire et al., 2018;
- Schiffer et al., 2016; Schmidt-Aursch & Jokat, 2005; Steffen et al., 2017] and ~45 km thick
- beneath Scandinavia [Artemieva & Thybo, 2013; Ebbing *et al.*, 2012].
- The pre-breakup crust in the region of the future NE Atlantic comprised the south-dipping
- 819 Ketilidian and Nagssugtoqidian orogens and the bivergent Caledonian orogen with east-
- 820 dipping subduction of Laurentia (Greenland) and west-dipping subduction of Baltica
- 821 (Scandinavia) (Figure 4). The GIFR thus formed over fossil forearc/volcanic front lithosphere
- that may initially have had a structure similar to that of the Zangbo Suture of the Himalaya
- orogen (Figure 17). North of the GIFR the supercontinent broke up longitudinally along the
- 824 Caledonian suture where the crust was thinner.
- We modeled the Caledonian frontal thrust as an orogenic belt where the lithosphere contrasts
- with that of the flanking Greenland and Scandinavia areas in a) increased crustal thickness,
- and b) eclogite from fossil subducted slabs embedded in the lithospheric mantle (Figure 4)
- 828 [Schiffer et al., 2014]. The eclogite is relatatively dense, potentially driving delamination, but
- is rheologically similar to dry peridotite [Petersen & Schiffer, 2016 and references therein].
- Additional weakening of the hydrated mantle wedge preserved under the suture would
- enhance the model behavior we describe below [Petersen & Schiffer, 2016]. For the mantle,
- we assume a pyrolite composition that is subject to melt depletion during model evolution.

- Figure 18 shows our initial, simplified model setup [Petersen et al., 2018]. Pre-rift continental
- crustal thickness is 40 km for the lithosphere adjacent to the orogen. The crust beneath the
- 835 200-km-wide orogen is 50 km thick and underlain by an additional 20-km-thick slab of
- 836 HVLC with an assumed mafic composition. Phase transitions and density are self-
- consistently calculated from pressure/temperature conditions throughout the model such that
- the topmost part of the body is above eclogite facies and the lower part is in the eclogite
- facies and thus negatively buoyant.
- Densities and entropy changes are pressure- and temperature-dependent and calculated using
- Perple_X-generated lookup tables [Connolly, 2005] based on the database of Stixrude and
- Lithogow-Bertelloni [2011]. We use a wide box (2000 km x 1000 km) to enable simulation
- of considerable extension distributed over a broad region, a grid resolution of 2 km, and a run
- time of 100 Myr at a full extension rate of 1 cm/a. Rifting of the lithosphere is kinematically
- forced by imposing plate separation at a rate of 0.5 cm/a via outwards perpendicular
- velocities at both left and right boundaries throughout the depth range of 0 240 km.
- A multigrid approach is employed to solve the coupled equations for conservation of mass,
- energy and momentum as described by Petersen *et al.* [2015; 2018]. For the continental crust,
- we assume plagioclase-like viscous behavior [Ranalli, 1995]. The HVLC is assumed to
- follow an eclogite flow law [Zhang & Green, 2007]. The upper mantle is assumed to follow a
- combined diffusion/dislocation creep flow law [Karato & Wu, 1993]. The lower mantle, here
- defined as the region where the pressure/temperature-dependent density exceeds 4300 kg/m³,
- approximately corresponding to Ringwoodite-out conditions, is assumed to follow the linear
- 854 flow law inferred by Čí ková et al. [2012].
- As the structure extends, rifting develops in the broad region where the crust is thickest. The
- 856 Moho temperature is highest there (i.e. ~800 C; Figure 18 central panels) due to greater
- burial and radiogenic heat production. During the first 10 Myr of widening, extensional strain
- within the crust is laterally distributed due to the delocalizing effect of flow in the lower crust
- 859 [e.g., Buck, 1991]. Thinning of the mantle lithosphere is not counteracted by this effect and
- 860 within 10 Myr it has been thinned by a factor of up ~2. This results in onset of decompression
- melting after ~12 Myr. At this point, the crust in the stretched orogen retains a large thickness
- of 30 40 km. This contrasts with the sequence of events where the crust is thin and brittle
- under which conditions decompression melting only onsets after breakup i.e. when complete
- thinning of the continental crust occurs [Petersen *et al.*, 2018].
- Thinning of the mantle lithosphere leads to lateral density gradients between the
- asthenosphere and displaced colder lithospheric mantle that destabilize the lithospheric
- mantle [Buck, 1986; Keen & Boutilier, 1995; Meissner, 1999]. Consequently, the mantle
- 868 lithosphere, including the already negatively buoyant HVLC, starts to delaminate at ~12 Myr
- 869 (Figure 18). As a result, asthenosphere at a potential temperature (T_P) of ~1325 C and crust at
- an initial temperature of ~600 800 C are rapidly juxtaposed. This leads to increased heat
- 871 flow into the crust which therefore remains ductile enough to flow and continues to extend in
- the delocalized, "wide rift mode" of Buck [1991]. The loci of extension repeatedly migrate
- laterally and this mode of deformation continues as long as lower crust is available. The loci
- 874 of extension only stabilize after ~70 Myr.
- Figure 18 shows the predicted structure after 51 Myr, approximately the present day, and a
- magnification of the 51-Myr lithology panel is shown in *. The continental crust is still intact
- across the now 1,200-km-wide ocean and extending diffusely. Decompression melting is

- occurring beneath two zones. The HVLC body has disintegrated and the largest pair of
- fragments are 200 300 km in diameter. These, along with carapaces of lithospheric mantle,
- have subsided to a depth near the base of the transition zone. Between them, a narrow arm of
- mantle upwells and flattens at the base of the crust to form a broad sill-like body ~200 km
- thick that underlies the entire ocean. Upwelling includes some material from just below the
- transition zone as a consequence of the sinking HVLC displacing uppermost lower-mantle
- 884 material.
- Full lithosphere breakup has not occurred by 51 Myr. It is imminent at 71 Myr (Figure 18).
- The lower crust beneath distal areas flows into the thinning extending zone and only when
- the supply of ductile lower crust is depleted does extension localize, leading to full
- lithosphere rupture and sea-floor spreading. This may take several tens of millions of years.
- In the case where the crust is thinner and/or HVLC is lacking modeling predicts transition to
- sea-floor spreading after only a few million years.
- The generic model presented here shows that it is possible for extending lithosphere to
- remain for as long as 70 Myr in a delocalized 'wide' stretching mode [senso Buck, 1991]
- with lower crust from distal areas flowing into the extending zone. Since the delamination,
- the mantle lithosphere has effectively been removed and decompression melting occurs
- where the mantle wells up beneath the rift system. Together, these interdependent processes
- provide a physical mechanism for how continental crust could be preserved beneath the GIFR
- despite more than 50 Myr of extension (Figure 20). At the same time, the model accounts for
- the magmatism observed on the GIFR in that it predicts decompression melting in the mantle.
- These melts rise, intrude and erupt, covering the continental crust as it stretches, and would
- produce crust similar to the "embryonic" crust proposed to occur in the Norway Basin
- 901 [Geoffroy, 2005; Gernigon *et al.*, 2012].
- The predictions of our model for present-day structure compare well with seismic
- tomography images (Figure 21). For example, a cross section through the full-waveform
- inversion tomographic model of Rickers et al. [2013] shows several features that are in close
- correspondence to those we predict. These include the flanking high-wave-speed bodies at
- 906 the bottom of the transition zone, a narrow, weak, vertical, low-wave-speed body between
- 907 them and a broader, stronger, low-wave-speed body in the top ~200 km underlying the entire
- ocean. The high-wave-speed bodies correspond to the delaminated lithospheric mantle and
- 909 the low-wave-speed anomalies correspond to the temperature anomalies predicted by the
- 910 modeling (Figure 19). A mantle temperature anomaly of ~ 30 C is predicted beneath the
- 911 entire ocean down to ~ 200 km depth as a result of upper mantle upwelling. The seismic
- anomaly could then be explained by this temperature anomaly and a resulting increase in the
- degree of partial melt by up to 0.5% [Foulger, 2012]. Such a temperature anomaly is
- onsistent with the low values predicted by Ribe et al. [1995] who modeled the topography of
- 915 the region, and the petrological estimates of Hole and Natland [this volume]. Seismic
- tomography images are notoriously variable in detail, in particular anomaly amplitudes
- 917 [Foulger et al., 2013], and we thus place most significance on the correspondence between
- 918 the shape of the predicted (Figure 19) and observed (Figure 21) anomalies.
- Our results differ from those of existing mechanical models in that breakup of the continental
- 920 crust is more protracted [e.g., Brune et al., 2014]. For example, Huismans and Beaumont
- 921 [2011] showed that extension of lithosphere with relatively weak crust results in pre-breakup
- 922 wide-rift-mode extension for ~35 Myr. Our model differs from theirs by having dense HVLC
- 923 that delaminates as a consequence of rifting thereby increasing heat flow into the crust. This

- enables wide rifting to persist for much longer than where no HVLC is present, even in the
- absence of an especially weak lower crustal rheology.
- The amount and detailed history of wide-mode extension is controlled by the thickness of the
- 927 initial crust and rheology-governing parameters such as initial thermal state, heat flow,
- 928 radiogenic heat production and crustal flow laws. We examined models that varied some of
- these parameters to investigate the sensitivity of our results to the assumed initial conditions.
- 930 We modeled crustal thicknesses of 35 km for the region and 40 km for the orogen, and
- 931 lithosphere thickness of 100 km with quartzite-like crustal rheology. Similar results to those
- described above were obtained. Factors we do not incorporate in our simple model that would
- 933 further encourage crustal stretching and delay breakup include increased basal heat flow
- and/or internal heat production and inclusion of 3D effects that would permit ductile mid-
- and lower crust to flow along the strike of the Caledonides towards the GIFR during
- 936 extension.

6 Geochemistry

- All aspects of the petrology and geochemistry of igneous rocks in the NE Atlantic Realm are
- onsistent with a model where Icelandic lower crust contains a substantial amount of
- ontinental crust. The geochemical and petrological work most powerful to test this model is
- that which addresses the composition and potential temperature (T_P) of the melt source.
- 942 6.1 Composition of the melt source
- The source of Icelandic lavas cannot be explained by mantle peridotite alone [e.g., Presnall &
- Gudfinnsson, 2011]. A component of continental material is required and some studies have
- presented evidence that this could be of Caledonian age [Breddam, 2002; Chauvel &
- 946 Hemond, 2000; Korenaga & Kelemen, 2000]. It could come from subducted slabs still
- remaining in the shallow mantle, as has been proposed earlier [Foulger & Anderson, 2005;
- Foulger et al., 2005]. The observations could also be explained by the upward flow of mantle
- melt through a substrate of stretched, magma-inflated continental crust similar to some
- 950 HVLC beneath the passive margins.
- 951 *Titanium*: The petrology and geochemistry of igneous rocks along the mid-Atlantic ridge
- change radically at the Icelandic margin. Low-TiO₂ basalts are found on the Reykjanes and
- Nolbeinsey Ridges and in the rift zones of Iceland. These rocks do not follow the MORB
- array of Klein and Langmuir [1987] but have the least Na₈ and Ti₈ of the entire global array.
- These lavas are probably derived mostly from a peridotitic MORB source.
- 956 Basalts with high-TiO₂ and FeO(T) signatures occur in Iceland, Scotland, east and west
- Greenland, but not on the Reykjanes or Kolbeinsey Ridges. These basalts cannot come from
- 958 MORB-source mantle—the source is required to have distinct Fe-Ti-rich material and other
- important geochemical indicators such as REE that are not found in MORB-source mantle.
- The extent of differentiation beneath Icelandic central volcanoes is also high enough to
- produce abundant silicic lavas—icelandite and rhyolite—in association with the FeO(T)-
- TiO₂-rich basalts. These rocks comprise 10% of the surface volcanics of Iceland but are not
- present on the adjacent submarine ridges and are uncommon on all other oceanic spreading
- 964 plate boundaries.

- A candidate for the source of such lavas is lower continental crust, possibly
- 966 pyroxenite/eclogite arising from gabbro with elevated TiO₂ and FeO(T) at pressures in the
- eclogite facies, along with refractory sub-continental lithospheric mantle (SCLM), originally
- 968 from the Greenland and European margins and still present in the central North Atlantic. A
- 969 hybrid source of this sort can explain the diversity of Icelandic magmas [Foulger &
- 970 Anderson, 2005; Foulger *et al.*, 2005; Korenaga, 2004; Korenaga & Kelemen, 2000].
- 971 Because there is no major isotopic anomaly, the source cannot be very old. Candidate
- material is common in continental lithosphere. For example, xenolith suites of lower crustal
- 973 cumulates from Permian lamprophyres in Scotland have the required characteristics [Downes
- 974 et al., 2007; Hole et al., 2015].
- The close proximity of the low- and high-Ti, high-FeO(T) basalts suggests that their different
- 976 sources are physically close together. It is clear that these sources have been tapped since the
- opening of the NE Atlantic as they are also seen in the same successions in the Skaergaard
- 978 intrusion in east Greenland [Larsen et al., 1999]. The high-TiO₂ and FeO(T) lavas found in
- 979 Iceland are typical of lavas derived from sub-continental lithospheric mantle and pyroxenite.
- No more than 20 30% of pyroxenite in a hybrid source is required to explain the
- 981 observations.
- 982 <u>Isotope ratios:</u> Elevated ⁸⁷Sr/⁸⁶Sr and Pb isotope ratios are found in basalts from east and
- 983 southeast Iceland [Prestvik et al., 2001]. This has been interpreted as requiring a component
- of continental material in the source beneath Iceland. That component could come from crust
- or detached SCLM buried beneath surface lavas [Foulger et al., 2003].
- 986 Zircons: Archaean and Jurassic zircons with Lewisian (1.8 Ga) and Mesozoic (~126 242
- 987 Ma) inheritance ages have been reported from lavas in NE Iceland. This has been interpreted
- as indicating ancient continental lithosphere beneath Iceland [Paquette et al., 2006;
- 989 Schaltegger et al., 2002]. A continental composition for Icelandic-type lower crust can
- 990 explain these results.
- 991 Water: Water in basalt glass from the mid-Atlantic Ridge indicates elevated contents in the
- 992 source from ~61 N across Iceland [Nichols et al., 2002]. The water contents are estimated to
- 993 be ~165 ppm at the southern end of the Reykjanes Ridge, rising to 620 920 ppm beneath
- Iceland. Such a component, and other volatiles such as CO₂ [Hole & Natland, this volume]
- decrease the solidus of a source rock and increase the volume of melt produced for a given T_P
- 996 (Section 6.2).
- 997 6.2 Temperature of the melt source
- The temperature of the melt source of Icelandic rocks is too low to be able to account for a
- 999 30-40-km-thick basaltic crust using any reasonable lithology [Hole & Natland, this volume].
- 1000 It is therefore an inevitable conclusion that much of the lower crust beneath the GIFR must
- arise from a process other than high-temperature partial melting of mantle peridotite.
- Geochemical work aimed at determining the potential temperature of NE Atlantic source
- 1003 rocks has used basalts from Iceland and high-MgO picrites from the Davis Strait [Clarke &
- Beutel, 2019; Hole & Natland, this volume]. The T_P for the source of MORB is generally
- used as the standard against which other calculated mantle temperatures are compared. The
- 1006 currently accepted value of this is 1350±40 C (Table 3) [Hole & Natland, this volume].

- A large range of temperatures, $T_P = 1400 1583$ C, has been suggested for the mantle
- beneath Iceland [Hole & Millett, 2016; Putirka, 2008]. The breadth of this range in itself
- indicates how difficult it is to derive a repeatable, reliable T_P using geochemistry and
- petrology. Difficulties include the lack of surface samples that correspond to an original
- mantle melt—crystalline rocks essentially always contain xenocrysts, and no picritic glass
- has been found in the NE Atlantic Realm [Presnall & Gudfinnsson, 2007]. The unknown
- source composition also introduces uncertainty. The geochemistry of Icelandic lavas requires
- there to be a component of recycled surface materials in the source and variable volatile
- 1015 contents including water [Nichols et al., 2002]. Ignoring any of these unknowns causes
- 1016 estimates of T_P to be erroneously high.
- 1017 Crystallization temperatures estimated from olivine-spinel melt equilibration, the so-called
- "aluminum-in-olivine" method, are independent of whole-rock composition. The
- temperatures yielded by this method are $T_P \sim 1375$ C and ~ 100 C higher for the Davis Strait
- picrites (Table 3) [Hole & Natland, this volume]. A summary of global maximum
- petrological estimates of T_P and ranges of olivine-spinel equilibrium crystallization
- temperatures for magnesian olivine are shown in Figure 22.
- Petrological estimates of the potential temperature T_P of the source of basalts in the NE
- 1024 Atlantic Realm suggest upper-bound T_P of ~1450 C for Iceland and ~1500 C for the picrites
- of Baffin Island, Disko Island and west Greenland [Hole & Natland, this volume]. There may
- thus have been a short-lived, localized burst of magma from a relatively hot source lasting ~2
- 1027 3 Myr when propagation of the Labrador Sea spreading center was blocked at the
- Nagssugtoqidian orogen, but there is no compelling evidence for a T_P anomaly $> \sim 100$ C
- before or after this anywhere in the NE Atlantic Realm.
- The melt volume produced at Iceland has also been used as a constraint in models for T_P .
- That work has assumed that the full thickness of the 30-40-km-thick seismic crustal layer is
- melt produced by steady state fractional melting of a peridotite mantle source. Production of
- just 20 km of igneous crust would require a T_P of ~1450 1550°C assuming a damp or dry
- peridotite source [Sarafian et al., 2017]. No credible lithology or temperature can explain the
- crustal thickness of ~40 km that has been measured for central Iceland [Darbyshire et al.,
- 1036 1998a; Foulger *et al.*, 2003].
- 1037 Crustal thickness beneath the active volcanic zones of Iceland varies from ~40 km (beneath
- 1038 Vatnajökull) to ~15 20 km (beneath the Reykjanes Peninsula extensional transform zone)
- 1039 [Foulger et al., 2003]. If the full thickness of crust everywhere is formed from melting in the
- mantle, unrealistically large lateral variations in temperature of the source of ~150 C over
- distances of ~125 km would be required [Hole & Natland, this volume].
- $1042 6.3 {}^{3}He/{}^{4}He$
- Elevated ³He/⁴He values are commonly assumed to indicate a core-mantle boundary
- provenance for the melt source. This association was originally suggested when it was found
- that some lavas from Hawaii contain high-³He/⁴He [Craig & Lupton, 1976]. It was reasoned
- that, over the lifetime of Earth, the ³He/⁴He of the mantle has progressively decreased from
- an original value of ~200 times the present-day atmospheric ratio (Ra) to ~8 \pm 2 Ra—the
- value most commonly observed in MORB. It was subsequently assumed that a lava with
- ³He/⁴He much larger than 8 Ra must have arisen from a primordial source, isolated for
- Earth's 4.6 Ga lifetime, deep in the mantle near the core-mantle boundary.

- This theory has long been contested and it has been counter-proposed that the helium instead
- resided for a long time in depleted, unradiogenic materials such as olivine in the sub-
- 1053 continental lithospheric mantle [Anderson, 2000a; b; 2001; Anderson et al., 2006; Foulger &
- Pearson, 2001; Natland, 2003; Parman et al., 2005]. That theory would fit the high-³He/⁴He
- values reported from Iceland and the Davis Strait [Starkey et al., 2009; Stuart et al., 2003] if
- the deeper parts of the crust beneath these regions contain ancient material, as we propose in
- this paper.

1058 7 Discussion

- 1059 7.1 The Greenland-Iceland-Faroe Ridge
- The model presented here proposes that in general Icelandic-type upper crust is mafic in
- nature, equivalent to Layers 2 3 of oceanic crust, whilst Icelandic-type lower crust is
- magma-dilated continental crust. The pre-existing SCLM mostly delaminated during the
- stretching process (Section 5) (Figure 18). The melt layer thus comprises Icelandic-type
- upper crust plus the melt that intruded into the continental crust below as plutons, dykes and
- sills. The location of Iceland with respect to the east Greenland and Faroe Volcanic margins
- fits the model of Geoffroy et al. [2015; submitted] of a dislocated C-block (Figure 5).
- This new model contributes to the > 40-year controversy regarding whether the crust beneath
- 1068 Iceland is thick or thin. A "thin crust" model, generally assumed in the 1970s and 1980s,
- attributed Icelandic-type upper crust to the melt layer—the subaerial equivalent of oceanic
- 1070 crust—and the layer currently termed "Icelandic-type lower crust" to hot, partially molten
- mantle [Björnsson et al., 2005]. From the 1990s, long seismic explosion profiles using
- modern digital recording were shot and deep reflecting horizons were discovered. A "thick
- 1073 crust" model was then introduced that interpreted the layer previously thought to be hot,
- partially molten mantle as Icelandic-type lower crust, the equivalent of oceanic layer 3, and
- part of the melt layer.
- Our findings support the thin-crust model with the caveat that Icelandic-type lower crust is
- indeed crust, and not hot mantle as previously proposed, but it is magma-inflated continental
- 1078 crust. This model agrees with long-sidelined magnetotelluric work in Iceland which detects a
- high-conductivity layer at ~10 20 km depth. This layer was proposed to mark the base of
- the crust [Beblo & Bjornsson, 1978; 1980; Beblo et al., 1983; Eysteinsson & Hermance,
- 1081 1985; Hermance & Grillot, 1974]. High-conductivity layers are common in continental mid-
- and lower crust [e.g., Muñoz et al., 2008]. Explosion seismology and receiver functions find
- 1083 the thickness of Icelandic-type upper crust to be ~3 10 km (Figure 9; Figure 10) [Darbyshire
- 1084 et al., 1998b; Foulger et al., 2003] which is comparable with the crustal thicknesses beneath
- the Reykjanes Ridge and the Kolbeinsey Ridge if additional magma dilating the Icelandic-
- 1086 type lower crust is taken into consideration. This is nevertheless up to ~40% thicker than the
- global average of 6 7 km. Mantle fusibility enhanced by pyroxenite and water (Section 6), a
- moderate elevation in temperature (Section 6.2), and bursts of volcanism accompanying
- frequent rift jumps (Section 4) can account for the enhanced melt volumes.
- The plate boundary traversing the GIFR cannot be likened to a conventional spreading ridge
- with segments connected by linear transform faults as is commonly depicted in simplified
- illustrations. Historically, motion in the GIFR region was postulated to have been taken up on
- a classic ~150-km-long sinistral transform fault named the Faroe Transform Fault or the
- 1094 Iceland Faroe Fracture Zone [Bott, 1985; Voppel et al., 1979] and this idea was reiterated in

- subsequent work [e.g., Blischke et al., 2017; Guarnieri, 2015]. Locations proposed for this
- feature include the north edge of the Iceland shelf, central Iceland, and the South Iceland
- 1097 Seismic Zone [Bott, 1974].
- There is, however, no observational evidence for such a structure [Gernigon et al., 2015;
- Schiffer et al., 2018] and it does not, even to a first order, fit the observations on the ground.
- Only a GIFR that deforms as a broad zone of distributed extension and shear can account for
- the reality of the geology of Iceland and adjacent regions [Schiffer et al., 2018].
- Our model may provide a long-awaited explanation for why the JMMC broke off east
- Greenland. Westerly migration of axes of extension on the GIFR may have changed the stress
- field in the diffusely extending continental area to the north and encouraged extension there
- to coalesce on the single most westerly zone which thereafter developed into the Kolbeinsey
- 1106 Ridge.
- 1107 7.2 Crustal flow
- Ductile crustal flow has been incorporated into earlier numerical models of continental
- breakup. A ductile, low-viscosity layer that decouples the upper lithosphere from the lower
- was incorporated in models of extending continental lithosphere by Huismans and Beaumont
- 1111 [2011; 2014]. Such a layer enables ultrawide regions of thinned, unruptured continental crust
- to develop along with distal extensional (sag) basins. Crustal thicknesses are maintained by
- widespread lateral flow of mid- and lower-crustal material from beneath surrounding regions.
- Lower crust may well up, further delaying full crustal breakup.
- In our model, subsidence resulting from progressive thinning or delamination of the mantle
- lithosphere is mitigated by hot asthenosphere rising to the base of the crust. This abruptly
- raises temperatures, increasing heat flow and further encourages ductile flow. Low extension
- rates, such as have characterized the NE Atlantic, tend to prolong the time to breakup and
- encourage diffuse extension because ductile flow and cooling can continue for longer. The
- crust may stretch unruptured for tens of millions of years and widen by 100s of kilometers
- with axes of extension migrating diachronously and laterally across the extending zone. Only
- after eventual rupture of the continental lithosphere can sea-floor spreading begin. Until that
- occurs, geochemical signatures of continental crust and mantle lithosphere are expected in
- overlying magmas that have risen through the continental material.
- Depth-dependent stretching, in particular involving the lower-crustal ductile flow that we
- model in Section 5, is both predicted by theory [McKenzie & Jackson, 2002] and required by
- observations from many regions. These include amagmatic margins, the Basin Range
- province, western USA [Gans, 1987] and deformation at collision zones, e.g., the Himalaya
- and Zagros mountain chains [e.g., Kusznir & Karner, 2007; Royden, 1996; Shen et al., 2001].
- Lower-crustal flow is actually observed where such crust is exhumed to the surface, e.g., at
- 1131 Ivrea in the Italian Alps, where lower-crustal granulite intruded by mafic plutons is exposed
- 1132 [e.g., Quick et al., 1995; Rutter et al., 1993].

1133 *7.3 Magmatism*

7.3.1 The concept of the North Atlantic Igneous Province

- The issues laid out in this paper bring into question the concept that the magmas popularly
- grouped into the North Atlantic Igneous Province (NAIP) can be viewed as a single
- magmatic entity [Peace et al., this volume]. The NAIP is generally considered to include the
- volcanic rocks in the region of the Davis Strait, the volcanic margins of east Greenland and
- Scandinavia, and the magmatism of the GIFR. These magmas are, however, only a subset of
- those in the region and many others are not typically included [Peace et al., this volume].
- 1141 These include melt embedded in the "amagmatic" margins of SW Greenland and Labrador,
- current volcanism at Jan Mayen, the Vestbakken Volcanic Province ~300 km south of
- Svalbard, conjugates in NE Greenland [Á Horni et al., 2016], magmatism at the west end of
- the CGFZ [Keen et al., 2014] and basaltic sills offshore Newfoundland detected in ODP site
- 210-1276 that are thought to extend throughout an area of ~20,000 km² [Deemer et al.,
- 1146 2010]. It is illogical to exclude these, especially since the Cretaceous(?) Anton Dohrn and
- Rockall seamounts are included in the NAIP [Jones *et al.*, 1994].
- The grouping of a select subset of magmas in the NE Atlantic Realm into a single province is
- predicated on and reinforces, the concept that they all arise from a single, generic source. A
- model of such simplicity that fits all observations has been elusive for over half a century.
- The obvious solution, and one that can readily account for the observations, is a model
- whereby each magmatic event occurs in response to local lithospheric tectonics and melts are
- locally sourced.
- The same reasoning may well apply to other volcanic provinces, e.g., the South Atlantic
- Volcanic Province. Generally included in this are the Paraná and Etendeka flood basalts, the
- volcanic rocks of the Rio Grande Rise and the Walvis Ridge, the currently active Tristan da
- 1157 Cunha archipelago and even kimberlites and carbonatites in Angola and the Democratic
- Republic of the Congo [see Foulger, 2018 for a review]. These volcanic elements contrast
- with one another in the extreme and each most likely erupted in reaction to local tectonic
- responses to global events and processes, with magmas locally sourced.

1161 7.3.2 Magma volume

- Estimates for the total volume of the magma generally lumped together as the NAIP are 2 -
- 1163 10 x 10⁶ km³ with a value of ~6.6 x 10⁶ km³ for the north Atlantic volcanic margins [Eldholm
- & Grue, 1994a]. Assuming these margins formed in ~3 Myr, Eldholm and Grue [1994a]
- calculate a magmatic rate of 2.2 km³/a and suggest the NAIP is one of the most voluminous
- igneous provinces in the world. That calculation assumes that the HVLC beneath the *Inner*
- SDRs is all igneous and formed contemporaneously with the volcanic margins. If this is not
- the case, the volume and magmatic rate for the north Atlantic volcanic margins must be
- downward-revised by up to 30%, i.e. to \sim 4.4 x 10^6 km³ for volume and 1.5 km³/a for
- magmatic rate. Eldholm and Grue [1994a] furthermore estimate a magmatic rate of ~ 0.2
- 1171 km³/a for Iceland. If the igneous crust on the GIFR is only 10 15 km thick, this rate must be
- downward-revised to 0.12 0.08 km³/a. The magmatic rate per rift kilometer would then be 2
- $-3 \times 10^{-4} \text{ km}^3/\text{a}$ compared with $\sim 4.8 \times 10^{-4} \text{ km}^3/\text{a}$ per rift kilometer for the global plate
- boundary.
- 1175

- 1176 These changes reconcile geological estimates with those derived from numerical modeling.
- 1177 Magmatism at the NE Atlantic rifted margins has been simulated using models of
- decompression melting in a convectively destabilized thermal boundary layer coupled with
- upper-mantle ("small-scale") convection [Geoffroy et al., 2007; Mutter & Zehnder, 1988;
- Simon et al., 2009]. These models explore whether the volumes and volume rates can be
- accounted for simply by breakup of the 100-200-km-thick lithosphere without additional ad
- 1182 hoc processes. Current numerical models slightly under-predict traditional geological
- estimates but could be reconciled with estimates lowered to take into account a wholly or
- partially continental affinity of HVLC.
- 1185 More accurate estimates of volume could also explain the extreme variations in magmatic
- thickness over short distances required by assumptions of HVLC igneous affinity. For
- example, the radical contrast between the unusually thin (4 7 km) oceanic crust beneath the
- 1188 Aegir Ridge [Greenhalgh & Kusznir, 2007] and a ~30 km igneous thickness beneath the
- adjacent GIFR defies reasonable explanation but the problem vanishes if the latter
- assumption is dropped.

1191 7.3.3 The chevron ridges

- Lithosphere- and asthenosphere-related mechanisms compete to explain the chevron ridges
- that flank the Reykjanes Ridge [Hey et al., 2008; Jones et al., 2002]. Martinez and Hey [this
- volume] suggest that the required oscillatory changes in magmatic production result from
- axially propagating mantle upwelling instabilities that travel with ridge-propagator tips along
- the Reykjanes Ridge. These originate in Iceland and the gradient in mantle properties along
- the Reykjanes Ridge results in the convective instabilities migrating systematically south
- along the Ridge. Upwelling is purely passive and the propagators behave in a wave-like
- manner without the flow of actual mantle material along the Ridge. In this model, the
- transition from linear to ridge/transform staircase plate boundary geometry at ~37 38 Ma
- failed to eliminate the structure of the deeper asthenospheric melting zone and the Reykjanes
- Ridge is restructuring itself to realign over that zone.
- Several of the propagators onset at the GIFR in concert with tectonic reorganizations there
- 1204 (Table 1) [Benediktsdóttir et al., 2012] inviting consideration of lithospheric triggers. The
- Reykjanes Ridge as a whole is oblique to the direction of plate motion but its axis comprises
- an array of right-stepping *en echelon* spreading segments, each of which strikes perpendicular
- to the direction of motion. Such fabric resembles a left-lateral transtension zone.
- 1208 The diachronous chevron crustal fabric began to form at ~37 38 Ma when the Reykjanes
- 1209 Ridge changed from a linear to a ridge-transform configuration with a ~30 counter-
- 1210 clockwise rotation in the direction of plate motion (Section 2.2.2) [Gaina et al., 2017]. From
- 1211 25-15 Ma slow, counter-clockwise rotation of the extension direction continued and from 15
- Ma present it rotated back [Gaina et al., 2017]. Slow counter-clockwise migration of the
- spreading direction would gradually hinder strike-slip motion on the transform segments and
- encourage evolution toward extension with a minor left-lateral shear overprint. Very slow
- changes in the direction of extension might be insufficient to trigger a sudden and major
- reorganization but enough to bring about the slow plate-boundary evolution observed.
- Regardless of whether a lithosphere- or asthenosphere-related mechanism is responsible for
- the chevron ridges, it is clear that shallow processes control them as their southerly
- propagation was temporarily blocked by several previously existing transform faults north of

- the present reorganization tip near the Bight transform fault. Furthermore, if their inception is
- related to tectonic reorganizations on the GIFR, then conversely the time at which the
- propagators set off from the GIFR could indicate the times of first-order tectonic
- reorganizations on the GIFR.
- The transform-eliminating rift propagators of the Reykjanes Ridge are unique in their degree
- of development but not entirely unknown elsewhere. Examples outside the NE Atlantic
- include a southward propagator eliminating a transform formerly at 21 40'N on the mid-
- 1227 Atlantic Ridge [Dannowski et al., 2011] and propagators on the faster-spreading (~100
- 1228 km/Myr) NE Pacific plate boundary that eliminated the Surveyor, Sila, Sedna and Pau
- transforms [Atwater & Severinghaus, 1989; Hey & Wilson, 1982; Shih & Molnar, 1975].
- Propagating small-scale convective instabilities have also been postulated to form volcanic
- ridges and seamount chains that flank parts of the East Pacific Rise in a direction parallel to
- plate motion [e.g, Forsyth *et al.*, 2006].

1233 7.3.4 The North Atlantic geoid high

- 1234 The GIFR sits at the apex of a ~3000-km-long bathymetric and geoid high (up to ~4000 m
- and 80 m respectively) that stretches from the Azores to the Jan Mayen Fracture Zone
- 1236 [Carminati & Doglioni, 2010; King, 2005; Marquart, 1991]. Without this high the Thulean
- land bridge and Iceland would not have been subaerial. Globally, the only other comparable
- geoid high extends through Indonesia and Melanesia and to the Tonga Trench. Major geoid
- highs with lower amplitudes or smaller spatial extents are associated with the SW Indian
- 1240 Ocean and the Andean mountain chain.
- The geoid highs associated with Indonesia, Melanesia and Tonga, and the Andean mountain
- chain are a consequence of accumulations of dense subducted slabs. The geoid high of the
- north Atlantic corresponds closely to the pre-breakup Caledonian orogen plus the south
- European/North African Hercynian orogen (Figure 23). A possible explanation for part of the
- geoid anomaly is thus residual, dense, subducted Caledonian and Hercynian slabs along with
- 1246 continental lower crust and mantle lithosphere distributed in the shallow mantle. Henry Dick
- and colleagues have long argued that the petrology and geochemistry of magmas on the SW
- 1248 Indian ridge require SCLM in the melt source [Cheng et al., 2016; Dick, 2015; Gao et al.,
- 1249 2016; Zhou & Dick, 2013]. That ridge is the current locus of extension between Africa and
- 1250 Antarctica which separated as part of Pangaea breakup beginning in the Jurassic. By analogy
- with the NE Atlantic, continental material might also remain in the mantle beneath the ocean
- there and the SW Indian geoid high might thus be explained in a similar way to that of the
- 1253 north Atlantic.

1254 7.3.5 Regions analogous to the GIFR

- There are clear parallels between the GIFR and the Davis Strait. The structure and tectonic
- development of the latter show similar characteristics to the GIFR but to a less extreme
- degree (Figure 24). The Davis Strait is colinear with the GIFR and both function as
- transtensional shear zones. Its primary feature is the long Ungava Fault Complex [Peace et
- 1259 al., 2017]. This is underlain by ~8 km of oceanic crust beneath which is ~8 km of HVLC
- with V_P up to 7.4 7.5 km/s [Chalmers & Pulvertaft, 2001; Funck et al., 2006; Funck et al.,
- 2007; Srivastava *et al.*, 1982] and density of 2850 3050 kg/m³ [Suckro *et al.*, 2013]. These
- values are similar to those of Icelandic-type lower crust.

- Like the GIFR, the bathymetric high that contains the 550-km-long Davis Strait is elongated
- in the direction approximately perpendicular to plate motion. It has water depths of < 700 m,
- 1265 contrasting with the adjacent > 2000-m-deep Labrador Sea and Baffin Bay. At the Davis
- 1266 Strait north-propagating rifting stalled at the confluence of the Nagssugtoqidian and Rinkian
- orogens and continued displaced by several hundred kilometers in a right-stepping sense. In
- the case of the GIFR, both north- and south-propagating oceanic rifting stalled at the
- 1269 confluence of the Nagssugtoqidian and Caledonian orogens.
- 1270 The Jan Mayen Fracture Zone formed where a major, pre-existing transverse structure
- formed a barrier to the south-propagating Mohns Ridge. It was also an episodic transtensional
- structure, has a history of migration of the locus of deformation, bathymetric highs and
- unusual volcanism, e.g., on the island of Jan Mayen and in the submarine Traill Ø and Vøring
- 1274 Spur igneous complexes [Gernigon et al., 2009; Kandilarov et al., 2015]. Continental crust is
- possibly trapped between parallel segments of the Zone.

7.3.6 Regions analogous to the NE Atlantic Realm

- The history, structure, tectonics and petrology of the NE Atlantic Realm are unusually
- 1278 complex but it represents an extreme example and not a unique case. Other regions that show
- similar features suggest that the style of breakup it exemplifies is generic. The NE Atlantic
- Realm may owe its extremity to the facts that the NE Atlantic was formed by two opposing
- propagators that stalled at a barrier, an unusually large microcontinent was captured, and the
- spreading rate was and is exceptionally slow.

- 1283 The South Atlantic Igneous Province also includes regions of shallow sea-floor, anomalously
- thick crust, anomalous volcanism and continental crust distributed in the ocean. It has a
- history of stalled spreading-ridge propagation, coincidence with a major pre-existing
- transverse structure and both shear and extensional deformation in a zone several hundred
- kilometers broad in the direction perpendicular to plate motion [Foulger, 2018; Kusznir & al.,
- 1288 2018]. Graça et al. [2019] recently presented evidence that the Rio Grande Rise, which
- 1289 contains continental material [Santos Ventura et al., 2019], and parts of the Walvis Ridge
- were once joined, but split apart by at least four ridge jumps. Such a process is very similar to
- that which we propose for the GIFR.
- The Lomonosov Ridge in the Arctic ocean can be viewed as an incipient microcontinent.
- West of India, the Laxmi basin comprises a pair of aborted conjugate volcanic passive
- margins with Outer SDRs that appear to be underlain by HVLC and flank an intra-oceanic
- microcontinent—a C-block [Geoffroy et al., submitted; Guan et al., 2019; Nemčok & Rybár,
- 1296 2017]. The Seychelles region in the West Indian Ocean, the Galapagos Islands region in the
- east Pacific [Foulger, 2010, p 100-101] and the Shatsky Rise [Korenaga & Sager, 2012;
- Sallares & Charvis, 2003] all display analogous features. Regions currently in the process of
- breaking up in a similar mode include the Afar area [Acton et al., 1991], the Imperial and
- 1300 Mexicali Valleys and Baja California (California and Mexico). The abundance of continental
- crustal fragments in the oceans is becoming increasingly clear, with much originating at
- locations where continental breakup was complicated by lithospheric heterogeneities.
- Despite the very different structure and context, tectonics comparable to those observed on
- the GIFR and in Iceland are also observed on the East Pacific Rise (EPR). There, "dueling"
- overlapping propagating ridge pairs with intermediate bookshelf shearing build ridge-
- perpendicular and ridge-oblique zones of crustal complexity (Figure 25) [Perram et al.,

- 1307 1993]. In oceanic settings overlapping ridge tips tend to form where lithosphere is weak and
- to migrate along-strike. Overlapping spreading centers are kinematically unstable and the tips
- inevitably fail episodically and are replaced by new ones. An unusual facet of the
- development of the GIFR that is not reported from the East Pacific Rise is the switching of
- the sense of overlap when the Aegir Ridge was replaced by the Kolbeinsey Ridge.
- 1312 Comparable styles of deformation are also observed in the Japan-, Manus-, Lau- and Mariana
- 1313 Trench back-arc basins [Kurashimo et al., 1996; Martinez et al., 2018; Taylor et al., 1994].
- Beneath back-arc basins the hydrous mantle environment above the dewatering slab does not
- become dehydrated and the attendant increase in viscosity tends to localize upwelling melt.
- As a result, extension does not become focused in a single rift zone but remains distributed
- between multiple, parallel rifts. Magnetic anomalies are disorganized and water also reduces
- the solidus, increasing melt production [Dunn & Martinez, 2011; Martinez et al., 2018].
- On land, similar petrologies, including high-TiO₂ basalts, association with abundant rhyolite,
- and likely provenance of the source in subcontinental material are observed in flood basalts
- that erupted through continental lithosphere. These include the Central Atlantic Magmatic
- Province [Peace *et al.*, this volume], the Deccan traps and the Columbia River Basalts.

1323 **8 Conclusions**

- 1324 Our main conclusions may be summarized:
- 1325 1. Disintegration of the Laurasian collage of cratons and orogens to form the Labrador Sea,
- Baffin Bay and the NE Atlantic Ocean lasted several tens of millions of years and
- occurred piecewise and diachronously via rift propagation.
- 1328 2. The GIFR formed where the south-propagating Aegir Ridge and the north-propagating,
- Reykjanes Ridge stalled at the junction of the Nagssugtoqidian and Caledonian orogens.
- 1330 The intervening ~300-km wide (northerly) and ~150-km long (easterly) continental
- block, the Iceland Microcontinent, along with flanking areas, extended by distributed,
- magma-assisted continental extension via multiple parallel migrating rifts with diffuse
- shear zones between them. The continental crust was capped by surface lavas. It stretched
- to form the 1000-km long Thulean continental land bridge which was not overrun by
- oceanic waters until ~10 -15 Ma.
- 1336Magma-assisted continental extension was enabled by ductile flow of low-viscosity mid-and lower crust.
- 4. Icelandic-type crust comprises the 3 10 km thick upper crust, equivalent to oceanic
- layers 2 3, underlain by lower crust up to ~ 30 km thick comprising magma-inflated
- 1340 continental crust.
- 5. The melt layer that caps the GIFR comprises the Icelandic-type upper crust plus magma injected into the Icelandic-type lower crust, and has a total thickness of ~10 15 km.
- 1343 6. The petrology and geochemistry of Icelandic lavas is consistent with inclusion of a component from underlying continental crust.
- 7. A largely continental Icelandic-type lower crust is consistent with the fact that no
- reasonable models of temperature or mantle petrology can generate the \sim 40 km of melt
- necessary to explain its entire thickness as wholly oceanic.
- 1348 8. The chevron ridges that flank the Reykjanes Ridge form in association with small-offset propagators initiated by tectonic reorganizations on the unstable GIFR.

1351			
1352 1353	10. The continuity of continental crust beneath the GIFR means that, at this latitude, Laurasia still has not yet entirely broken up. An implication of this is that the GIFR could be considered to be a new kind of plate boundary.		
1354 1355 1356	11. A model whereby continental breakup is characterized by diachronous rifting, strong influence from pre-existing structures, distributed continental material in the new oceans, and anomalous volcanism matches many other oceanic regions.		
1357			
1358	Acknowledgments		
1359	Erin K. Beutel and D. Barrie Clarke made valuable contributions to the discussions that led to		
1000	this manuscript. CS's postdoctoral fellowship at Durham University was financed by the		
1360	this interest per est a posturation with the state of the		
1360 1361	Carlsberg Foundation. F. Martinez and R. Hey are supported by US NSF grants OCE-		
1361	Carlsberg Foundation. F. Martinez and R. Hey are supported by US NSF grants OCE-		

Table 1: Chronology of major tectonic events in the NE Atlantic. Timescale after Gradstein *et al.* [2012]. Chevron ridge # after Jones *et al.* [2002].

Date (Ma)	Chevron ridge #	Magnetic chron	Event
58-57		C26	Beginning of opening of the Labrador Sea.
56-52		C24-22	First magnetic anomaly on the proto-Reykjanes Ridge.
54		C24r	Beginning of opening of the North Atlantic Ocean on the Aegir Ridge and west of the Lofoten margin.
54-ca 46		C24-21	Rift to drift transition, Faroe-Shetland and Hatton margins.
54.2-50			Spreading propagated from the Greenland Fracture Zone south to the Jan Mayen Fracture Zone.
52		C23	Aegir Ridge reaches its maximum southerly extent.
50-48		C21	~30-40 clockwise rotation of direction of plate motion .
48		C22-21	Onset of fan-shaped spreading about the Aegir Ridge. Pulse of extension in the southern JMMC. No major change south of the GIFR.
40		C18	Counter-clockwise rotation of direction of plate motion.
38-37	7	C17	Reykjanes Ridge becomes stair-step. First chevron ridge begins to form.
36		C13	Cessation of spreading in the Labrador Sea.
33-29		C12-10	Counter-clockwise rotation of direction of plate motion.
31-28	6	C12-10	Extinction of the ultra-slow Aegir Ridge. Second chevron ridge begins to form about the Reykjanes Ridge
24		C6/7	First unambiguous magnetic anomaly about the Kolbeinsey Ridge.
15-10		C5A/C5	Breaching of the Thulean land bridge.
14	5		Rift jump in Iceland from North West Syncline to Snæfellsnes Zone and Húnaflói Volcanic Zone, propagator "Loki" starts to travel south down Reykjanes Ridge forming third chevron ridge.
9	4		Propagator "Fenrir" starts to travel south down Reykjanes Ridge forming fourth chevron ridge.
7	3		Extinction of Snæfellsnes Zone, propagator "Sleipnir" starts to travel south down Reykjanes Ridge forming fifth chevron ridge.
5	2		Propagator "Hel" starts to travel south down Reykjanes Ridge forming sixth chevron ridge.
2	1		EVZ in Iceland forms, propagator "Frigg" starts to travel south down Reykjanes Ridge forming seventh chevron ridge.

Table 2: Rift zones indicated by geological observations on land in Iceland.

Name	Acronym	Tectonic status
North West Syncline	NWS	Extinct
Austurbrún Syncline	AS	Extinct
East Iceland Zone	EIZ	Extinct
Snæfellsnes Zone	SZ	Oblique, non extensional
Húnaflói Volcanic Zone	HVZ	Extinct
Mödrudalsfjallgardar Zone	MZ	Extinct
Reykjanes Peninsula Zone	RPZ	Oblique, extensional
Western Volcanic Zone	WVZ	Active, waning
Hofsjökull Zone	HZ	Active, very short
Northern Volcanic Zone	NVZ	Active
Öræfajökull-Snæfell Zone	ÖVZ	Active, non extensional
Eastern Volcanic Zone	EVZ	Active, propagating

Table 3: Potential temperatures required to produce 20 km of melt for various source compositions [from Hole & Natland, this volume].

Source composition	T_P C	
dry peridotite	1550	
dry peridotite + 10% pyroxenite	1540	
dry peridotite + 40% pyroxenite	1470	
damp peridotite + pyroxenite	1450	
damp peridotite	1450	
pyroxenite	1325-1450	
Baffin Island picrites (T _{Ol-Sp})	1500	

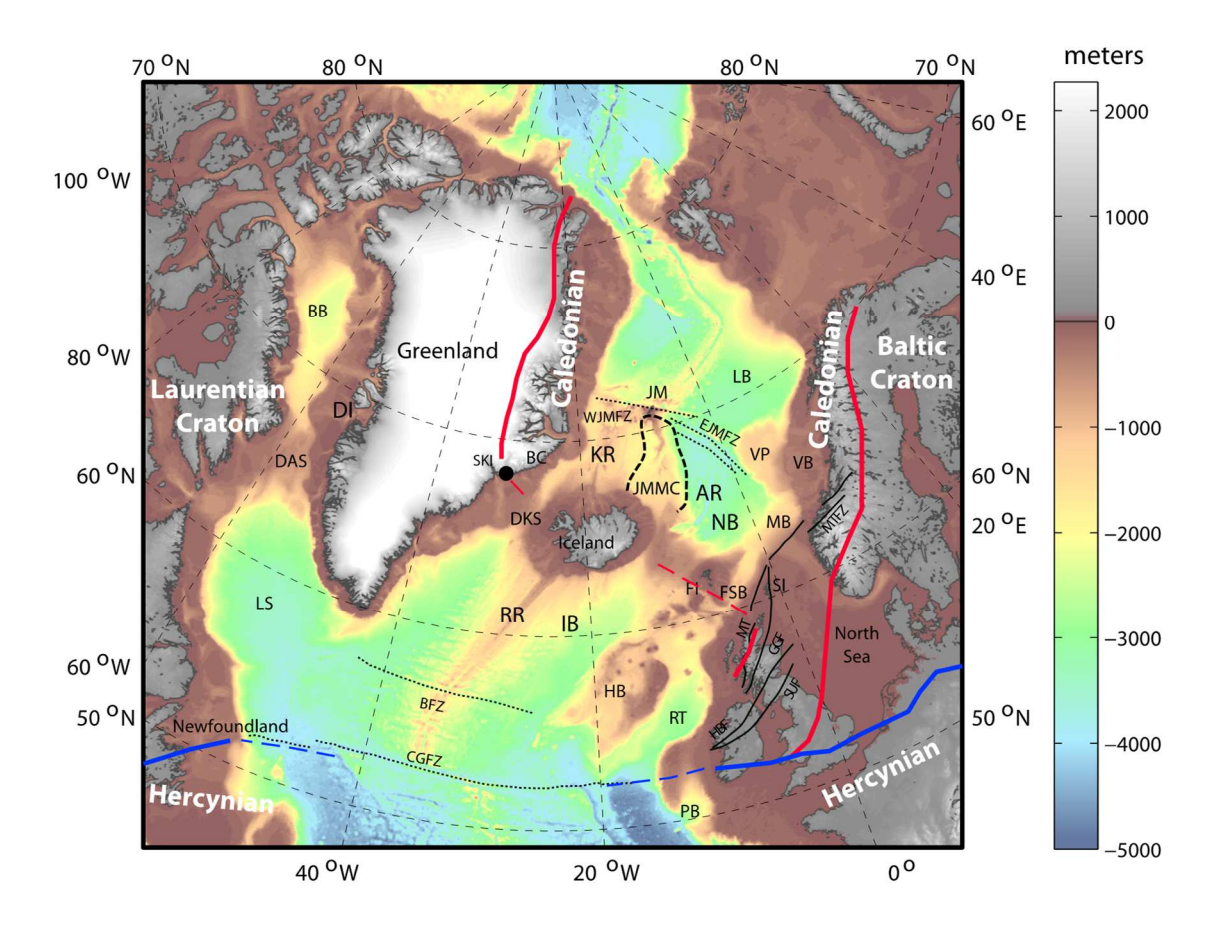


Figure 1: Regional map of the North East Atlantic Realm showing features and places mentioned in the text. Bathymetry is shown in color and topography in land areas in gray. BB: Baffin Bay, DAS: Davis Strait, DI: Disko Island, LS: Labrador Sea, CGFZ: Charlie-Gibbs Fracture Zone, BFZ: Bight Fracture Zone, RR: Reykjanes Ridge, IB: Iceland basin, DKS: Denmark Strait, SKI: Skaergaard intrusion, BC: Blosseville coast, KR: Kolbeinsey Ridge, JMMC: Jan Mayen Microcontinent Complex, AR: Aegir Ridge, NB: Norway basin, WJMFZ, EJMFZ: West and East Jan Mayen Fracture Zones, JM: Jan Mayen, LB: Lofoten basin, VP: Vøring Plateau, VB: Vøring basin, MB: Møre basin, FI: Faroe Islands, SI: Shetland Islands, FSB: Faroe-Shetland basin, MT: Moine Thrust, GGF: Great Glen Fault, HBF: Highland Boundary Fault, SUF: Southern Upland Fault, MTFZ: Møre-Trøndelag Fault Zone, HB: Hatton basin, RT: Rockall Trough, PB: Porcupine basin. Red lines: boundaries of the Caledonian orogen and associated thrusts, blue lines: northern boundary of the Hercynian orogen, both dashed where extrapolated into the younger Atlantic Ocean.

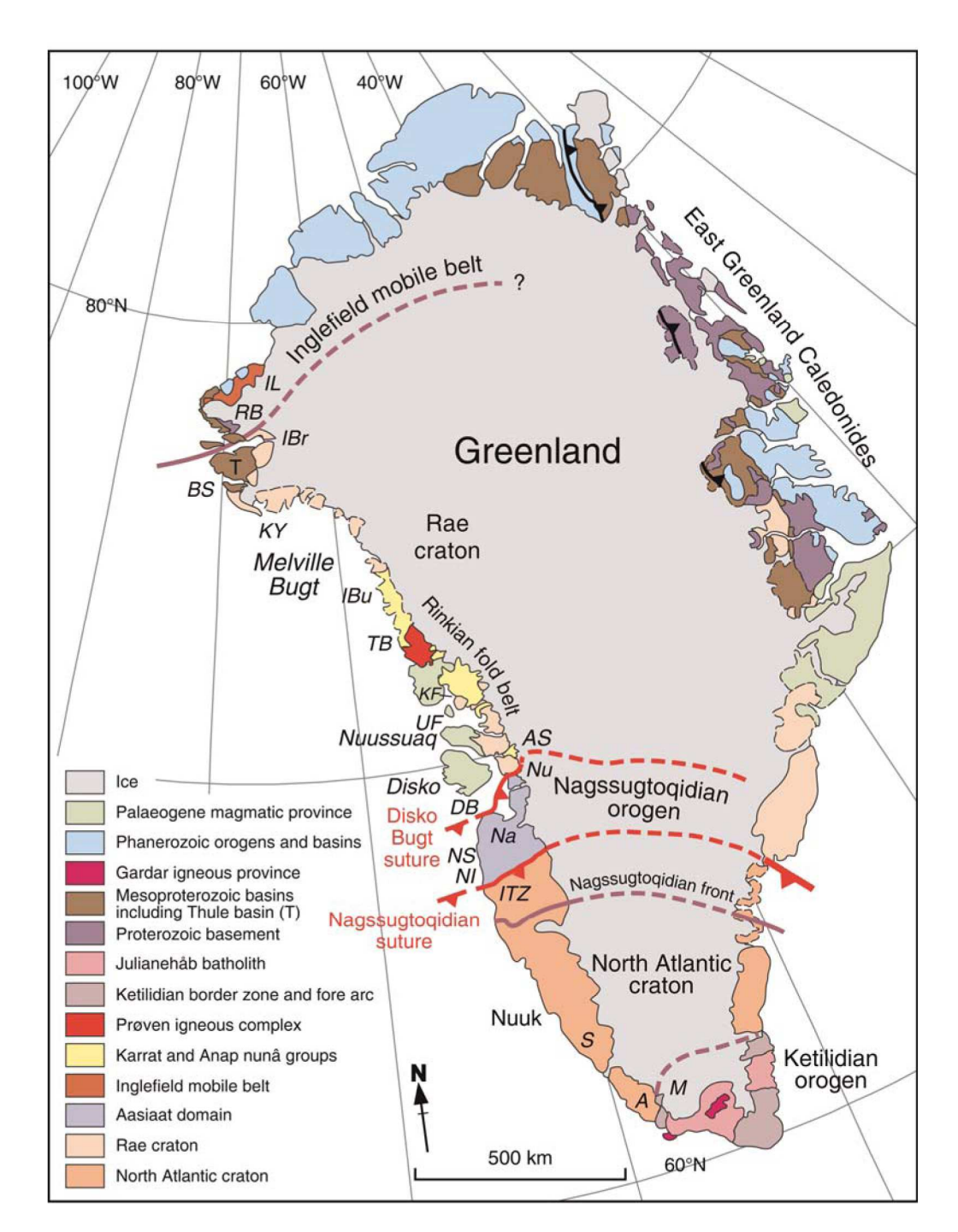


Figure 2: Schematic map of Greenland showing features referred to in the text. A: Arsuk, AS: Ataa Sund, BS: Bylot Sund, DB: Disko Bugt, IBr: Inglefield Bredning, IBu: Inussulik Bugt, IL: Inglefield Land, ITZ: Ikertoq thrust zone, KF: Karrat Fjord, KY: Kap York, M: Midternæs, Na: Naternaq, NI: Nordre Isortoq, NS: Nordre Strømfjord, Nu: Nunatarsuaq, RB: Rensselaer Bugt, S: Sermilik, T: Thule basin, TB: Tasiussaq Bugt, UF: Uummannaq Fjord [from St-Onge *et al.*, 2009].

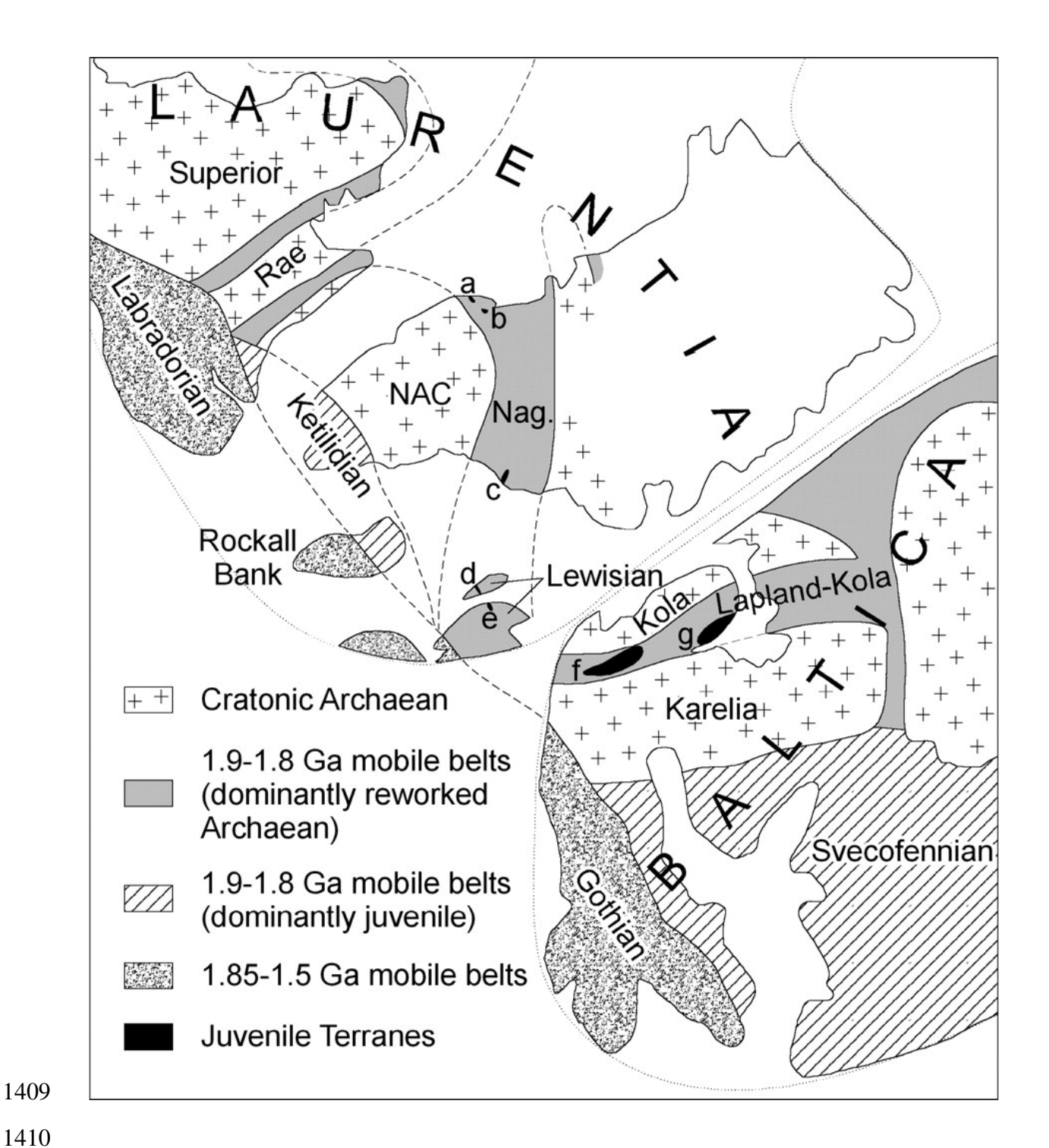


Figure 3: Reconstruction of the North Atlantic Realm at 1265 Ma. NAC: North Atlantic Craton, Nag: Nagssugtoqidian. Juvenile terranes: a: Sissimuit Charnockite, b: Arfersiorfic diorite, c: Ammassalik Intrusive Complex, d: South Harris Complex, e: Loch Maree Group, f: Lapland-Kola Granulite Belt, g: Tersk and Umba terranes [from Mason *et al.*, 2004].

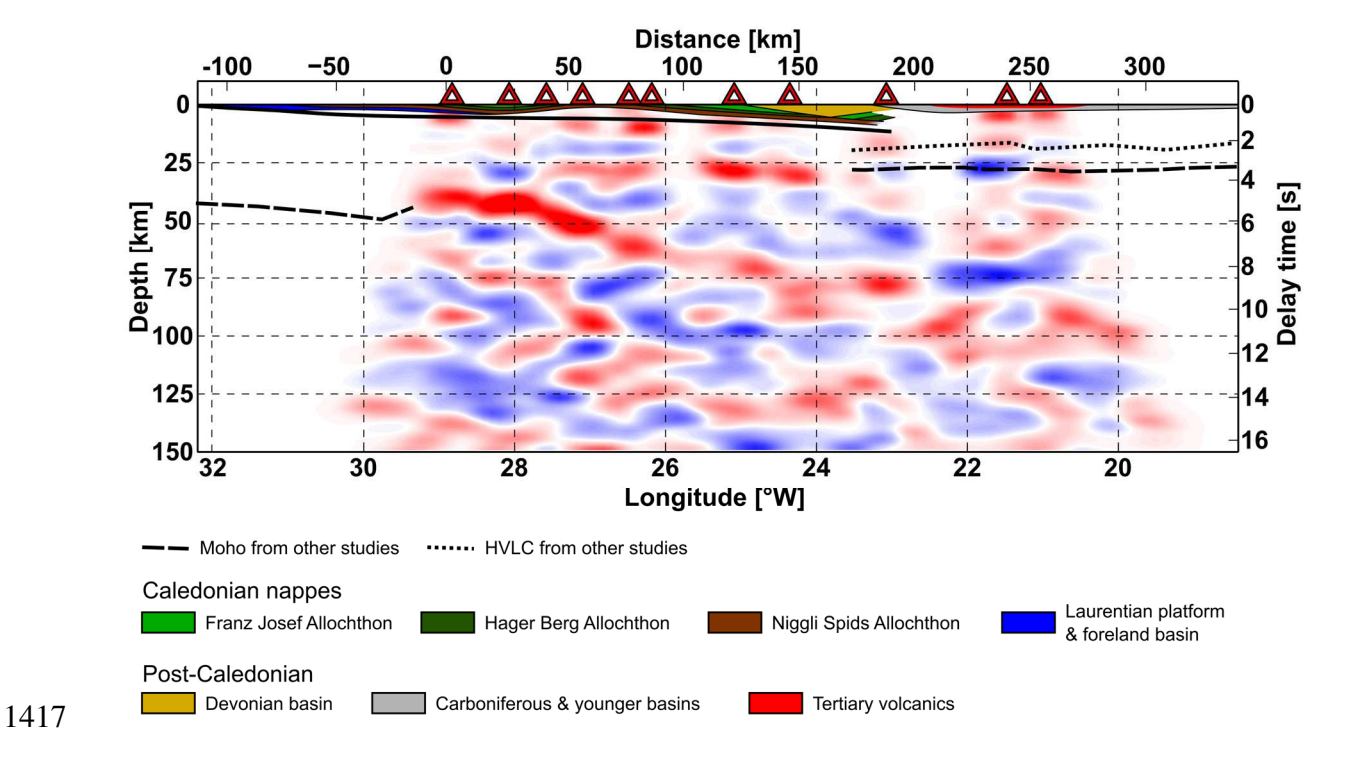


Figure 4: Receiver function image of the crust and upper mantle under central east Greenland from Schiffer *et al.* [2014] showing the Central Fjord structure. A geological cross-section based on Gee [2015] is overlain showing the Caledonian nappes and foreland basin, and the Devonian basin. Younger sedimentary basins are from Schlindwein & Jokat [2000]. Extrapolated Moho depths are from Schiffer *et al.* [2016].

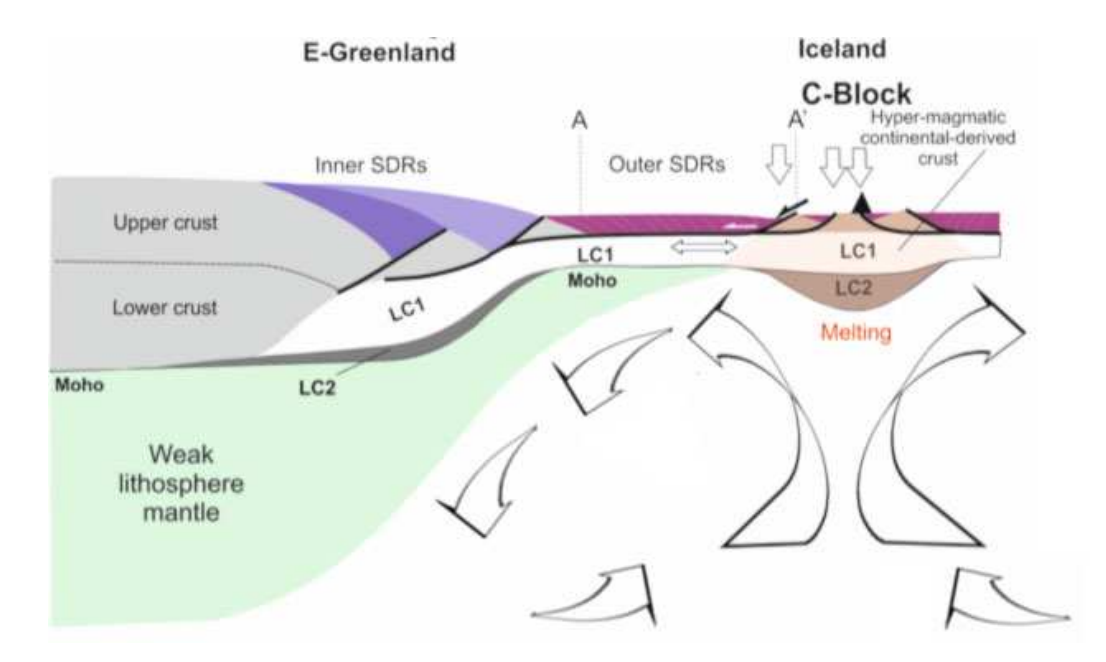


Figure 5: Schematic diagram illustrating the generalized structure of Inner- and Outer-SDRs

and a possible "C-Block" under Iceland. Outer-SDRs comprise thick subaerial eruptive layers underlain by hyper-extended middle crust and high- V_P mafic material of uncertain affinity but similar in structure to massively sill-intruded lower crust. Ductile flow and magma-assisted inflation can extend such crust to many times its original length. Material eroded from the underlying lithospheric mantle may be distributed in the direction of extension and incorporated in the underlying asthenosphere. LC1: sill-injected continent-derived ductile crust. LC2: highly reflective, undeformed layer, tectonically disconnected from LC1, and with much higher V_P (7.6-7.8 km/s) [adapted from Geoffroy et al., submitted].

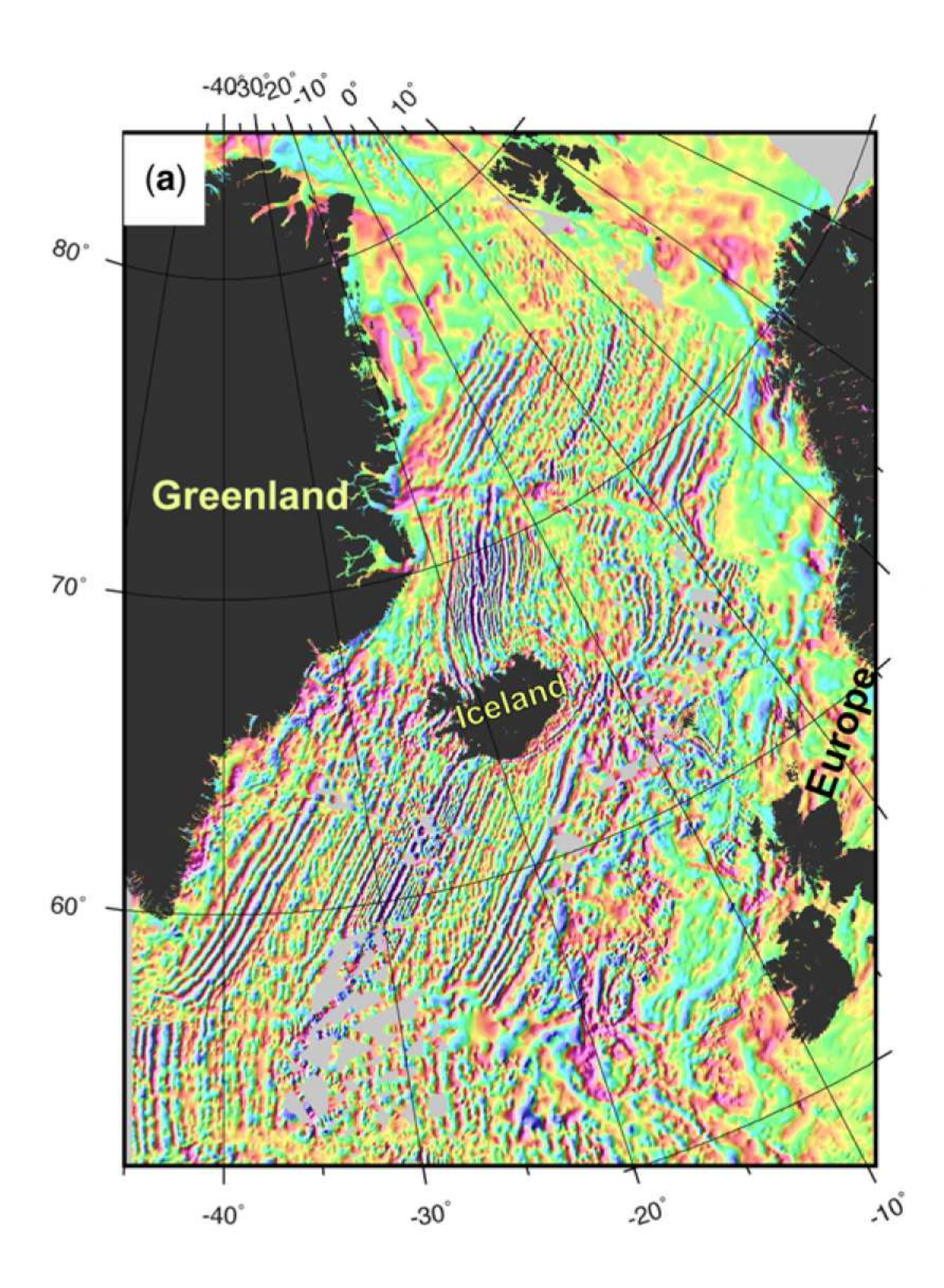


Figure 6: Magnetic anomalies in the North Atlantic Ocean [from Gaina et al., 2017].

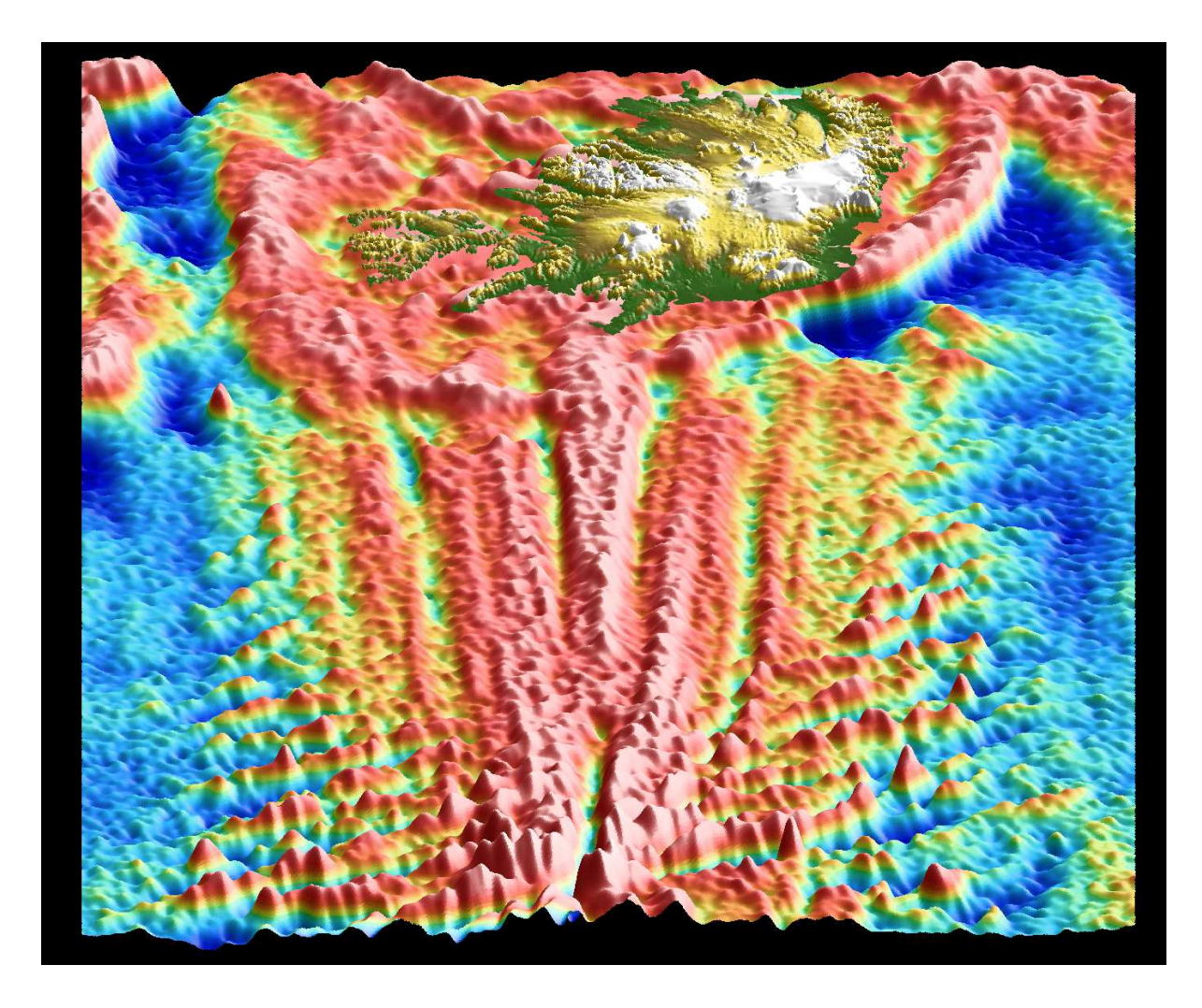


Figure 7: Perspective view along the Reykjanes Ridge looking towards Iceland showing the flanking chevron ridges converging with the spreading axis. Fracture-zone traces delineating former transform faults that have been eliminated can be seen as oblique cross-cutting structures in the lower part of the figure. Submarine areas show satellite-derived Free Air gravity anomalies from Sandwell *et al.* [2014] with the land topography of Iceland superimposed.

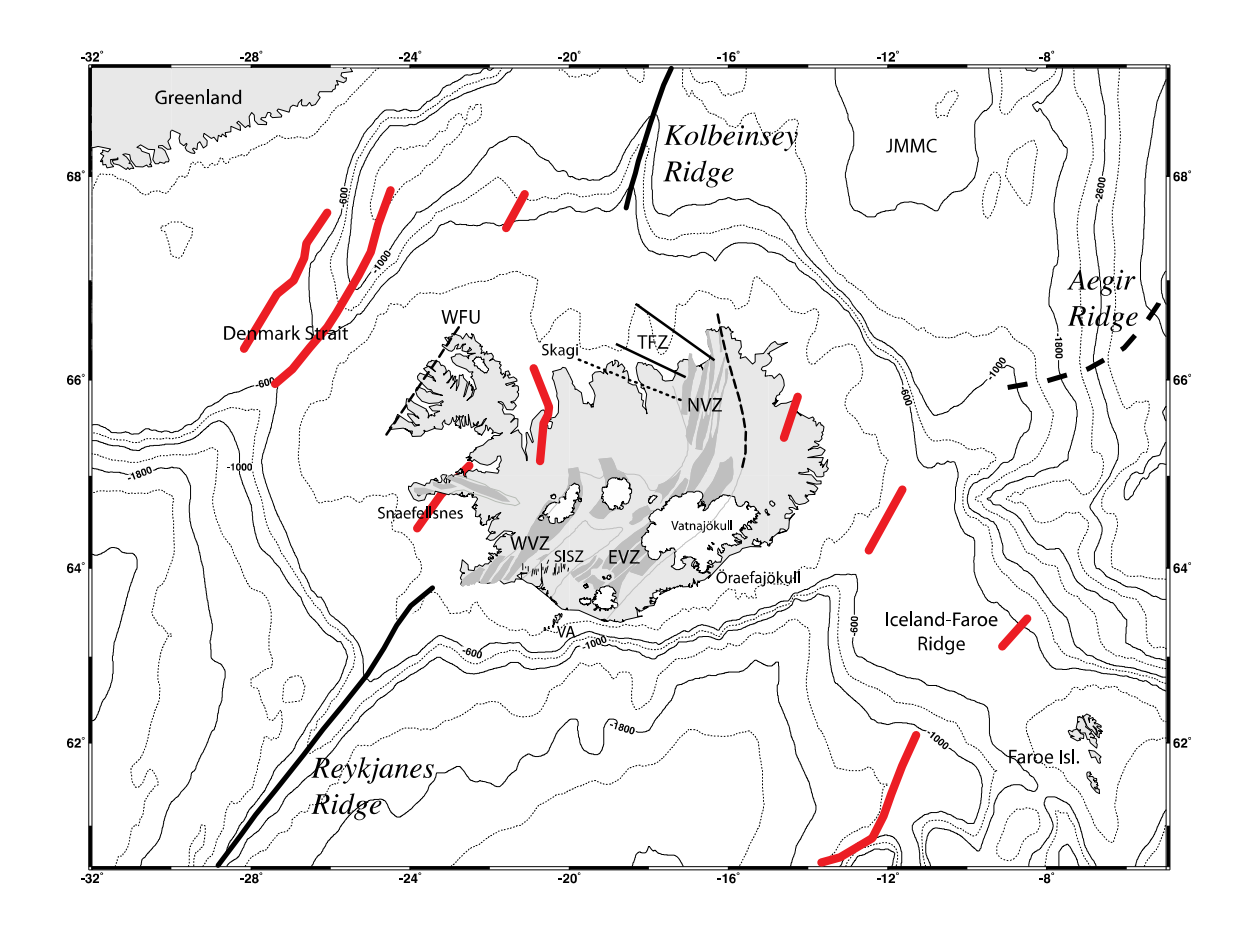


Figure 8: The Greenland-Iceland-Faroe Ridge and surrounding areas showing bathymetry and tectonic features. JMMC: Jan Mayen Microcontinent Complex. Thick black lines: axes of Reykjanes and Kolbeinsey Ridges, thin gray lines on land: outlines of neovolcanic zones, dark grey: currently active extensional volcanic systems, dashed black lines: extinct rifts on land, thin black lines: individual faults of the South Iceland Seismic Zone (SISZ), white: glaciers. WVZ, EVZ, NVZ: Western, Eastern, Northern Volcanic Zones, TFZ: Tjörnes Fracture Zone comprising two main shear zones and one (dotted) known only from earthquake epicenters (see also Figure 15). Thick red lines: extinct rift zones from Hjartarson *et al.* [2017].

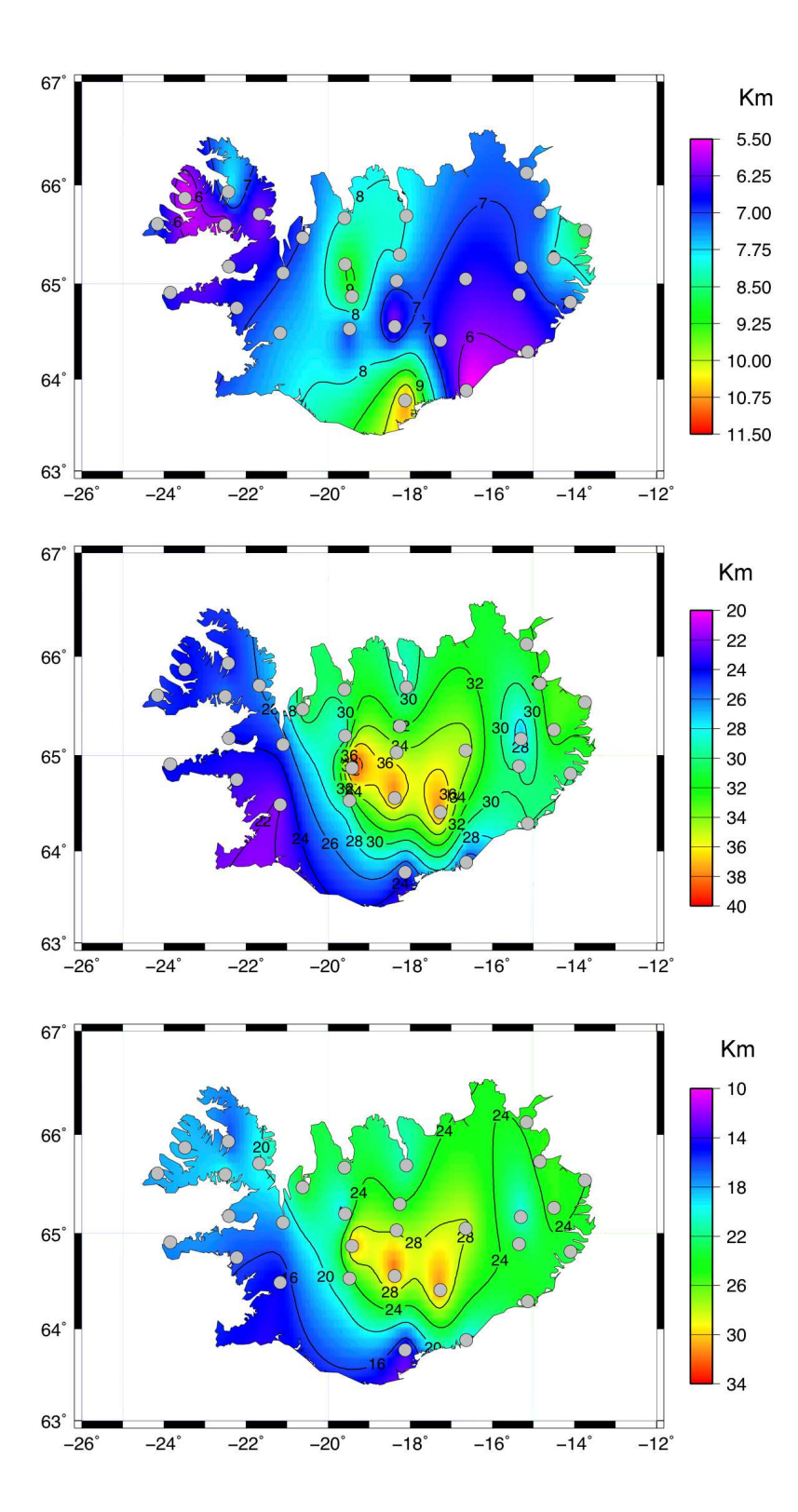


Figure 9: Compilation of results from receiver function analysis in Iceland. Top: Depth to the base of the upper crust, middle: depth to the base of the lower crust, bottom: thickness of the lower crust [data from Foulger *et al.*, 2003].

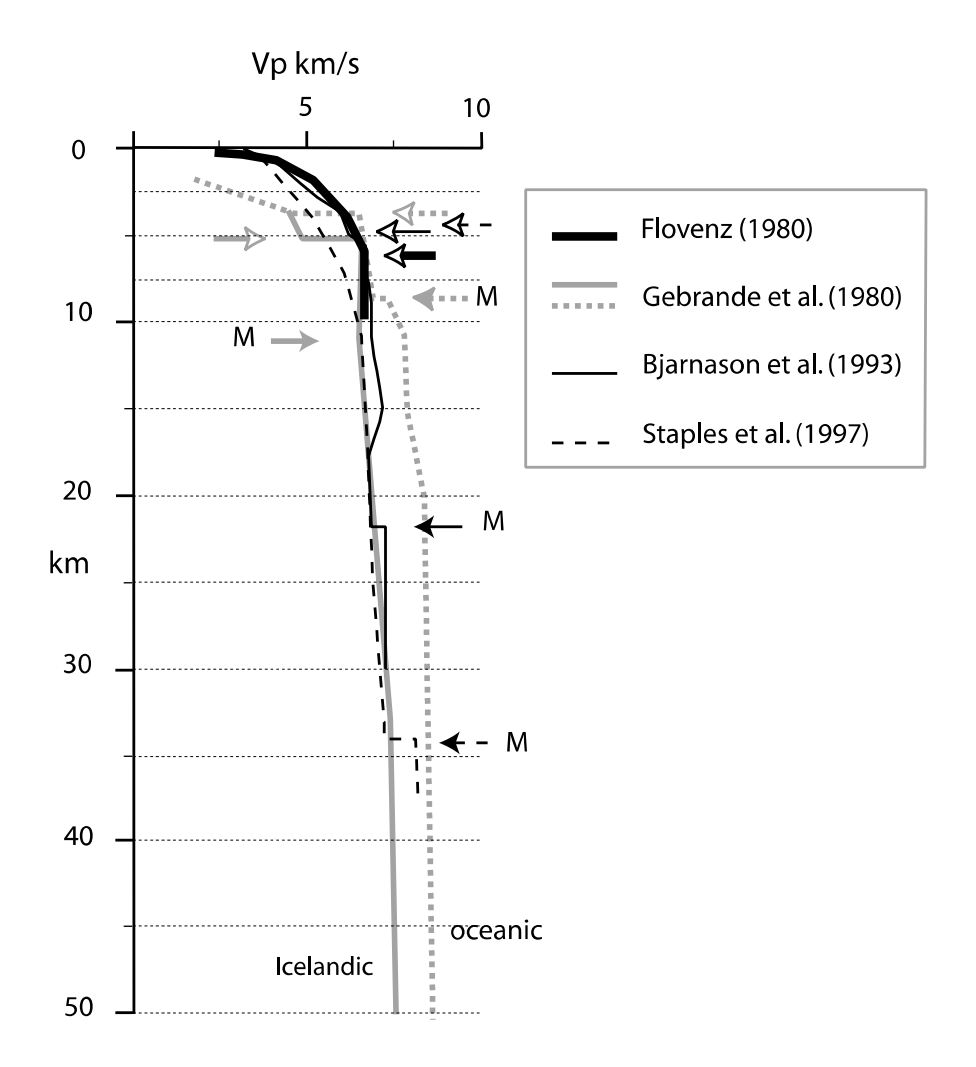


Figure 10: Velocity-depth profiles showing the average one-dimensional seismic structure of Icelandic-type crust from explosion profiles shot in Iceland and in 10-Ma oceanic crust south of Iceland [Gebrande *et al.*, 1980]. Open-headed arrows, estimates of the base of the upper crust from various studies; solid-headed arrows, estimates of the base of the lower crust; M, proposed Moho identifications [from Bjarnason *et al.*, 1993; Flovenz, 1980; Foulger *et al.*, 2003; Staples *et al.*, 1997].

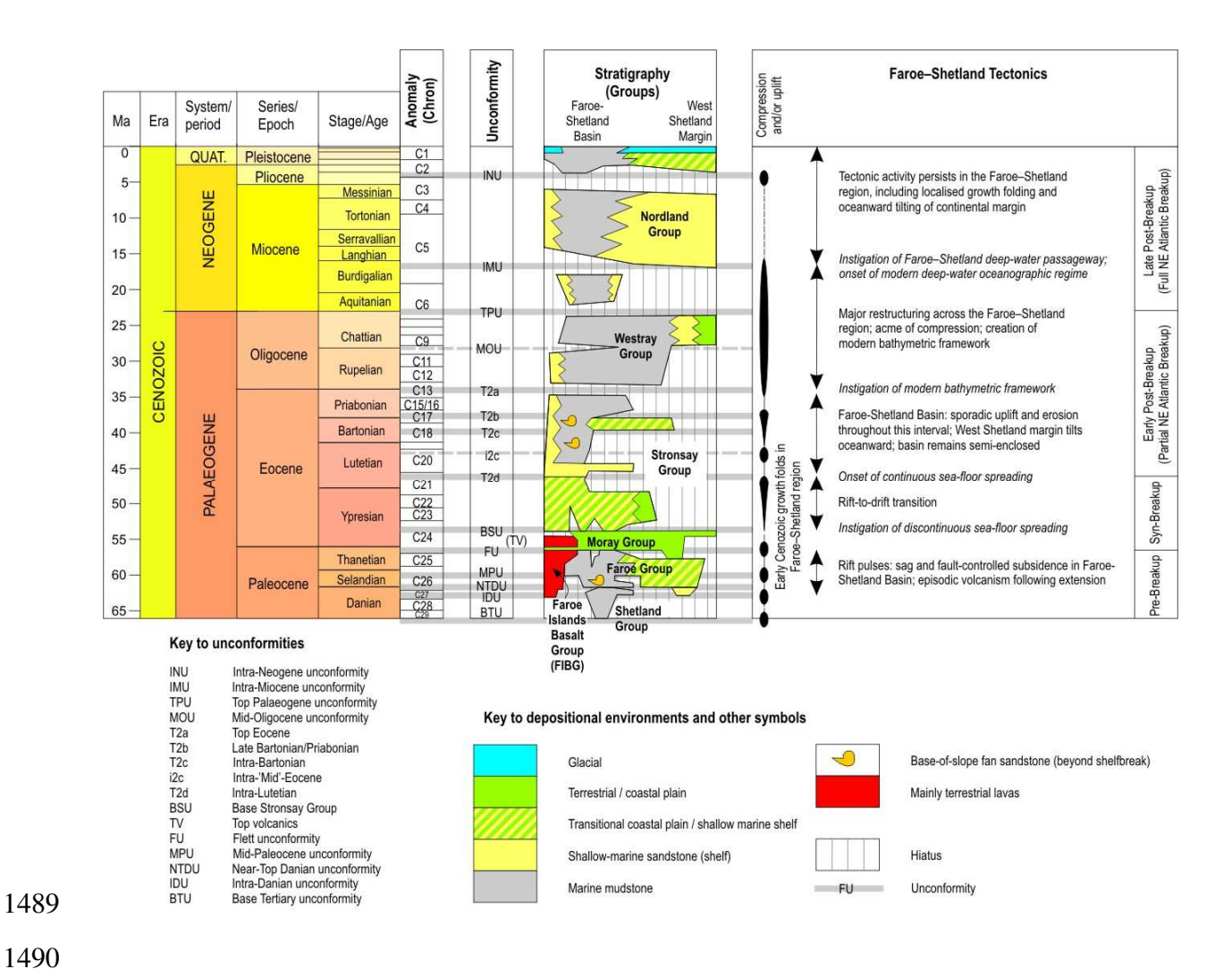


Figure 11: Cenozoic tectonostratigraphy for the Faroe-Shetland basin. The compilation of the stratigraphy and Faroe-Shetland tectonics is based mainly on Stoker *et al.* [2013; 2018; 2005b]. Additional information: 'Stratigraphy' and 'Unconformity' columns [Mudge, 2015], 'Faroe-Shetland Tectonics' column [Blischke *et al.*, 2017; Dean *et al.*, 1999; Ellis & Stoker, 2014; Johnson *et al.*, 2005; Ólavsdóttir *et al.*, 2013a; Stoker *et al.*, 2012; Stoker *et al.*, 2005a], timescale [Gradstein *et al.*, 2012].

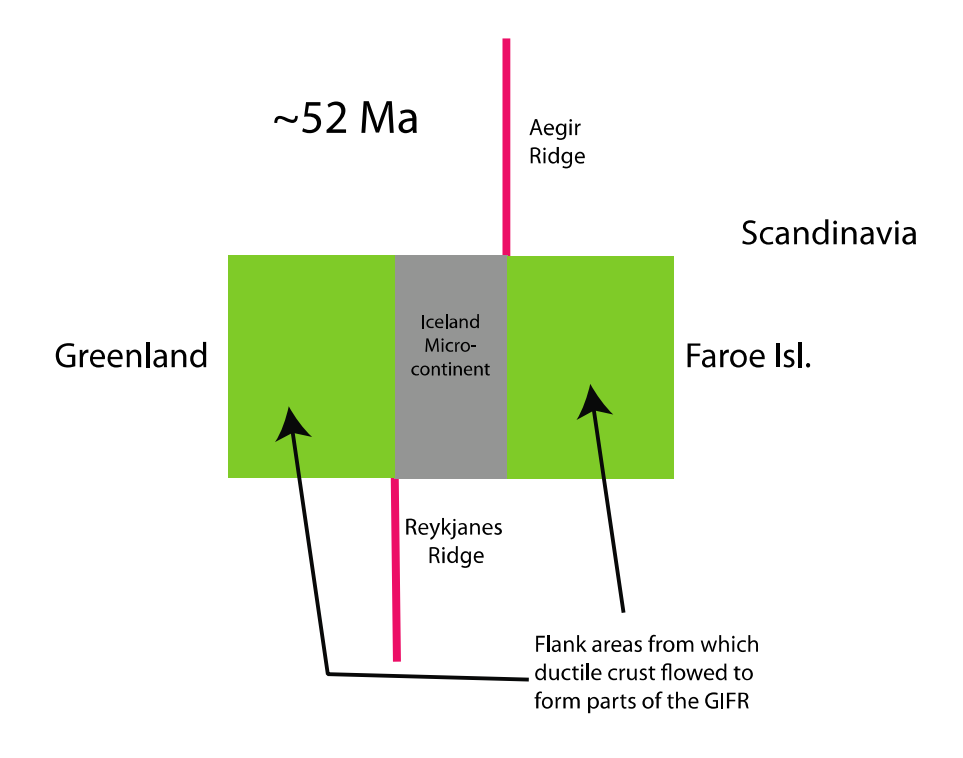


Figure 12: Schematic diagram illustrating the Iceland Microcontinent.

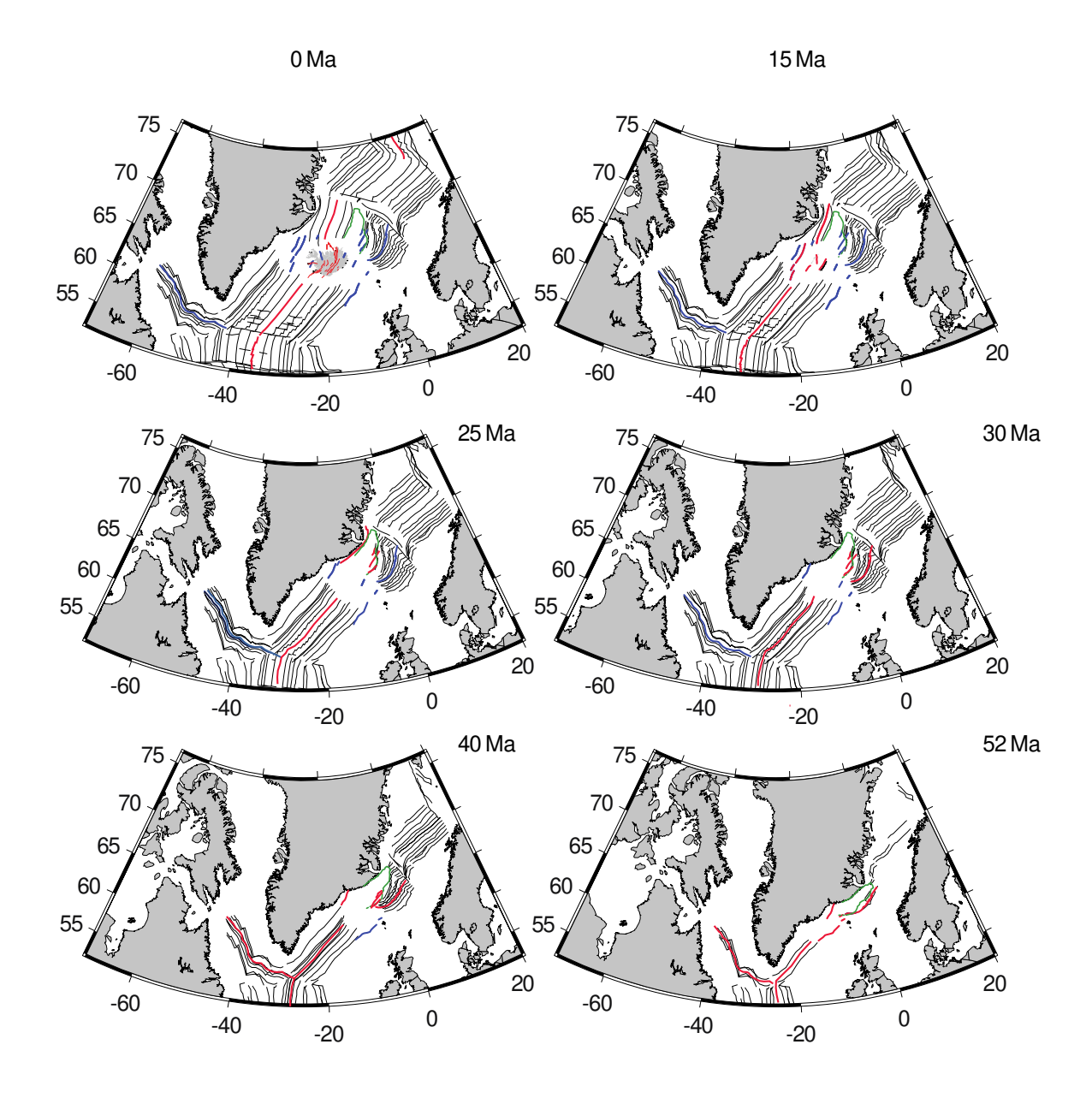


Figure 13: Locations of known extensional axes during opening of the NE Atlantic Ocean. Basemap and magnetic chrons (black lines) from GPlates using a Lambert Conformal Conic projection. Isochrons are from Müller *et al.* [2016]. Spreading ridges: Red—active, blue—extinct. Locations of some extinct offshore spreading axes are from Hjartarson *et al.* [2017] and Brandsdóttir *et al.* [2015]. Green: approximate boundary of Jan Mayen Microplate Complex. Areas where there is no direct evidence for rifts or spreading axes are left white.

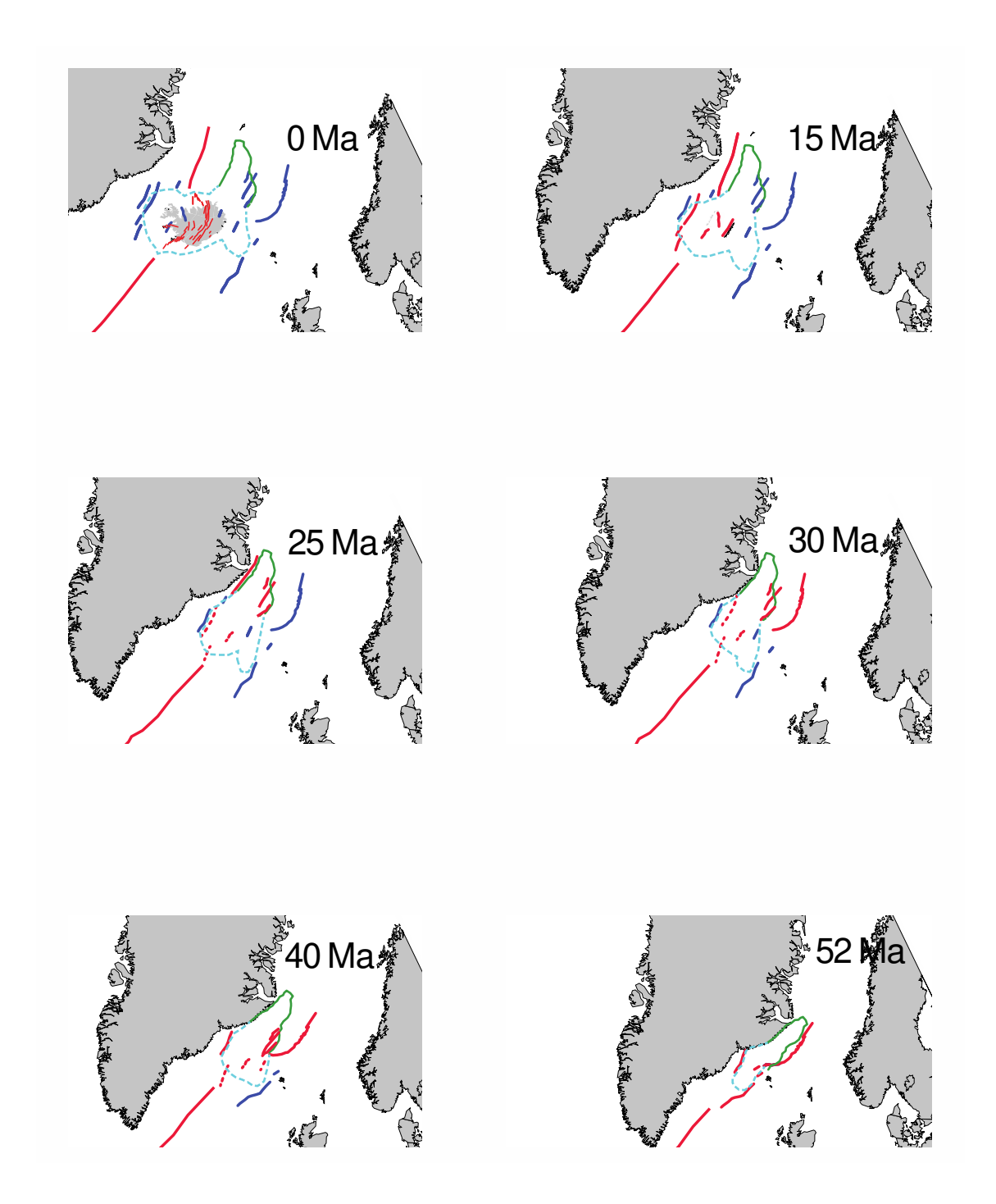


Figure 14: Speculative reconstruction of the sequence of extensional deformation on the GIFR and surroundings. Outline of land areas and locations of known extensional axes are from Figure 13 with the latter shown as solid lines. Red: active, blue: extinct. Dashed lines show speculative positions of ridges at times when observational data are lacking. Green solid line: approximate boundary of Jan Mayen Microplate Complex. Pale blue dashed line: approximate boundary of Iceland Microcontinent. This, and the Jan Mayen Microplate Complex expand with time as a result of magma inflation and ductile flow.

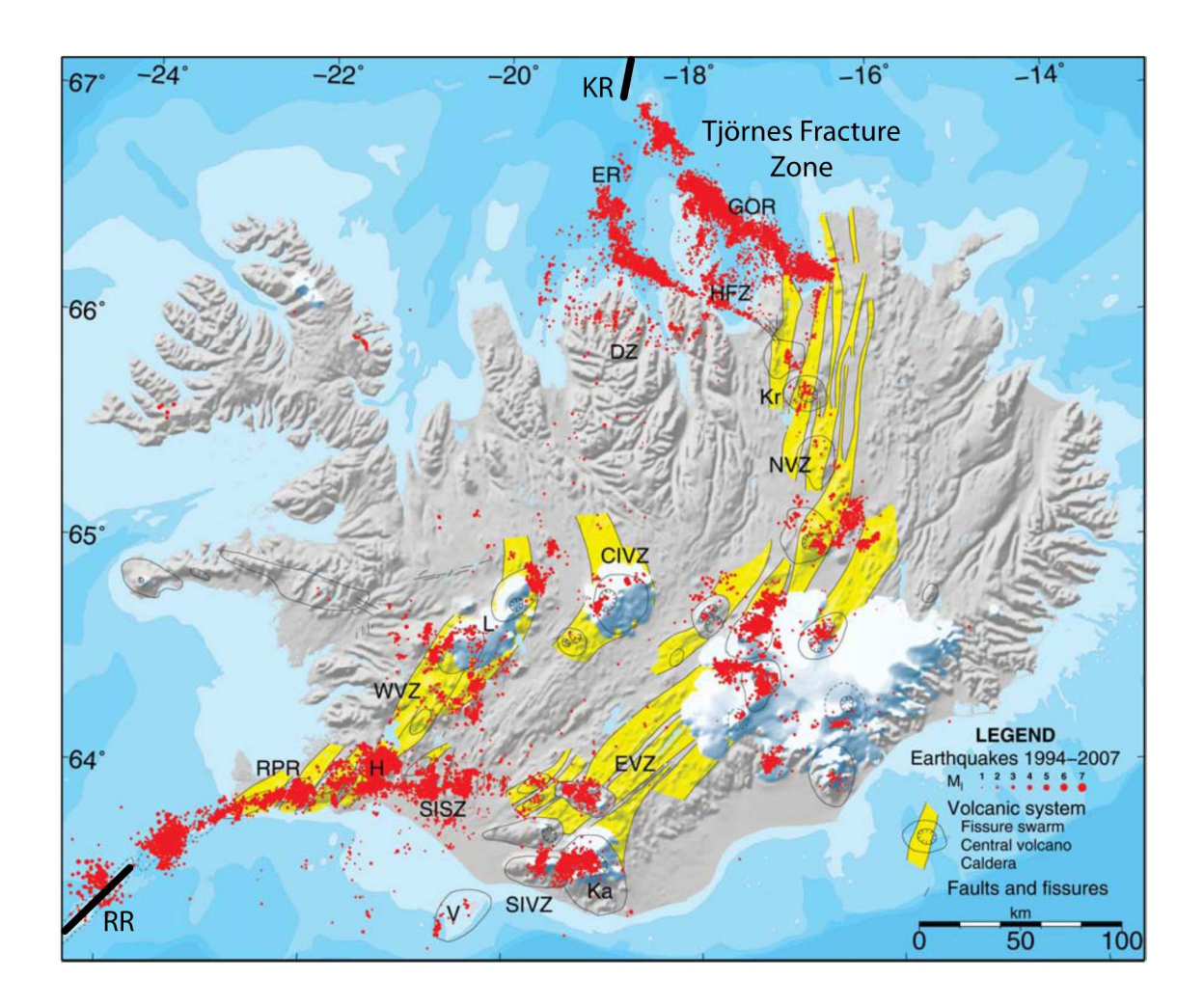
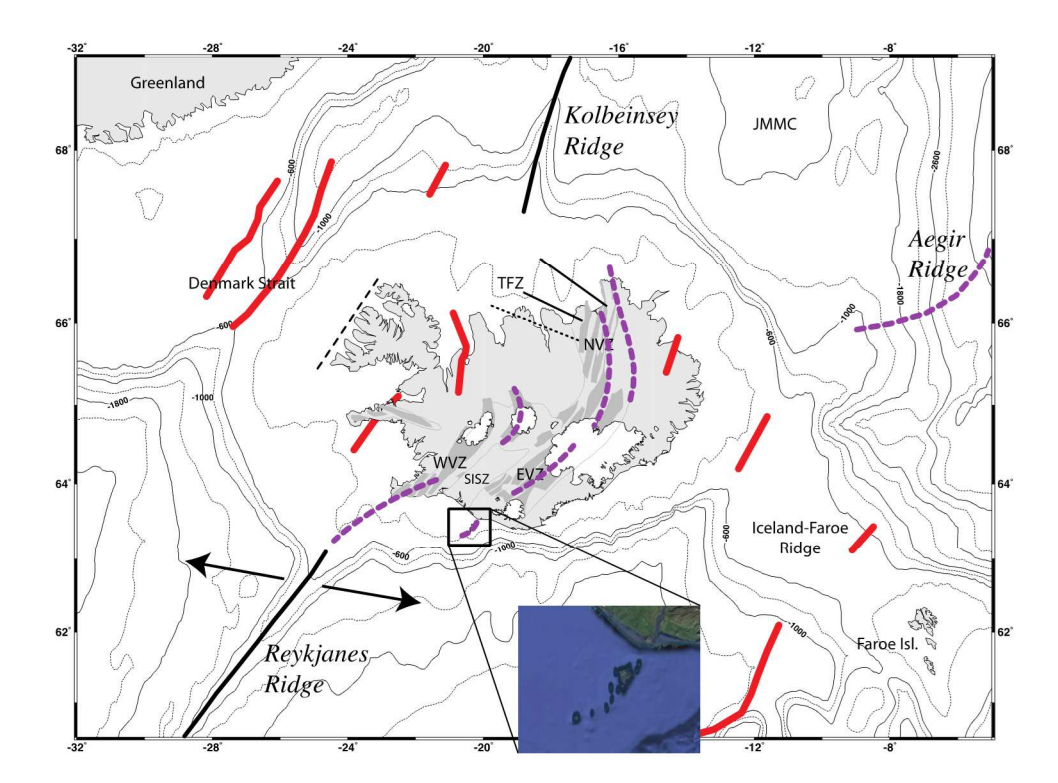


Figure 15: Map of Iceland from Einarsson [2008] showing earthquakes 1994-2007 from the database of the Icelandic Meteorological Office. Yellow: volcanic systems. The Tjörnes Fracture Zone comprises GOR: the Grímsey Oblique Rift, HFZ: the Húsavík-Flatey Zone, ER: the Eyjafjardaráll Rift, DZ: the Dalvík Zone. Other abbreviations are RR: Reykjanes Ridge, KR: Kolbeinsey Ridge, RPR: Reykjanes Peninsula Rift Zone (also known as the Reykjanes Peninsula extensional transform zone), WVZ: Western Volcanic Zone, SISZ: South Iceland Seismic Zone, EVZ: Eastern Volcanic Zone, CIVZ: Central Iceland Volcanic Zone, NVZ: Northern Volcanic Zone, SIVZ: South Iceland Volcanic Zone, Kr, Ka, H and L: the central volcanoes Krafla, Katla, Hengill and Langjökull, V: the Vestmannaeyjar archipelago.



1539

1540

Figure 16: Similar to Figure 8 but showing additionally lines of curved sections of plate boundary that resemble curving, approaching crack tips (dashed magenta lines). Inset: expanded view of Vestmannaeyjar archipelago. Bold arrows: current direction of regional plate motion. For other details and abbreviations see caption of Figure 8.

1545

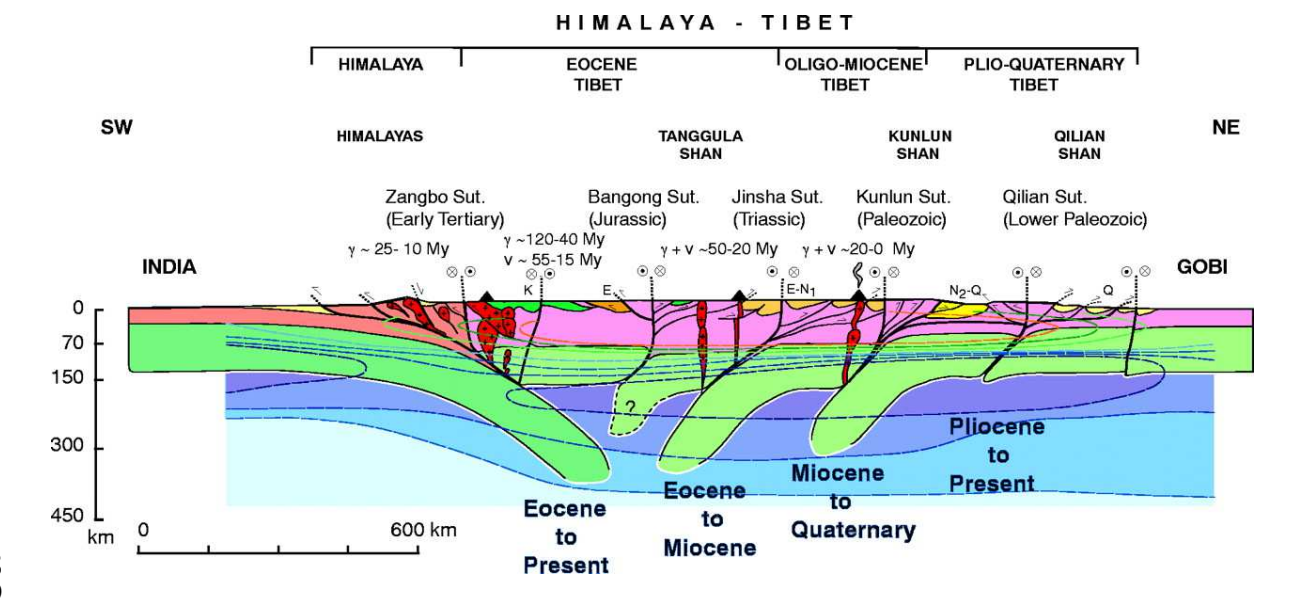


Figure 17: Schematic figure of the lithospheric structure of a well-studied, currently intact

trapped fossil slabs that thicken the crust locally. Deeper parts of the slabs are in the dense

intrusives, yellow and dark green: sedimentary basins. The orogen is underlain by an array of

orogen—the Himalaya-Tibet orogen. Green: lithospheric mantle, red and pink: crust or

eclogite facies and negatively buoyant [from Tapponnier et al., 2001].

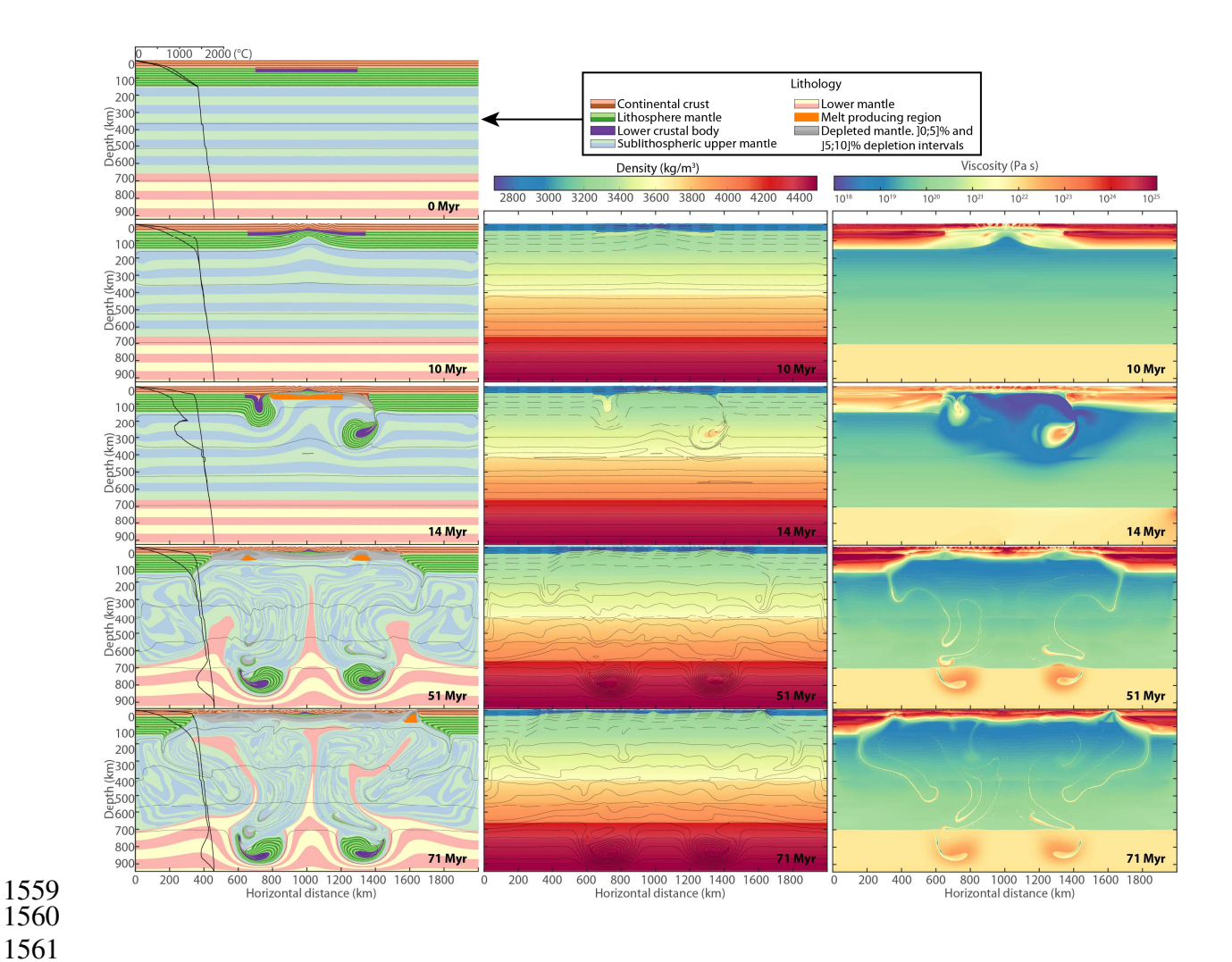


Figure 18: Simplified thermo-mechanical model of Cenozoic extension of the western frontal thrust of the Caledonian suture. Left panels: Lithology at selected times, thick black lines: minimum/maximum temperature profiles as a function of depth, thin black lines: isotherms from 1400 C with 100 C intervals. Upper left panel: initial model configuration. Central panels: density evolution, dashed black lines: isotherms from 0 C to 1400 C at 200 C intervals, full black lines: isotherms from 1450 C at 25 C intervals. Right panels: effective viscosity evolution.

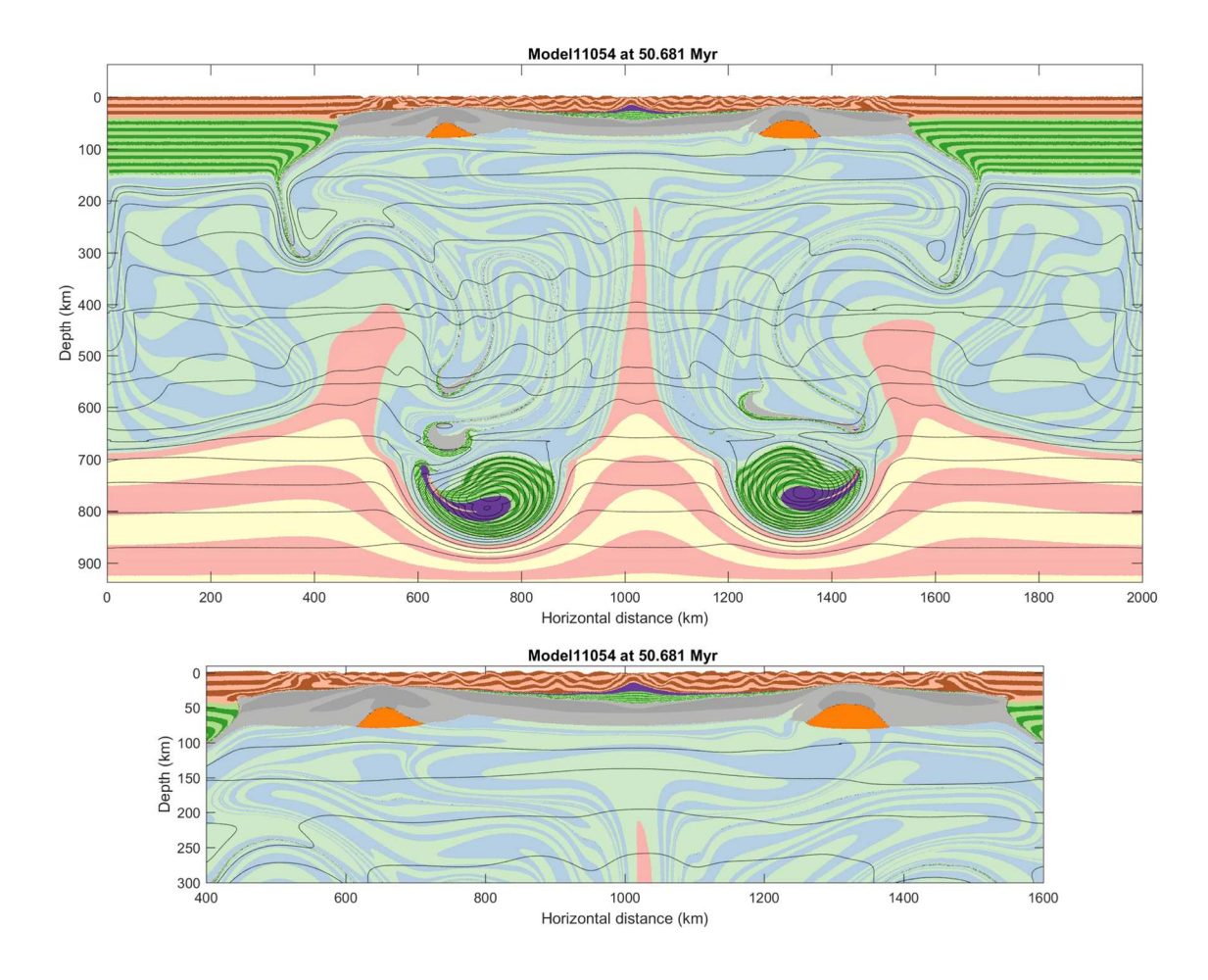


Figure 19: Expanded view of the lithology panel for 50.6 Myr, from Figure 18. See that Figure for details.

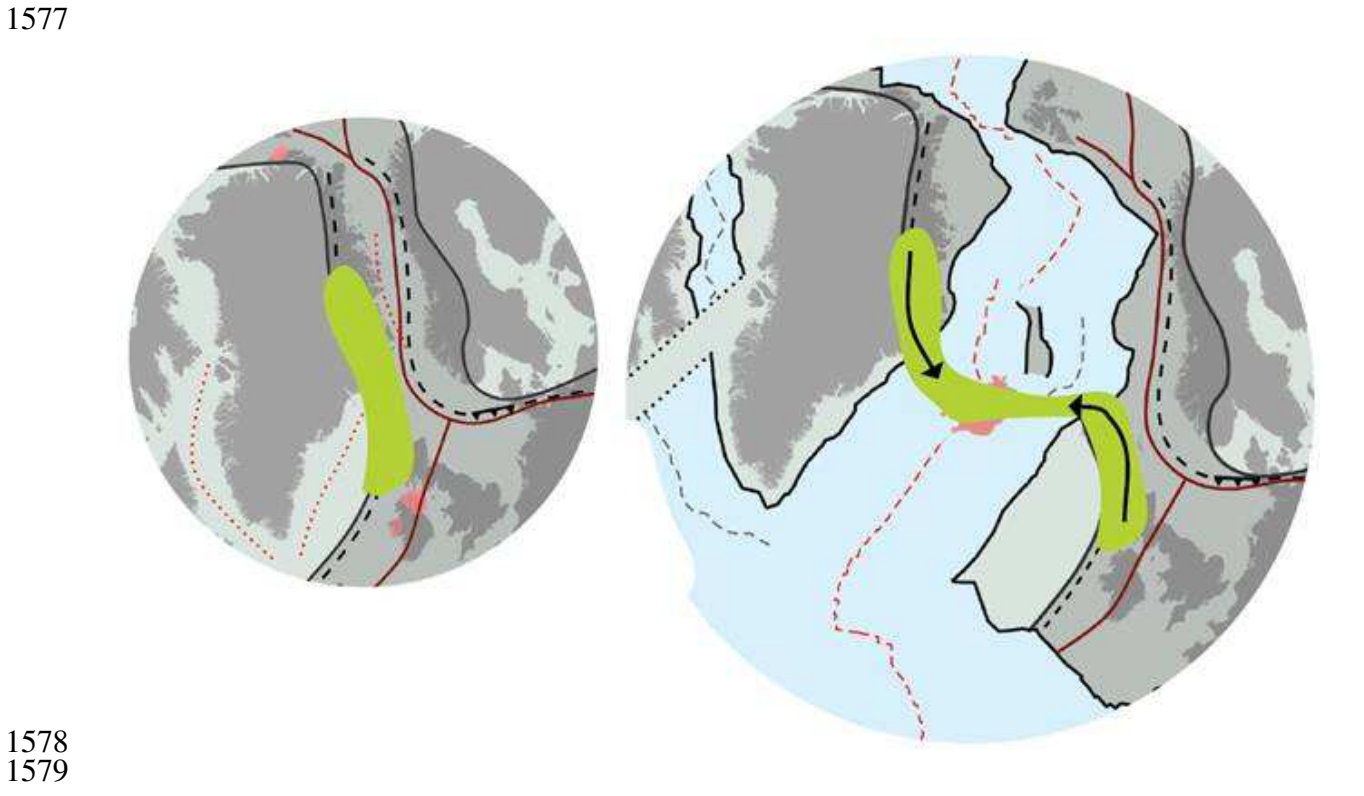


Figure 20: Map view sketch of our model. Green: the Caledonian frontal thrust zone where

1579

the crust is relatively thick prior to breakup, arrows: lateral inflow of weak lower crust into the extending, thinning zone. The persistence of continental crust beneath the GIFR maintains a warm, weak lithosphere and encourages distributed deformation and lateral rift jumps to persist.

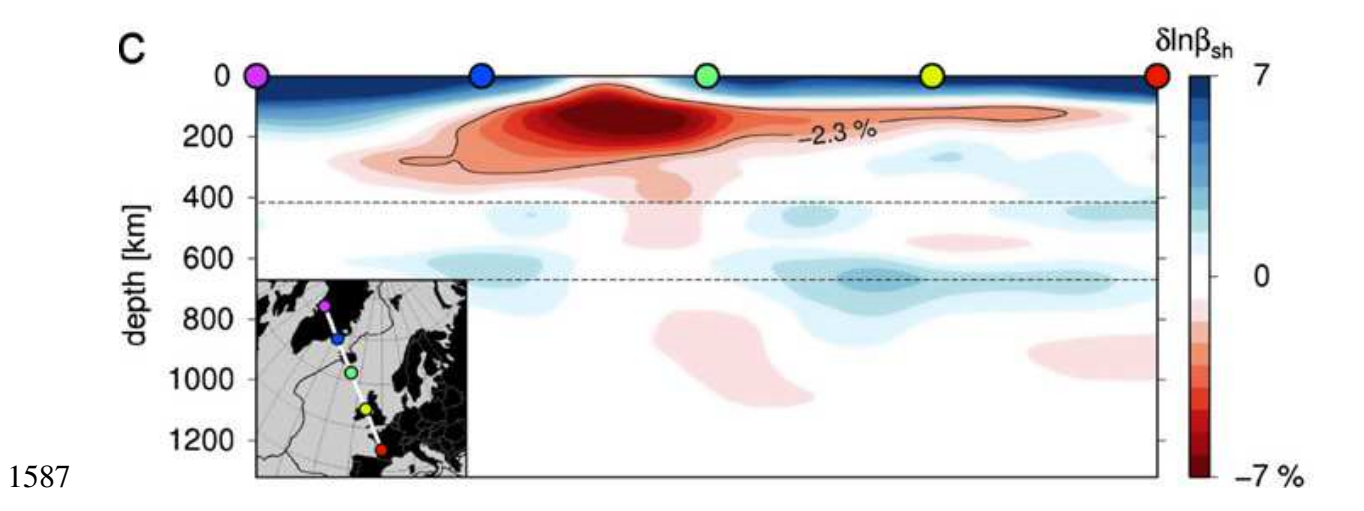


Figure 21: Cross section through the full-waveform inversion tomographic model of Rickers *et al.* [2013]. Colored dots are spaced at intervals of 1000 km. Compare with lower left panel of Figure 18.

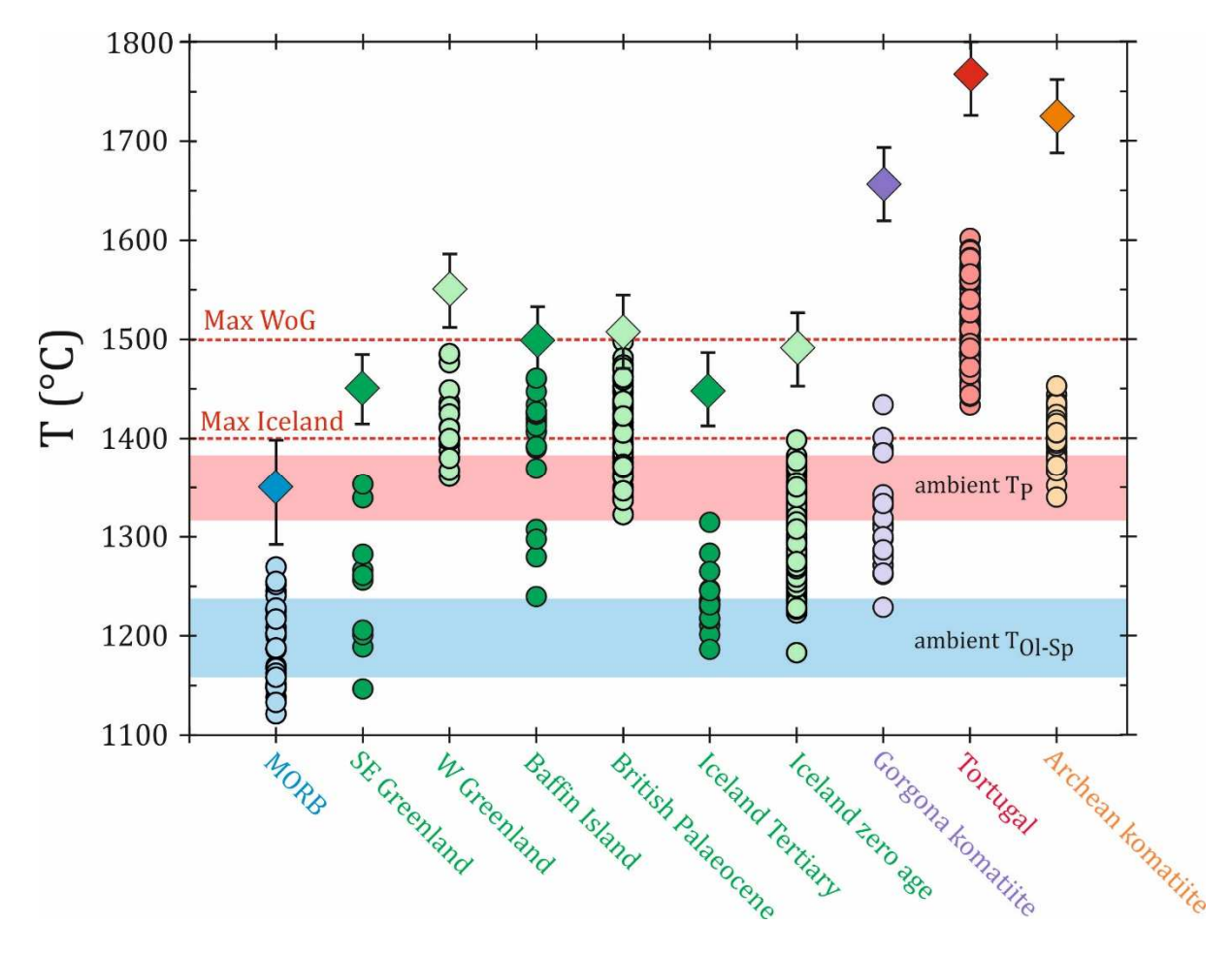


Figure 22: Summary of global maximum petrological estimates of T_P (diamonds \pm 40 C; Herzberg & Asimow [2015]) and olivine-spinel equilibrium crystallization temperatures (T_{Ol-SP}) for magnesian olivine (dots). The lower light-blue shaded region represents the range of T_{Ol} for olivine which crystallized from near-primary magmas formed at ambient $T_P \sim 1350 \pm 40$ C (upper pink-shaded region). The horizontal dashed lines represent the maximum estimated T_P for Iceland and West of Greenland (WoG; Disko Island, Baffin Island) from Hole and Natland [this volume]. Data sources for T_{Ol-SP} : MORB, Gorgona komatiite and Archean komatiite: Coogan *et al.* [2014], British Palaeocene, Baffin Island, West Greenland (Disko Island): Coogan *et al.* [2014], Spice *et al.* [2016], Iceland: Matthews *et al.* [2016], Spice *et al.* [2016], Tortugal: Trela *et al.* (2017). Petrological estimates from Herzberg and Asimow [2008; 2015], Hole [2015], Hole and Millett [2016] and Trela *et al.* [2017].

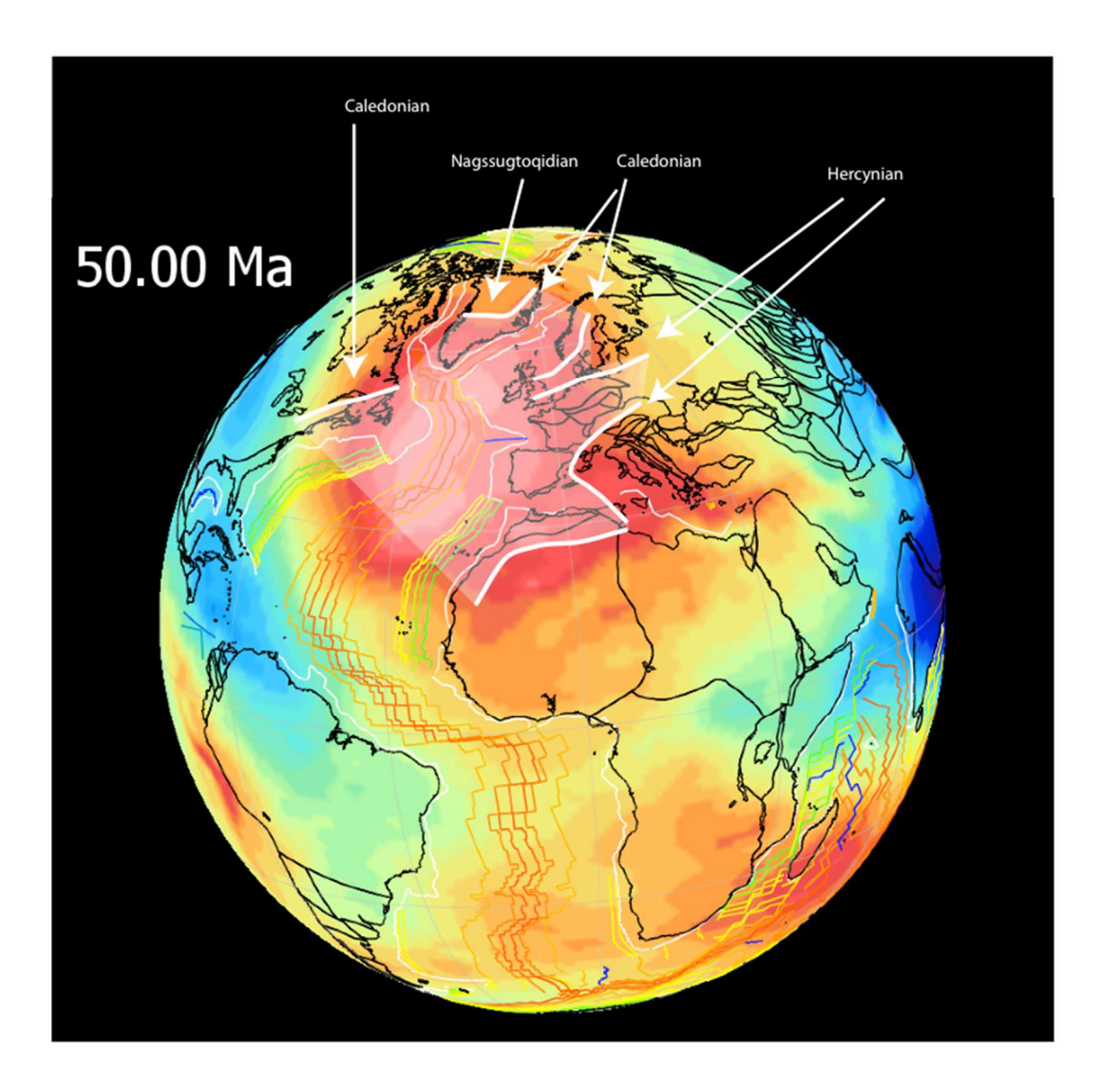


Figure 23: Continents reassembled to 50 Ma with the location of the future NE Atlantic centered over the present-day geoid high (red area). Thick white lines outline the Caledonian, Nagssugtoqidian, and Hercynian orogens. The area encompassed by these orogens is shaded and corresponds to the majority of the region of the geoid high.

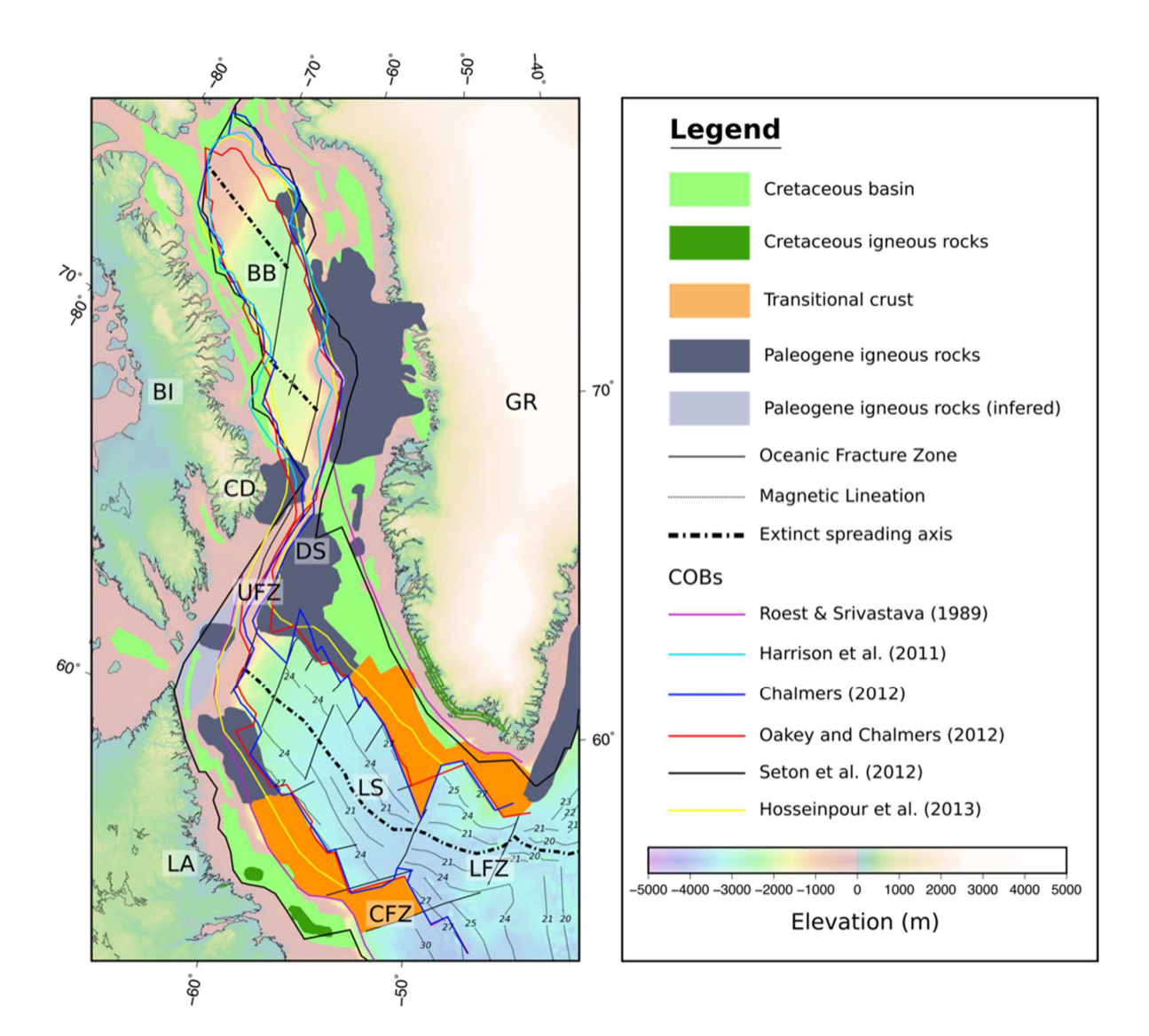


Figure 24: Structural map of the oceanic region west of Greenland showing Cretaceous basins and the extent of Paleogene volcanics, including inferred continuation as shown in Abdelmalak *et al.* [2018]. Different proposed continent-ocean boundaries are also shown. The magnetic lineations and fracture zones are reproduced from Chalmers [2012]. BB: Baffin Bay, BI: Baffin Island, CFZ: Cartwright Fracture Zone, DS: Davis Strait, GR: Greenland, LFZ: Leif Fracture Zone, LS: Labrador Sea, UFZ: Ungava Fault Zone, LA: Labrador. Elevation data are from Smith and Sandwell [1997].



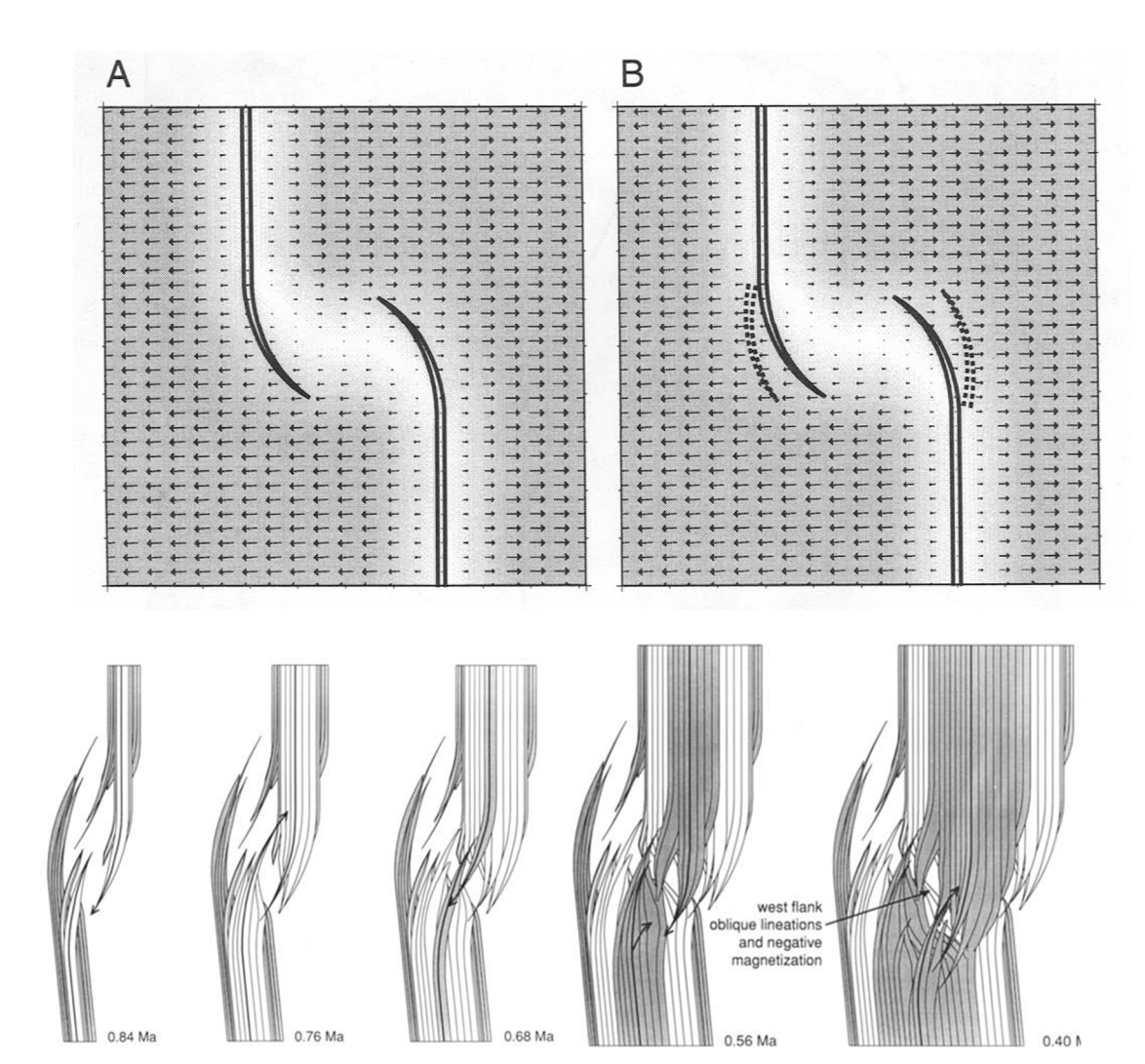


Figure 25: Schematic diagrams showing models of spreading ridge evolution observed on the East Pacific Rise. Top panels: ridges in the region 26 S - 32 S between the Easter and Juan Fernandez microplates. Parallel, solid lines: active ridges, parallel dashed lines: extinct ridges. The structure is modeled as a brittle layer overlying and weakly coupled with an underlying ductile layer. Deformation in this layer is shown by shading with gray indicating uniform motion and white indicating little or no motion. Arrows show displacement. Extension occurs in the overlap zone on curved, overlapping ridges that progressively migrate outward, are removed from the magma supply, become extinct, and are replaced by new ridges. Distributed bookshelf faulting occurs in the overlap zone [from Martínez *et al.*, 1997]. Bottom panels: Model for the evolution of the East Pacific Rise at 20 40'S showing a possible origin of rotated blocks. Shading indicates magnetization polarities. The ridge tips alternate between propagation and retreat, leading to the term "dueling propagators" [from Perram *et al.*, 1993].

1666

1667

1668

1652 References

- 1653 Á Horni, J., J. R. Hopper, and e. al. (2016), Regional distribution of volcanism within the
- North Atlantic Igneous Province, in The North-East Atlantic Region: A Reappraisal of
- 1655 Crustal Structure, Tectono-Stratigraphy and Magmatic Evolution, edited by G. Péron-
- Pinvidic, J. Hopper, M. S. Stoker, C. Gaina, H. Doornenbal, T. Funck and U. Árting, Geological Society, London, Special Publications.
- Abdelmalak, M. M., J. I. Faleide, S. Planke, L. Gernigon, D. Zastrozhnov, G. E. Shephard, and R. Myklebust (2017), The T-Reflection and the Deep Crustal Structure of the Vøring Margin, Offshore mid-Norway, Tectonics, 36, 2497-2523.
- Abdelmalak, M. M., S. Planke, S. Polteau, E. H. Hartz, J. I. Faleide, C. Tegner, D. A. Jerram, J. M. Millett, and R. Myklebust (2018), Breakup volcanism and plate tectonics in the NW Atlantic, Tectonophysics.
- Acton, G. D., S. Stein, and J. F. Engeln (1991), Block rotation and continental extension in Afar: A comparison to oceanic microplate systems, Tectonics, 10, 501-526.
 - Ady, B. E., and R. C. Whittaker (2018), Examining the influence of tectonic inheritance on the evolution of the North Atlantic using a palinspastic deformable plate reconstruction, Geological Society, London, Special Publications, 470, SP470.479.
- Amundsen, H. E. F., U. Schaltegger, B. Jamtveit, W. L. Griffin, Y. Y. Podladchikov, T.
 Torsvik, and K. Gronvold (2002), Reading the LIPs of Iceland and Mauritius,
 Proceedings of the 15th Kongsberg Seminar, Kongsberg, Norway.
- Andersen, M. S., T. Nielsen, A. B. Sørensen, L. O. Boldreel, and A. Kuijpers (2000), Cenozoic sediment distribution and tectonic movements in the Faroe region, Global and Planetary Change, 24, 239-259.
- Anderson, D. L. (2000a), The statistics of helium isotopes along the global spreading ridge system and the Central Limit Theorem, Geophys. Res. Lett., 27, 2401-2404.
- Anderson, D. L. (2000b), The statistics and distribution of helium in the mantle, Int. Geol. Rev., 42, 289-311.
- 1679 Anderson, D. L. (2001), A statistical test of the two reservoir model for helium, Earth planet. Sci. Lett., 193, 77-82.
- Anderson, D. L., G. R. Foulger, and A. Meibom (2006), Helium: Fundamental models, edited, G. R. Foulger, http://www.mantleplumes.org/.
- Angenheister, G., H. Gebrande, H. Miller, P. Goldflam, W. Weigel, W. R. Jacoby, G.
 Palmason, S. Bjornsson, P. Einarsson, N. I. Pavlenkova, S. M. Zverev, I. V. Litvinenko,
 B. Loncarevic, and S. C. Solomon (1980), Reykjanes ridge Iceland seismic experiment
 (RRISP 77), J. Geophys., 47, 228-238.
- Artemieva, I. M., and H. Thybo (2013), EUNAseis: A seismic model for Moho and crustal structure in Europe, Greenland, and the North Atlantic region, Tectonophysics, 609, 97-153.
- Atwater, T., and J. Severinghaus (1989), Tectonic maps of the northeast Pacific, *in* The
 Eastern Pacific Ocean and Hawaii, edited by E. L. Winterer, D. M. Hussong and R. W.
 Decker, pp. 15-20, Geological Society of America, Boulder, Colorado.
- Barnett-Moore, N., D. R. Müller, S. Williams, J. Skogseid, and M. Seton (2018), A reconstruction of the North Atlantic since the earliest Jurassic, Basin Research, 30, 160-185.
- Bauer, K., S. Neben, B. Schreckenberger, R. Emmermann, K. Hinz, N. Fechner, K. Gohl, A.
 Schulze, R. B. Trumbull, and K. Weber (2000), Deep structure of the Namibia

- 1698 continental margin as derived from integrated geophysical studies, J. Geophys. Res., 105, 25829–25853.
- Beblo, M., and A. Bjornsson (1978), Magnetotelluric investigation of the lower crust and upper mantle beneath Iceland, J. Geophys., 45, 1-16.
- Beblo, M., and A. Bjornsson (1980), Model of Electrical-Resistivity beneath Ne Iceland, Correlation with Temperature, Journal of Geophysics-Zeitschrift Fur Geophysik, 47, 184-190.
- Beblo, M., A. Bjornsson, K. Arnason, B. Stein, and P. Wolfgram (1983), Electrical conductivity beneath Iceland Constraints imposed by magnetotelluric results on temperature, partial melt, crust and mantle structure, J. Geophys., 53, 16-23.
- Benediktsdóttir, Á., R. Hey, F. Martinez, and Á. Höskuldsson (2012), Detailed tectonic evolution of the Reykjanes Ridge during the past 15 Ma, Geochem. Geophys. Geosys., 1710
- Benson, R. N. (2003), Age Estimates of the Seaward-Dipping Volcanic Wedge, Earliest
 Oceanic Crust, and Earliest Drift-Stage Sediments Along the North American Atlantic
 Continental Margin, *in* The Central Atlantic Magmatic Province: Insights from
 Fragments of Pangea, edited by W. Hames, J. Mchone, P. Renne and C. Ruppel, pp. 61–
 American Geophysical Union.
- Bergerat, F., and J. Angelier (2000), The South Iceland Seismic Zone: tectonic and sismotectonic analyses revealing the evolution from rifting to transform motion, J. Geodyn., 29, 211-231.
- Berzin, R., O. Oncken, J. H. Knapp, A. Pérez-Estaún, T. Hismatulin, N. Yunusov, and A.
 Lipilin (1996), Orogenic Evolution of the Ural Mountains: Results from an Integrated
 Seismic Experiment, Science, 274, 220.
- Bingen, B., and G. Viola (2018), The early-Sveconorwegian orogeny in southern Norway:
 Tectonic model involving delamination of the sub-continental lithospheric mantle,
 Precamb. Res., 313, 170-204.
- Bjarnason, I. T., W. Menke, O. G. Flovenz, and D. Caress (1993), Tomographic image of the mid-Atlantic plate boundary in south-western Iceland, J. Geophys. Res., 98, 6607-6622.
- Bjornsson, A., G. Johnsen, S. Sigurdsson, G. Thorbergsson, and E. Tryggvason (1979),
 Rifting of the Plate Boundary in North Iceland 1975-1978, J. Geophys. Res., 84, 30293038.
- Björnsson, A., H. Eysteinsson, and M. Beblo (2005), Crustal formation and magma genesis beneath Iceland: magnetotelluric constraints, *in* Plates, Plumes, and Paradigms, edited by G. R. Foulger, J.H. Natland, D.C. Presnall and D.L. Anderson, pp. 665-686, Geological Society of America.
- Blischke, A., C. Gaina, J. R. Hopper, G. Peron-Pinvidic, B. Brandsdottir, P. Guarnieri, O. Erlendsson, and K. Gunnarsson (2017), The Jan Mayen microcontinent: an update of its architecture, structural development and role during the transition from the Ægir Ridge to the mid-oceanic Kolbeinsey Ridge, *in* The NE Atlantic Region: A Reappraisal of Crustal Structure, Tectonostratigraphy and Magmatic Evolution, edited by G. Peron-Pinvidic, J. R. Hopper, M. S. Stoker, C. Gaina, J. C. Doornenbal, T. Funck and U. E. Arting, pp. 299-337, Geological Society, London, Special Publications.
- Bohnhoff, M., and J. Makris (2004), Crustal structure of the southeastern Iceland-Faeroe Ridge (IFR) from wide aperture seismic data, J. Geodyn., 37, 233-252.
- Bonatti, E. (1985), Punctiform initiation of seafloor spreading in the Red Sea during transition from a continental to an oceanic rift, Nature, 316, 33.

- Bott, M. H. P. (1974), Deep structure, evolution and origin of the Icelandic transverse ridge,
- *in* Geodynamics of Iceland and the North Atlantic Area, edited by L. Kristjansson, pp.
- 1747 33-48, D. Reidel Publishing Company, Dordrecht.
- Bott, M. H. P. (1985), Plate tectonic evolution of the Icelandic transverse ridge and adjacent regions, JGR, 90, 9953-9960.
- Bott, M. H. P., J. Sunderland, P. J. Smith, U. Casten, and S. Saxov (1974), Evidence for continental crust beneath the Faeroe Islands, Nature, 248, 202.
- Bourgeois, O., O. Dauteuil, and E. Hallot (2005), Rifting above a mantle plume: structure and development of the Iceland Plateau, Geodinamica Acta, 18, 59-80.
- Brandsdóttir, B., E. E. E. Hooft, R. Mjelde, and Y. Murai (2015), Origin and evolution of the Kolbeinsey Ridge and Iceland Plateau, N-Atlantic, Geochem. Geophys. Geosys., 16, 612–634.
- Breddam, K. (2002), Kistufell: Primitive melt from the Iceland mantle plume, J. Pet., 43, 345-373.
- Breivik, A. J., R. Mjelde, J. I. Faleide, and Y. Murai (2006), Rates of continental breakup magmatism and seafloor spreading in the Norway Basin–Iceland plume interaction, Journal of Geophysical Research: Solid Earth, 111.
- Breivik, A. J., R. Mjelde, J. I. Faleide, and Y. Murai (2012), The eastern Jan Mayen microcontinent volcanic margin, Geophys. J. Int., 188, 798-818.
- Bronner, A., D. Sauter, G. Manatschal, G. Péron-Pinvidic, and M. Munschy (2011),
 Magmatic breakup as an explanation for magnetic anomalies at magma-poor rifted
 margins, Nature Geoscience, 4, 549.
- Brooks, C. K. (2011), The East Greenland rifted volcanic margin, Geological Survey of Denmark and Greenland Bulletin, 24, 1-96.
- Brune, S., C. Heine, M. Pérez-Gussinyé, and S. V. Sobolev (2014), Rift migration explains continental margin asymmetry and crustal hyper-extension, Nature Communications, 5.
- Buck, R. W. (1986), Small-scale convection induced by passive rifting: the cause for uplift of rift shoulders, Earth planet. Sci. Lett., 77, 362–372.
- Buck, W. R. (1991), Modes of continental lithospheric extension, Journal of Geophysical Research: Solid Earth, 96, 20161-20178.
- Buiter, S. J. H., and T. H. Torsvik (2014), A review of Wilson Cycle plate margins: A role for mantle plumes in continental break-up along sutures?, Gondwana Research, 26, 627-653.
- 1778 Carminati, E., and C. Doglioni (2010), North Atlantic geoid high, volcanism and glaciations, Geophys. Res. Lett., 37.
- 1780 Chalmers, J. A. (2012), Labrador Sea, Davis Strait, and Baffin Bay, *in* Regional Geology and 1781 Tectonics: Phanerozoic Passive Margins, Cratonic Basins and Global Tectonic Maps, 1782 edited by D. G. Roberts and A. W. Bally, pp. 384-435, Elsevier, Boston.
- 1783 Chalmers, J. A., and K. H. Laursen (1995), Labrador Sea: The extent of continental and oceanic crust and the timing of the onset of seafloor spreading, Marine and Petroleum Geology, 12, 205–217.
- 1786 Chalmers, J. A., and T. C. R. Pulvertaft (2001), Development of the continental margins of 1787 the Labrador Sea: a review, Geological Society, London, Special Publications, 187, 77.
- 1788 Chauvel, C., and C. Hemond (2000), Melting of a complete section of recycled oceanic crust:
 1789 Trace element and Pb isotopic evidence from Iceland, Geochem. Geophys. Geosys., 1,
 1790 1999GC000002.
- 1791 Chauvet, F., L. Geoffroy, H. Guillou, R. Maury, B. Le Gall, A. Agranier, and A. Viana (2019), Eocene continental breakup in Baffin Bay 757.

- 1793 Cheng, H., H. Zhou, Q. Yang, L. Zhang, F. Ji, and H. Dick (2016), Jurassic zircons from the Southwest Indian Ridge, Scientific Reports, 6, 26260.
- 1795 Chenin, P., G. Manatschal, L. L. Lavier, and D. Erratt (2015), Assessing the impact of 1796 orogenic inheritance on the architecture, timing and magmatic budget of the North 1797 Atlantic rift system: a mapping approach, Journal of the Geological Society, 172, 711.
- 1798 Christensen, N. I. (2004), Serpentinites, Peridotites, and Seismology, Int. Geol. Rev., 46, 795-816.
- 1800 Čí ková, H., A. P. van den Berg, W. Spakman, and C. Matyska (2012), The viscosity of
 1801 Earth's lower mantle inferred from sinking speed of subducted lithosphere, Phys. Earth
 1802 Planet. Int., 200-201, 56-62.
- Clarke, D. B., and E. K. Beutel (2019), Davis Strait Paleocene Picrites: Products of a Plume or Plates?, Earth-Science Reviews, this volume.
- Clerc, C., L. Jolivet, and J.-C. Ringenbach (2015), Ductile extensional shear zones in the lower crust of a passive margin, Earth planet. Sci. Lett., 431, 1-7.
- Connelly, J. N., K. Thrane, A. W. Krawiec, and A. A. Garde (2006), Linking the
 Palaeoproterozoic Nagssugtoqidian and Rinkian orogens through the Disko Bugt region
 of West Greenland, Journal of the Geological Society, 163, 319.
- 1810 Connolly, J. A. D. (2005), Computation of phase equilibria by linear programming: A tool for geodynamic modeling and its application to subduction zone decarbonation, Earth planet. Sci. Lett., 236, 524-541.
- 1813 Coogan, L. A., A. D. Saunders, and R. N. Wilson (2014), Aluminum-in-olivine thermometry 1814 of primitive basalts: Evidence of an anomalously hot mantle source for large igneous 1815 provinces, Chem. Geol., 368, 1-10.
- Craig, H., and J. E. Lupton (1976), Primordial neon, helium, and hydrogen in oceanic basalts, Earth planet. Sci. Lett., 31, 369-385.
- Dalhoff, F., L. M. Larsen, J. R. Ineson, S. Stouge, J. A. Bojesen-Koefoed, S. Lassen, A. Kuijpers, J. A. Rasmussen, and H. Nøhr-Hansen (2006), Continental crust in the Davis Strait: new evidence from seabed sampling, Geological Survey of Denmark and Greenland Bulletin, 10, 33–36.
- Dannowski, A., I. Grevemeyer, J. Phipps Morgan, C. R. Ranero, M. Maia, and G. Klein (2011), Crustal structure of the propagating TAMMAR ridge segment on the Mid-Atlantic Ridge, 21.5°N, Geochemistry, Geophysics, Geosystems, 12.
- Darbyshire, F. A., I. T. Bjarnason, R. S. White, and O. G. Flovenz (1998a), Crustal structure above the Iceland mantle plume imaged by the ICEMELT refraction profile, Geophys. J. Int., 135, 1131-1149.
- Darbyshire, F. A., I. T. Bjarnason, R. S. White, and I. G. Flovenz (1998b), Crustal structure above the Iceland mantle plume imaged by the ICEMELT refraction profile, Geophys. J. Int., 135, 1131-1149.
- Darbyshire, F. A., T. Dahl-Jensen, T. B. Larsen, P. H. Voss, and G. Joyal (2018), Crust and uppermost-mantle structure of Greenland and the Northwest Atlantic from Rayleigh wave group velocity tomography, Geophys. J. Int., 212, 1546-1569.
- Dean, K., K. McLachlan, and A. Chambers (1999), Rifting and the development of the
 Faeroe-Shetland Basin, Proceedings of the 5th Conference Petroleum Geology of
 Northwest Europe, London, pp. 533–544.
- Deemer, S., C. A. Hurich, and J. Hall (2010), Post-rift flood-basalt-like volcanism on the Newfoundland Basin nonvolcanic margin: The U event mapped with spectral decomposition 494, 1-16 pp.

- 1840 Denk, T., F. Grímsson, R. Zetter, and L. A. Símonarson (2011), The Biogeographic History 1841 of Iceland - The North Atlantic Land Bridge Revisited, in Late Cainozoic Floras of 1842 Iceland, edited, pp. 647-668, Springer Science+Business Media B.V.
- 1843 Detrick, R. S., J. G. Sclater, and J. Thiede (1977), The subsidence of aseismic ridges, Earth 1844 planet. Sci. Lett., 34, 185-196.
- 1845 Dewey, J. F., and R. A. Strachan (2003), Changing Silurian–Devonian relative plate motion in the Caledonides: sinistral transpression to sinistral transtension, Journal of the 1846 1847 Geological Society, 160, 219.
- 1848 Dick, H. J. B. (2015), The Southwest Indian Ridge: Remelting the Gondwanan Mantle, Acta 1849 Geologica Sinica - English Edition, 89, 27-27.
- 1850 Doré, A. G., E. R. Lundin, C. Fichler, and O. Olesen (1997), Patterns of basement structure and reactivation along the NE Atlantic margin, J. geol. Soc. Lon., 154, 85–92. 1851
- 1852 Downes, H., B. G. J. Upton, A. D. J. Connolly, and J.-L. Bodinier (2007), Petrology and geochemistry of a cumulate xenolith suite from Bute: evidence for late Palaeozoic crustal 1853 1854 underplating beneath SW Scotland, Journal of the Geological Society, London, 164, 1855 1217-1231.
- 1856 Du, Z., and G. R. Foulger (1999), The crustal structure beneath the Northwest Fjords, 1857 Iceland, from receiver functions and surface waves, Geophys. J. Int., 139, 419-432.
- 1858 Du, Z., G. R. Foulger, B. R. Julian, R. M. Allen, G. Nolet, W. J. Morgan, B. H. Bergsson, P. Erlendsson, S. Jakobsdottir, S. Ragnarsson, R. Stefansson, and K. Vogfjord (2002), 1859 1860 Crustal structure beneath western and eastern Iceland from surface waves and receiver
- 1861 functions, Geophys. J. Int., 149, 349-363.
- Du, Z. J., and G. R. Foulger (2001), Variation in the crustal structure across central Iceland, 1862 Geophys. J. Int., 145, 246-264. 1863
- 1864 Dunbar, J. A., and D. S. Sawyer (1988), Continental rifting at pre-existing lithospheric weaknesses, Nature, 333, 450. 1865
- 1866 Dunn, R., and F. Martinez (2011), Contrasting crustal production and rapid mantle transitions beneath backarc ridges, Nature, 469, 198-202. 1867
- Eagles, G., L. Pérez-Díaz, and N. Scarselli (2015), Getting over continent ocean boundaries, 1868 1869 Earth-Science Reviews, 151, 244-265.
- Ebbing, J., E. Lundin, O. Olesen, and E. K. Hansen (2006), The mid-Norwegian margin: a 1870 1871 discussion of crustal lineaments, mafic intrusions, and remnants of the Caledonian root 1872 by 3D density modelling and structural interpretation, Journal of the Geological Society, 1873 163, 47.
- 1874 Ebbing, J., R. W. England, T. Korja, T. Lauritsen, O. Olesen, W. Stratford, and C. Weidle 1875 (2012), Structure of the Scandes lithosphere from surface to depth, Tectonophysics, 536-1876 537, 1-24,
- 1877 Ebdon, C. C., P. J. Granger, H. D. Johnson, and A. M. Evans (1995), Early Tertiary evolution 1878 and sequence stratigraphy of the Faeroe-Shetland Basin: implications for hydrocarbon prospectivity, in The Tectonics, Sedimentation and Palaeoceanography of the North 1879 1880 Atlantic Region, edited by R. A. Scrutton, M. S. Stoker, G. B. Shimmield and A. W.
- 1881 Tudhope, pp. 51–69, Geological Society, London, Special Publications, London.
- Einarsson, P. (1988), The South Iceland Seismic Zone, Episodes, 11, 34-35. 1882
- 1883 Einarsson, P. (1991), Earthquakes and present-day tectonism in Iceland, Tectonophysics, 1884 189, 261-279.
- 1885 Einarsson, P. (2008), Plate boundaries, rifts and transforms in Iceland, Jökull, 58, 35-58.
- Eldholm, O., and K. Grue (1994a), North Atlantic volcanic margins: Dimensions and 1886 1887 production rates, J. Geophys. Res., 99, 2955–2968.

- Eldholm, O., and K. Grue (1994b), North Atlantic volcanic margins: Dimensions and production rates, Journal of Geophysical Research: Solid Earth, 99, 2955-2968.
- Eldholm, O., J. Thiede, and E. Taylor (1989), Evolution of the Vøring Volcanic Margin, Proceedings of the ODP, Scientific Results, pp 1033-1065 104.
- Elliott, G. M., and L. M. Parson (2008), Influence of margin segmentation upon the break-up of the Hatton Bank rifted margin, NE Atlantic, Tectonophysics, 457, 161-176.
- Ellis, D., and M. S. Stoker (2014), The Faroe–Shetland Basin: a regional perspective from the Paleocene to the present day and its relationship to the opening of the North Atlantic Ocean, *in* Hydrocarbon Exploration to Exploitation West of Shetlands, edited by S. J. C. Cannon and D. Ellis, Geological Society, London, London.
- Engeln, J. F., S. Stein, J. Werner, and R. G. Gordon (1988), Microplate and shear zone models for oceanic spreading center reorganizations, Journal of Geophysical Research: Solid Earth, 93, 2839-2856.
- Escartin, J., G. Hirth, and B. Evans (2001), Strength of slightly serpentinized peridotites: Implications for the tectonics of oceanic lithosphere, Geology, 29, 1023-1026.
- Eysteinsson, H., and J. Hermance (1985), Magnetotelluric measurements across the eastern neovolcanic zone in south Iceland, JGR, 90, 10,093-010,103.
- Fichler, C., T. Odinsen, H. Rueslåtten, O. Olesen, J. E. Vindstad, and S. Wienecke (2011), Crustal inhomogeneities in the Northern North Sea from potential field modeling: Inherited structure and serpentinites?, Tectonophysics, 510, 172-185.
- Flovenz, O. G. (1980), Seismic structure of the Icelandic crust above layer three and the relation between body wave velocity and the alteration of the basaltic crust, J. Geophys., 47, 211-220.
- Forsyth, D. W., N. Harmon, D. S. Scheirer, and R. A. Duncan (2006), Distribution of recent volcanism and the morphology of seamounts and ridges in the GLIMPSE study area:

 Implications for the lithospheric cracking hypothesis for the origin of intraplate, non-hot spot volcanic chains, J. Geophys. Res., 111, B11407.
- Fossen, H. (2010), Extensional tectonics in the North Atlantic Caledonides: a regional view, Geological Society, London, Special Publications, 335, 767.
- 1917 Foulger, G. R. (2006), Older crust underlies Iceland, Geophys. J. Int., 165, 672-676.
- Foulger, G. R. (2010), Plates vs Plumes: A Geological Controversy, Wiley-Blackwell, Chichester, U.K., xii+328 pp.
- 1920 Foulger, G. R. (2012), Are 'hot spots' hot spots?, J. Geodyn., 58, 1-28.
- Foulger, G. R. (2018), Origin of the South Atlantic igneous province, J. Volc. Geotherm. Res., 355, 2-20.
- Foulger, G. R., and D. G. Pearson (2001), Is Iceland underlain by a plume in the lower mantle? Seismology and helium isotopes, Geophys. J. Int., 145, F1-F5.
- Foulger, G. R., and D. L. Anderson (2005), A cool model for the Iceland hot spot, J. Volc. Geotherm. Res., 141, 1-22.
- 1927 Foulger, G. R., Z. Du, and B. R. Julian (2003), Icelandic-type crust, Geophys. J. Int., 155, 567-590.
- Foulger, G. R., J. H. Natland, and D. L. Anderson (2005), A source for Icelandic magmas in remelted Iapetus crust, J. Volc. Geotherm. Res., 141, 23-44.
- Foulger, G. R., C. H. Jahn, G. Seeber, P. Einarsson, B. R. Julian, and K. Heki (1992), Postrifting stress relaxation at the divergent plate boundary in Northeast Iceland, Nature, 358, 488-490.
- Foulger, G. R., G. F. Panza, I. M. Artemieva, I. D. Bastow, F. Cammarano, J. R. Evans, W.
- B. Hamilton, B. R. Julian, M. Lustrino, H. Thybo, and T. B. Yanovskaya (2013), Caveats
- on tomographic images, Terra Nova, 25, 259-281.

- Fountain, D. M., T. M. Boundy, H. Austrheim, and P. Rey (1994), Eclogite-facies shear zones—deep crustal reflectors?, Tectonophysics, 232, 411-424.
- Funck, T., H. R. Jackson, S. A. Dehler, and I. D. Reid (2006), A refraction seismic transect from Greenland to Ellesmere Island, Canada: The crustal structure in southern Nares Strait, Polarforschung, 74, 94–112.
- Funck, T., H. R. Jackson, K. E. Louden, and F. Klingelhoefer (2007), Seismic study of the transform-rifted margin in Davis Strait between Baffin Island (Canada) and Greenland: What happens when a plume meets a transform, J. Geophys. Res., 112, B04402.
- Funck, T., M. S. Andersen, J. Keser Neish, and T. Dahl-Jensen (2008), A refraction seismic transect from the Faroe Islands to the Hatton-Rockall Basin, Journal of Geophysical Research: Solid Earth, 113.
- Funck, T., K. Gohl, V. Damm, and I. Heyde (2012), Tectonic evolution of southern Baffin Bay and Davis Strait: Results from a seismic refraction transect between Canada and Greenland, J. Geophys. Res., 117, B04107.
- Funck, T., W. H. Geissler, G. S. Kimbell, S. Gradmann, O. Erlendsson, K. McDermott, and U. K. Petersen (2016), Moho and basement depth in the NE Atlantic Ocean based on seismic refraction data and receiver functions, *in* The NE Atlantic Region: A Reappraisal of Crustal Structure, Tectonostratigraphy and Magmatic Evolution, edited by G. Peron-Pinvidic, J. R. Hopper, M. S. Stoker, C. Gaina, J. C. Doornenbal, T. Funck and U. E. Arting, pp. 207 231, Geological Society, London, Special Publications, London.
- Funck, T., W. H. Geissler, G. S. Kimbell, S. Gradmann, Ö. Erlendsson, K. McDermott, and U. K. Petersen (2017), Moho and basement depth in the NE Atlantic Ocean based on seismic refraction data and receiver functions, Geological Society, London, Special Publications, 447, 207.
- Gaina, C., L. Gernigon, and P. Ball (2009), Palaeocene–Recent plate boundaries in the NE Atlantic and the formation of the Jan Mayen microcontinent, Journal of the Geological Society, London, 166, 1–16.
- Gaina, C., A. Nasuti, G. S. Kimbell, and A. Blischke (2017), Break-up and seafloor spreading
 domains in the NE Atlantic, Geological Society, London, Special Publications, 447, 393 417.
- 1967 Gans, P. B. (1987), An open-system, two-layer crustal stretching model for the Eastern Great Basin, Tectonics, 6, 1-12.
- Gao, C., H. J. B. Dick, Y. Liu, and H. Zhou (2016), Melt extraction and mantle source at a Southwest Indian Ridge Dragon Bone amagmatic segment on the Marion Rise, Lithos, 246-247, 48-60.
- Garde, A. A., M. A. Hamilton, B. Chadwick, J. Grocott, and K. J. McCaffrey (2002), The Ketilidian orogen of South Greenland: geochronology, tectonics, magmatism, and forearc accretion during Palaeoproterozoic oblique convergence, Canadian Journal of Earth Sciences, 39, 765-793.
- Gasser, D. (2014), The Caledonides of Greenland, Svalbard and other Arctic areas: status of research and open questions, Geological Society, London, Special Publications, 390, 93.
- 1978 Gebrande, H., H. Miller, and P. Einarsson (1980), Seismic structure of Iceland along RRISP-1979 Profile I, J. Geophys., 47, 239-249.
- Gee, D. G., H. Fossen, N. Henriksen, and A. K. Higgins (2008a), From the Early Paleozoic Platforms of Baltica and Laurentia to the Caledonide Orogen of Scandinavia and Greenland, Episodes, 31, 44-51.
- Gee, D. G., H. Fossen, N. Henriksen, and K. Higgins (2008b), From the early Paleozoic platforms of Baltica and Laurentia to the Caledonide orogen of Scandinavia and Greenland, Episodes, 44–51.

- Gee, J. (2015), Caledonides of Scandinavia, Greenland, and Svalbard, *in* Reference Module in Earth Systems and Environmental Sciences, edited by S. A. Elias, Elsevier.
- 1988 Geoffroy, L. (2005), Volcanic passive margins, Comptes Rendus Geoscience, 337, 1395-1408.
- 1990 Geoffroy, L., E. B. Burov, and P. Werner (2015), Volcanic passive margins: another way to break up continents, Scientific Reports, 5, 14828.
- Geoffroy, L., C. Aubourg, J.-P. Callot, and J.-A. Barrat (2007), Mechanisms of crustal growth in large igneous provinces: The north Atlantic province as a case study, *in* Plates, Plumes, and Planetary Processes, edited by G. R. Foulger and D. M. Jurdy, pp. 747-774, Geological Society of America, Boulder, CO.
- Geoffroy, L., H. Guan, L. Gernigon, G. R. Foulger, and P. Werner (submitted), C-Blocks and the extent of continental material in oceans: the Laxmi Basin case study, Geophys. J. Int.

1999

2000 2001

2002

2003

2011

2012

- Gernigon, L., J.-C. Ringenbach, S. Planke, and B. L. Gall (2004), Deep structures and breakup along volcanic rifted margins: insights from integrated studies along the outer Vøring Basin (Norway), Marine and Petroleum Geology, 21, 363–372.
- Gernigon, L., A. Blischke, A. Nasuti, and M. Sand (2015), Conjugate volcanic rifted margins, seafloor spreading, and microcontinent: Insights from new high-resolution aeromagnetic surveys in the Norway Basin, Tectonics, 34.
- Gernigon, L., F. Lucazeau, F. Brigaud, e.-C. Ringenbach, S. Planke, and B. L. Gall (2006), A moderate melting model for the Vøring margin (Norway) based on structural observations and a thermo-kinematical modelling: Implication for the meaning of the lower crustal bodies, Tectonophysics, 412, 255-278.
- Gernigon, L., C. Gaina, O. Olesen, P. J. Ball, G. Péron-Pinvidic, and T. Yamasaki (2012),
 The Norway Basin revisited: From continental breakup to spreading ridge extinction,
 Marine and Petroleum Geology, 35, 1-19.
 - Gernigon, L., D. Franke, L. Geoffroy, C. Schiffer, G. R. Foulger, M. Stoker, and e. al. (this volume), Crustal fragmentation, magmatism, and the diachronous breakup of the Norwegian-Greenland Sea, Earth-Science Reviews.
- Gernigon, L., O. Olesen, J. Ebbing, S. Wienecke, C. Gaina, J. O. Mogaard, M. Sand, and R.
 Myklebust (2009), Geophysical insights and early spreading history in the vicinity of the
 Jan Mayen Fracture Zone, Norwegian–Greenland Sea, Tectonophysics, 468, 185–205.
- 2017 Gerya, T. (2011), Origin and models of oceanic transform faults, Tectonophysics.
- Gillard, M., D. Sauter, J. Tugend, S. Tomasi, M.-E. Epin, and G. Manatschal (2017), Birth of an oceanic spreading center at a magma-poor rift system, Scientific Reports, 7, 15072.
- Goodwin, T., D. Cox, and J. Trueman (2009), Paleocene sedimentary models in the subbasalt around the Munkagrunnur–East Faroes Ridge, Proceedings of the Faroe Islands Exploration Conference, 2nd Conference, pp. 267–285.
- Graça, M. C., N. Kusznir, and N. S. Gomes Stanton (2019), Crustal thickness mapping of the central South Atlantic and the geodynamic development of the Rio Grande Rise and Walvis Ridge, Marine and Petroleum Geology, 101, 230-242.
- Gradstein, F. M., J. G. Ogg, M. D. Schmitz, and G. M. Ogg (2012), The Geologic Time Scale 2027 2012, Elsevier, Amsterdam.
- Greenhalgh, E. E., and N. J. Kusznir (2007), Evidence for thin oceanic crust on the extinct Aegir Ridge, Norwegian Basin, NE Atlantic derived from satellite gravity inversion, Geophys. Res. Lett., 34, L06305.
- Grocott, J., and K. J. W. McCaffrey (2017), Basin evolution and destruction in an Early
 Proterozoic continental margin: the Rinkian fold–thrust belt of central West Greenland,
 Journal of the Geological Society.

- Guan, H., L. Geoffroy, L. Gernigon, F. Chauvet, C. Grigné, and P. Werner (2019), Magmatic ocean-continent transitions, Marine and Petroleum Geology, 104, 438-450.
- Guarnieri, P. (2015), Pre-break-up palaeostress state along the East Greenland margin, J. geol. Soc. Lon., 172, 727–739.
- Gudlaugsson, S. T., K. Gunnarsson, M. Sand, and J. Skogseid (1988), Tectonic and volcanic events at the Jan Mayen Ridge microcontinent, *in* Early Tertiary Volcanism and the Opening of the NE Atlantic, edited by A. C. Morton and L. M. Parson, pp. 85-93, Geological Society Special Publications.
- Gudmundsson, O. (2003), The dense root of the Iceland crust, Earth planet. Sci. Lett., 206, 427-440.
- Haller, J. (1971), Geology of the East Greenland Caledonides, Interscience, New York.
- Hansen, J., D. A. Jerram, K. McCaffrey, and S. R. Passey (2009), The onset of the North Atlantic Igneous Province in a rifting perspective, Geological Magazine, 146, 309-325.
- Harry, D. L., D. S. Sawyer, and W. P. Leeman (1993), The mechanics of continental extension in western North America: implications for the magmatic and structural evolution of the Great Basin, Earth planet. Sci. Lett., 117, 59-71.
- Heki, K., G. R. Foulger, B. R. Julian, and C.-H. Jahn (1993), Plate dynamics near divergent boundaries: Geophysical implications of postrifting crustal deformation in NE Iceland, J. Geophys. Res., 98, 14279-14297.
- Henriksen, N. (1999), Conclusion of the 1:500 000 mapping project in the Caledonian fold belt in North-East Greenland, Geology of Greenland Survey Bulletin, 183, 10-22.
- Henriksen, N., and A. K. Higgins (1976), East Greenland Caledonian fold belt, *in* Geology of Greenland, edited by A. Escher and W. S. Watt, pp. 182–246, Geological Survey of Greenland, Copenhagen.
- Hermance, J. F., and L. R. Grillot (1974), Constraints on temperatures beneath Iceland from magnetotelluric data, Phys. Earth Planet. Int., 8, 1-12.
- Heron, P., A. Peace, K. McCaffrey, J. K. Welford, R. Wilson, and R. N. Pysklywec (2019),
 Segmentation of rifts through structural inheritance: Creation of the Davis Strait,
 Tectonics, in press.
- Herzberg, C., and P. D. Asimow (2008), Petrology of some oceanic island basalts:

 PRIMELT2.XLS software for primary magma calculation, Geochemistry, Geophysics,
 Geosystems, 9.
- Herzberg, C., and P. D. Asimow (2015), PRIMELT3 MEGA.XLSM software for primary magma calculation: Peridotite primary magma MgO contents from the liquidus to the solidus, Geochemistry, Geophysics, Geosystems, 16, 563-578.
- Hey, R., F. Martinez, Á. Höskuldsson, and Á. Benediktsdóttir (2008), Propagating Rift Origin of the V-Shaped Ridges South of Iceland, paper presented at IAVCEI 2008 General assembly, 17-22 August, 2008.
- Hey, R., F. Martinez, A. Höskuldsson, and A. Benediktsdóttir (2010), Propagating rift model for the V-shaped ridges south of Iceland, Geochem. Geophys. Geosys., 11.
- Hey, R., F. Martinez, Á. Höskuldsson, D. E. Eason, J. Sleeper, S. Thordarson, Á.
 Benediktsdóttir, and S. Merkuryev (2016), Multibeam investigation of the active North
 Atlantic plate boundary reorganization tip, Earth planet. Sci. Lett., 435, 115-123.
- Hey, R. N., and D. S. Wilson (1982), Propagating rift explanation for the tectonic evolution of the northeast Pacific—the pseudomovie, Earth planet. Sci. Lett., 58, 167-188.
- Hjartarson, A., O. Erlendsson, and A. Blischke (2017), The Greenland–Iceland–Faroe Ridge Complex, *in* The NE Atlantic Region: A Reappraisal of Crustal Structure,
- Tectonostratigraphy and Magmatic Evolution, edited by G. Peron-Pinvidic, J. R. Hopper,

- 2082 M. S. Stoker, C. Gaina, J. C. Doornenbal, T. Funck and U. E. Arting, pp. 127-148, Geological Society, London, Special Publications.
- Hofton, M. A., and G. R. Foulger (1996a), Post-rifting anelastic deformation around the spreading plate boundary, north Iceland, 2: Implications of the model derived from the 1987-1992 deformation field, J. Geophys. Res., 101, 25,423 425,436.
- Hofton, M. A., and G. R. Foulger (1996b), Post-rifting anelastic deformation around the spreading plate boundary, north Iceland, 1: Modeling of the 1987-1992 deformation field using a viscoelastic Earth structure, JGR, 101, 25,403 425,421.
- Holbrook, W. S., H. C. Larsen, J. Korenaga, T. Dahl-Jensen, I. D. Reid, P. B. Kelemen, J. R. Hopper, G. M. Kent, D. Lizarralde, S. Bernstein, and R. S. Detrick (2001), Mantle thermal structure and active upwelling during continental breakup in the north Atlantic, Earth planet. Sci. Lett., 190, 251-266.
- Holdsworth, R. E., A. Morton, D. Frei, A. Gerdes, R. A. Strachan, E. Dempsey, C. Warren, and A. Whitham (2018), The nature and significance of the Faroe-Shetland Terrane: linking Archaean basement blocks across the North Atlantic, Precamb. Res., in press. Hole, M. J. (2015), The generation of continental flood basalts by decompression melting of
 - Hole, M. J. (2015), The generation of continental flood basalts by decompression melting of internally heated mantle, Geology, 43, 311-314.
- Hole, M. J., and J. M. Millett (2016), Controls of mantle potential temperature and lithospheric thickness on magmatism in the North Atlantic Igneous Province, J. Pet., 57, 417-436.
- Hole, M. J., and J. H. Natland (this volume), Magmatism in the North Atlantic Igneous Province; mantle temperatures, rifting and geodynamics, Earth-Science Reviews.

- Hole, M. J., R. M. Ellam, D. I. M. Macdonald, and S. P. Kelley (2015), Gondwana break-up related magmatism in the Falkland Islands, J. geol. Soc. Lon., 173, 108–126.
- Hopper, J. R., T. Dahl-Jensen, W. S. Holbrook, H. C. Larsen, D. Lizarralde, J. Korenaga, G. M. Kent, and P. B. Kelemen (2003), Structure of the SE Greenland margin from seismic reflection and refraction data: Implications for nascent spreading center subsidence and asymmetric crustal accretion during North Atlantic opening, Journal of Geophysical Research: Solid Earth, 108.
- Huismans, R., and C. Beaumont (2011), Depth-dependent extension, two-stage breakup and cratonic underplating at rifted margins, Nature, 473, 74.
- Huismans, R. S., and C. Beaumont (2014), Rifted continental margins: The case for depthdependent extension, Earth planet. Sci. Lett., 407, 148-162.
- Jamtveit, B., R. Brooker, K. Brooks, L. M. Larsen, and T. Pedersen (2001), The water content of olivines from the North Atlantic Volcanic Province, Earth planet. Sci. Lett., 186, 401-415.
- Johannesson, H., and K. Saemundsson (1998), Geological Map of Iceland at 1/500 000, Geological Map of Iceland, 1:500 000. Bedrock Geology.
- Johnson, H., J. D. Ritchie, K. Hitchen, D. B. McInroy, and G. S. Kimbell (2005), Aspects of the Cenozoic deformational history of the northeast Faroe-Shetland Basin, Wyville-Thomson Ridge and Hatton Bank areas, Proceedings of the Petroleum Geology: NW Europe and Global Perspectives, 6th Conference, pp. 993–1007.
- Jones, E. J. W., R. Siddall, M. F. Thirlwall, P. N. Chroston, and A. J. Lloyd (1994), Anton Dohrn Seamount and the evolution of the Rockall Trough, Oceanologica Acta, 17, 237-247.
- Jones, S. M. (2003), Test of a ridge–plume interaction model using oceanic crustal structure around Iceland, Earth planet. Sci. Lett., 208, 205-218.

- Jones, S. M., N. White, and J. Maclennan (2002), V-shaped ridges around Iceland;
- implications for spatial and temporal patterns of mantle convection, Geochem. Geophys. Geosys., 3, 2002GC000361.
- 2132 Kandilarov, A., R. Mjelde, E. Flueh, and R. B. Pedersen (2015), Vp/Vs-ratios and anisotropy
- on the northern Jan Mayen Ridge, North Atlantic, determined from ocean bottom seismic data, Polar Science, 9, 293-310.
- Karato, S.-i., and P. Wu (1993), Rheology of the Upper Mantle: A Synthesis, Science, 260, 2136 771.
- Keen, C. E., and R. R. Boutilier (1995), Lithosphere-asthenosphere interactions below rifts, Rifted Ocean-Continent Boundaries, 17-30.
- Keen, C. E., L. T. Dafoe, and K. Dickie (2014), A volcanic province near the western
 termination of the Charlie-Gibbs Fracture Zone at the rifted margin, offshore northeast
 Newfoundland, Tectonics, 33, 1133–1153.
- Keen, C. E., K. Dickie, and L. T. Dafoe (2018), Structural characteristics of the oceancontinent transition along the rifted continental margin, offshore central Labrador, Marine and Petroleum Geology, 89, 443-463.
- King, S. D. (2005), North Atlantic topographic and geoid anomalies: the result of a narrow ocean basin and cratonic roots?, *in* Plates, Plumes, and Paradigms, edited by G. R. Foulger, J.H. Natland, D.C. Presnall and D.L. Anderson, pp. 653-664, Geological

Society of America, Boulder, CO.

- Klein, E. M., and C. H. Langmuir (1987), Global correlations of ocean ridge basalt chemistry with axial depth and crustal thickness, J. Geophys. Res., 92, 8089-8115.
- Kodaira, S., R. Mjelde, K. Gunnarsson, H. Shiobara, and H. Shimamura (1998), Structure of the Jan Mayen microcontinent and implications for its evolution, Geophys. J. Int., 132, 383-400.
- Korenaga, J. (2004), Mantle mixing and continental breakup magmatism, Earth planet. Sci. Lett., 218, 463-473.
- Korenaga, J., and P. B. Kelemen (2000), Major element heterogeneity in the mantle source of the north Atlantic igneous province, Earth planet. Sci. Lett., 184, 251-268.
- Korenaga, J., and W. W. Sager (2012), Seismic tomography of Shatsky Rise by adaptive importance sampling, Journal of Geophysical Research: Solid Earth, 117.
- Korenaga, J., P. B. Kelemen, and W. S. Holbrook (2002), Methods for resolving the origin of
 large igneous provinces from crustal seismology, J. Geophys. Res., 107, 2178,
 doi:2110.1029/2001JB001030.
- Krabbendam, M. (2001), When the Wilson Cycle breaks down: how orogens can produce strong lithosphere and inhibit their future reworking, Geological Society, London, Special Publications, 184, 57.
- Kumar, P., R. Kind, K. Priestley, and T. Dahl-Jensen (2007), Crustal structure of Iceland and Greenland from receiver function studies, Journal of Geophysical Research: Solid Earth, 112.
- Kurashimo, E., M. Shinohara, K. Suyehiro, J. Kasahara, and N. Hirata (1996), Seismic
 evidence for stretched continental crust in the Japan Sea, Geophys. Res. Lett., 23, 30673070.
- Kusznir, N., and e. al. (2018), Intra-ocean Ridge Jumps, Oceanic Plateaus & Upper Mantle Inheritance, Earth Science Reviews, submitted.
- Kusznir, N. J., and G. D. Karner (2007), Continental lithospheric thinning and breakup in response to upwelling divergent mantle flow: application to the Woodlark,
- Newfoundland and Iberia margins, *in* Imaging, Mapping and Modelling Continental

- Lithosphere Extension and Breakup, edited by G. D. Karner, G. Manatschal and L. M. Pinheiro, pp. 389-419, Geological Society of London, Special Publications.
- Lamers, E., and S. M. M. Carmichael (1999), The Paleocene deepwater sandstone play West
 of Shetland, Proceedings of the Petroleum Geology of Northwest Europe, 5th
 Conference, pp. 645–659.
- Larsen, L. M., R. Waagstein, A. K. Pedersen, and M. Storey (1999), Trans-Atlantic
 correlation of the Palaeogene volcanic successions in the Faeroe Islands and East
 Greenland, Journal of the Geological Society, 156, 1081-1095.
- Larsen, L. M., L. M. Heaman, R. A. Creaser, R. A. Duncan, R. Frei, and M. Hutchinson (2009), Tectonomagnetic events during stretching and basin formation in the Labrador Sea and the Davis Strait: evidence from age and composition of Mesozoic to Palaeogene dyke swarms in West Greenland, Journal of the Geological Society, London, 166, 999–1012.
- Lundin, E., and T. Doré (2005), The fixity of the Iceland "hotspot" on the Mid-Atlantic
 Ridge: observational evidence, mechanisms and implications for Atlantic volcanic
 margins, *in* Plates, Plumes, and Paradigms, edited by G. R. Foulger, J.H. Natland, D.C.
 Presnall and D.L. Anderson, pp. 627-652, Geological Society of America.
- Lundin, E. R., and A. G. Doré (2011), Hyperextension, serpentinization, and weakening: A new paradigm for rifted margin compressional deformation, Geology, 39, 347-350.
- Lundin, E. R., and A. G. Doré (2018), Non-Wilsonian break-up predisposed by transforms:
 examples from the North Atlantic and Arctic, *in* Fifty Years of the Wilson Cycle
 Concept in Plate Tectonics, edited by R. W. Wilson, G. A. Houseman, K. J. W.
 Mccaffrey, A. G. Doré and S. J. H. Buiter, Geological Society, London, Special
 Publications.
- Lundin, E. R., A. G. Doré, and T. F. Redfield (2018), Magmatism and extension rates at rifted margins, Petroleum Geoscience.
- Manton, B., S. Planke, D. Zastrozhnov, M. M. Abdelmalak, J. Millett, D. Maharjan, S.
 Polteau, J. I. Faleide, L. Gernigon, and R. Myklebust (2018), Pre-Cretaceous
 Prospectivity of the Outer Møre and Vøring Basins Constrained by New 3D Seismic
 Data, paper presented at 80th EAGE Conference and Exhibition.
- Marquart, G. (1991), Interpretations of Geoid Anomalies around the Iceland Hotspot, Geophys. J. Int., 106, 149-160.
- Martinez, F., and R. N. Hey (this volume), Reykjanes Ridge evolution by plate kinematics and propagating small-scale mantle convection within a regional upper mantle anomaly, Earth-Science Reviews.
- Martinez, F., R. J. Stern, K. A. Kelley, Y. Ohara, J. D. Sleeper, J. M. Ribeiro, and M. Brounce (2018), Diffuse extension of the southern Mariana margin, J. Geophys. Res., 123, 892–916.
- Martínez, F., R. N. Hey, and P. D. Johnson (1997), The East ridge system 28.5–32°S East Pacific rise: Implications for overlapping spreading center development, Earth planet. Sci. Lett., 151, 13-31.
- Mason, A. J., R. R. Parrish, and T. S. Brewer (2004), U–Pb geochronology of Lewisian orthogneisses in the Outer Hebrides, Scotland: implications for the tectonic setting and correlation of the South Harris Complex, Journal of the Geological Society, 161, 45.
- Matthews, S., O. Shorttle, and J. Maclennan (2016), The temperature of the Icelandic mantle from olivine-spinel aluminum exchange thermometry, Geochemistry, Geophysics, Geosystems, 17, 4725-4752.
- McKenzie, D., and J. Jackson (2002), Conditions for flow in the continental crust, Tectonics, 21, 5-1-5-7.

- Meissner, R. (1999), Terrane accumulation and collapse in central Europe: seismic and rheological constraints, Tectonophysics, 305, 93-107.
- Menke, W. (1999), Crustal isostasy indicates anomalous densities beneath Iceland, Geophys. Res. Lett., 26, 1215-1218.
- 2230 Menke, W., and V. Levin (1994), Cold crust in a hot spot, Geophys. Res. Lett., 21, 1967-2231 1970.
- Menke, W., V. Levin, and R. Sethi (1995), Seismic attenuation in the crust at the mid-Atlantic plate boundary in south-west Iceland, Geophys. J. Int., 122, 175-182.
- Meyer, R., J. G. H. Hertogen, R. B. Pedersen, L. Viereck-Götte, and M. Abratis (2009), Elements and isotopic measurements of magmatic rock samples from ODP Hole 104-642E, in Supplement to: Meyer, R. et al. (2009): Interaction of mantle derived melts with crust during the emplacement of the Vöring Plateau, N.E. Atlantic. Marine Geology, 261(1-4), 3-16, edited, PANGAEA.
- Mjelde, R., A. Goncharov, and R. D. Müller (2013), The Moho: Boundary above upper mantle peridotites or lower crustal eclogites? A global review and new interpretations for passive margins, Tectonophysics, 609, 636-650.
- Mjelde, R., S. Kodaira, H. Shimamura, T. Kanazawa, H. Shiobara, E. W. Berg, and O. Riise (1997), Crustal structure of the central part of the Vøring Basin, mid-Norway margin, from ocean bottom seismographs, Tectonophysics, 277, 235-257.
- Mjelde, R., R. Aurvåg, S. Kodaira, H. Shimamura, K. Gunnarsson, A. Nakanishi, and H. Shiobara (2002), Vp/Vs-ratios from the central Kolbeinsey Ridge to the Jan Mayen Basin, North Atlantic; implications for lithology, porosity and present-day stress field, Mar. Geophys. Res., 23, 123-145.
- Mjelde, R., P. Digranes, H. Shimamura, H. Shiobara, S. Kodaira, H. Brekke, T. Egebjerg, N.
 Sørenes, and S. Thorbjørnsen (1998), Crustal structure of the northern part of the Vøring
 Basin, mid-Norway margin, from wide-angle seismic and gravity data, Tectonophysics,
 293, 175-205.
- Mjelde, R., P. Digranes, M. Van Schaack, H. Simamura, H. Shiobara, S. Kodaira, O. Naess,
 N. Sørenes, and E. Vagnes (2001), Crustal structure of the outer Voring Plateau, offshore
 Norway, from ocean bottom seismic and gravity data, J. Geophys. Res., 106, 6769-6791.
- Mudge, D. C. (2015), Regional controls on Lower Tertiary sandstone distribution in the
 North Sea and NE Atlantic margin basins, *in* Tertiary Deep-Marine Reservoirs of the
 North Sea Region, edited by T. McKie, P. T. S. Rose, A. J. Hartley, D. W. Jones and T.
 L. Armstrong, pp. 17–42, Geological Society, London, Special Publications.
- Müller, R. D., M. Seton, S. Zahirovic, S. E. Williams, K. J. Matthews, N. M. Wright, G. E.
 Shephard, K. T. Maloney, N. Barnett-Moore, M. Hosseinpour, D. J. Bower, and J.
 Cannon (2016), Ocean basin evolution and global-scale plate reorganization events since
 Pangea breakup, Ann. Rev. Earth Planet. Sci., 44, 107.
- Muñoz, G., A. Mateus, J. Pous, W. Heise, F. Monteiro Santos, and E. Almeida (2008),
 Unraveling middle-crust conductive layers in Paleozoic Orogens through 3D modeling
 of magnetotelluric data: The Ossa-Morena Zone case study (SW Iberian Variscides),
 Journal of Geophysical Research: Solid Earth, 113.
- Müntener, O., G. Manatschal, L. Desmurs, and T. Pettke (2010), Plagioclase Peridotites in Ocean–Continent Transitions: Refertilized Mantle Domains Generated by Melt Stagnation in the Shallow Mantle Lithosphere, J. Pet., 51, 255-294.
- Mutter, J. C., and C. M. Zehnder (1988), Deep crustal structure and magmatic processes; the inception of seafloor spreading in the Norwegian-Greenland Sea, *in* Early Tertiary volcanism and the opening of the NE Atlantic, edited by A. C. Morton and L. M. Parson, pp. 35-48.

- Natland, J. H. (2003), Capture of helium and other volatiles during the growth of olivine phenocrysts in picritic basalts from the Juan Fernandez Islands, J. Pet., 44, 421-456.
- Nemčok, M., and S. Rybár (2017), Rift-drift transition in a magma-rich system: the Gop Rift-Laxmi Basin case study, West India, Geological Society, London, Special Publications, 445, 95.

2284

2285

2293

2294

2295

2296

2297

22982299

2300

2301

23022303

2304

2305

2306

2307

2308

2309

2310

2311

- Nichols, A. R. L., M. R. Carroll, and A. Hoskuldsson (2002), Is the Iceland hot spot also wet?

 Evidence from the water contents of undegassed submarine and subglacial pillow basalts, Earth planet. Sci. Lett., 202, 77-87.
 - Nirrengarten, M., G. Manatschal, J. Tugend, N. Kusznir, and D. Sauter (2018), Kinematic Evolution of the Southern North Atlantic: Implications for the Formation of Hyperextended Rift Systems, Tectonics, 37, 89-118.
- O'Reilly, B. M., F. Hauser, A. W. B. Jacob, and P. M. Shannon (1996), The lithosphere below the Rockall Trough: wide-angle seismic evidence for extensive serpentinisation, Tectonophysics, 255, 1-23.
- Oakey, G. N., and J. A. Chalmers (2012), A new model for the Paleogene motion of Greenland relative to North America: Plate reconstructions of the Davis Strait and Nares Strait regions between Canada and Greenland, Journal of Geophysical Research: Solid Earth, 117.
 - Ólavsdóttir, J., L. O. Boldreel, and M. S. Andersen (2010), Development of a shelf-margin delta due to uplift of Munkagrunnut Ridge at the margin of Faroe-Shetland Basin: a seismic sequence stratigraphic study, Petroleum Geoscience, 16, 91-103.
 - Ólavsdóttir, J., M. S. Andersen, and L. O. Boldreel (2013a), Seismic stratigraphic analysis of the Cenozoic sediments in the NW Faroe–Shetland Basin Implications for inherited structural control of sediment distribution, Marine and Petroleum Geology, 46, 19–35.
 - Ólavsdóttir, J., M. S. Andersen, and L. O. Boldreel (2013b), Seismic stratigraphic analysis of the Cenozoic sediments in the NW Faroe Shetland Basin–Implications for inherited structural control of sediment distribution, Marine and Petroleum Geology, 46, 19-35.
 - Ólavsdóttir, J., Ó. R. Eidesgaard, and M. S. Stoker (2017), The stratigraphy and structure of the Faroese continental margin, *in* The NE Atlantic Region: A Reappraisal of Crustal Structure, Tectonostratigraphy and Magmatic Evolution, edited by G. Péron-Pinvidic, J. R. Hopper, M. S. Stoker, C. Gaina, J. C. Doornenbal, T. Funck and U. E. Árting, pp. 339–356, Geological Society, London, Special Publications, London.
 - Palmason, G. (1971), Crustal structure of Iceland from explosion seismology, Soc. Sci. Isl. Greinar V, 187 pp., Reykjavik.
 - Paquette, J., O. Sigmarsson, and M. Tiepolo (2006), Continental basement under Iceland revealed by old zircons, paper presented at American Geophysical Union, Fall Meeting.
 - Parman, S. W., Kurz, M.D., S. R. Hart, and T. L. Grove (2005), Helium solubility in olivine and implications for high ³He/⁴He in ocean island basalts, Nature, 437, 1140-1143.
- Passey, S. R., and D. W. Jolley (2009), A revised lithostratigraphic nomenclature for the Palaeogene Faroe Islands basalt Group, NE Atlantic ocean, Earth and Environmental Science Transaction of the Royal Society of Edinburgh, 99, 127-158.
- Peace, A., K. McCaffrey, J. Imber, J. Hunen, R. Hobbs, and R. Wilson (2018), The role of pre-existing structures during rifting, continental breakup and transform system development, offshore West Greenland, Basin Research, 30, 373-394.
- Peace, A., K. McCaffrey, J. Imber, J. Phethean, G. Nowell, K. Gerdes, and E. Dempsey (2016), An evaluation of Mesozoic rift-related magmatism on the margins of the Labrador Sea: Implications for rifting and passive margin asymmetry, Geosphere, 12.

- Peace, A. J., D. Franke, A. Doré, G. R. Foulger, N. Kusznir, J. G. McHone, J. Phethean, S.
- Rocchi, S. Schiffer, M. Schnabel, and J. K. Welford (this volume), Pangea dispersal and Large Igneous Provinces in search for causative mechanisms, Earth-Science Reviews.
- Peace, A. L., G. R. Foulger, C. Schiffer, and K. J. W. McCaffrey (2017), Evolution of Labrador Sea-Baffin Bay: Plate or plume processes?, Geoscience Canada, 44, 91-102.
- Peace, A. L., E. D. Dempsey, C. Schiffer, J. K. Welford, and J. W. Ken (submitted), Evidence for basement reactivation during the opening of the Labrador Sea from the Makkovik Province, Labrador, Canada: Insights from field-data and numerical models, Geosciences.
- Perlt, J., M. Heinert, and W. Niemeier (2008), The continental margin in Iceland A snapshot derived from combined GPS networks, Tectonophysics, 447, 155-166.
- Peron-Pinvidic, G., and G. Manatschal (2010), From microcontinents to extensional allochthons: witnesses of how continents rift and break apart?, Petroleum Geoscience, 16, 1-10.
- Peron-Pinvidic, G., G. Manatschal, and P. T. Osmundsen (2013), Structural comparison of archetypal Atlantic rifted margins: A review of observations and concepts, Marine and Petroleum Geology, 43, 21-47.
- Peron-Pinvidic, G., L. Gernigon, C. Gaina, and P. Ball (2012), Insights from the Jan Mayen system in the Norwegian–Greenland sea—I. Mapping of a microcontinent, Geophys. J. Int., 191, 385-412.
- Perram, L. J., M.-H. Cormier, and K. C. Macdonald (1993), Magnetic and tectonic studies of the dueling propagating spreading centers at 20°40′S on the East Pacific Rise: Evidence for crustal rotations, Journal of Geophysical Research: Solid Earth, 98, 13835-13850.
- Petersen, K., J. Armitage, S. Nielsen, and H. Thybo (2015), Mantle temperature as a control on the time scale of thermal evolution of extensional basins. Earth planet. Sci. Lett., 409, 61–70.
- Petersen, K. D., and C. Schiffer (2016), Wilson Cycle Passive Margins: Control of orogenic inheritance on continental breakup, Gondwana Research, 39, 131-144.
- Petersen, K. D., C. Schiffer, and T. Nagel (2018), LIP formation and protracted lower mantle upwelling induced by rifting and delamination, Scientific Reports, 8, 16578.
- Pharaoh, T. C. (1999), Palaeozoic terranes and their lithospheric boundaries within the Trans-European Suture Zone (TESZ): a review, Tectonophysics, 314, 17-41.
- Planke, S., P. A. Symonds, E. Alvestad, and J. Skogseid (2000), Seismic volcanostratigraphy of large-volume basaltic extrusive complexes on rifted margins, Journal of Geophysical Research: Solid Earth, 105, 19335-19351.
- Pollitz, F. F., and I. S. Sacks (1996), Viscosity structure beneath northeast Iceland, JGR, 101, 17,771-717,793.
- Presnall, D., and G. Gudfinnsson (2011), Oceanic volcanism from the low-velocity zone without mantle plumes, J. Pet., 52, 1533-1546.
- Presnall, D. C., and G. Gudfinnsson (2007), Global Na8-Fe8 Systematics of MORBs: Implications for Mantle Heterogeneity, Temperature, and Plumes, paper presented at European Geophysical Union General Assembly, 15-20 April, 2007.
- Prestvik, T., S. Goldberg, H. Karlsson, and K. Gronvold (2001), Anomalous strontium and lead isotope signatures in the off-rift Oraefajokull central volcano in south-east Iceland. Evidence for enriched endmember(s) of the Iceland mantle plume?, Earth planet. Sci.
- 2367 Lett., 190, 211-220.
- Putirka, K. D. (2008), Excess temperatures at ocean islands: Implications for mantle layering and convection, Geology, 36, 283-286.

- Quick, J. E., S. Sinigoi, and A. Mayer (1995), Emplacement of mantle peridotite in the lower continental crust, Ivrea-Verbano zone, northwest Italy, Geology, 23, 739-742.
- 2372 Ranalli, G. (1995), Rheology of the Earth, Springer.
- 2373 Reston, T. J., J. Pennell, A. Stubenrauch, I. Walker, and M. Pérez-Gussinyé (2001),
- Detachment faulting, mantle serpentinization, and serpentinite- mud volcanism beneath the Porcupine Basin, southwest of Ireland, Geology, 29, 587-590.
- Reynisson, R. F., J. Ebbing, E. Lundin, and P. T. Osmundsen (2011), Properties and distribution of lower crustal bodies on the mid-Norwegian margin, edited, pp. 843-854, Geological Society, London.
- Ribe, N. M., U. R. Christensen, and J. Theissing (1995), The dynamics of plume-ridge interaction, 1: Ridge-centered plumes, Earth planet. Sci. Lett., 134, 155-168.
- Richard, K. R., R. S. White, R. W. England, and J. Fruehn (1999), Crustal structure east of the Faroe Islands; mapping sub-basalt sediments using wide-angle seismic data, Petroleum Geoscience, 5, 161-172.
- Rickers, F., A. Fichtner, and J. Trampert (2013), The Iceland–Jan Mayen plume system and its impact on mantle dynamics in the North Atlantic region: Evidence from full-waveform inversion, Earth planet. Sci. Lett., 367, 39-51.
- Ritchie, J. D., H. D. Johnson, M. F. Quinn, and R. W. Gatliff (2008), Cenozoic compressional deformation within the Faroe-Shetland Basin and adjacent areas, *in* The Nature and Origin of Compression in Passive Margins, edited by H. D. Johnson, A. G. Doré, R. E. Holdsworth, R. W. Gatliff, E. R. Lundin and J. D. Ritchie, pp. 121–136, Geological Society, London, Special Publications.
- Roberts, D. (2003), The Scandinavian Caledonides: event chronology, palaeogeographic settings and likely, modern analogues, Tectonophysics, 365, 283-299.
- Roberts, D. G., M. Thompson, B. Mitchener, J. Hossack, S. Carmichael, and H. M. Bjornseth (1999), Palaeozoic to Tertiary rift and basin dynamics: mid-Norway to the Bay of Biscay a new context for hydrocarbon prospectivity in the deep water frontier, Proceedings of the 5th Conference of the Petroleum Geology of Northwest Europe, London, pp. 7-40.
- Roest, W. R., and S. P. Srivastava (1989), Sea-floor spreading in the Labrador Sea: a new reconstruction, Geology, 17, 1000–1003.
- 2400 Rognvaldsson, S. T., A. Gudmundsson, and R. Slunga (1998), Seismotectonic analysis of the 2401 Tjornes Fracture Zone, an active transform fault in north Iceland, Journal of Geophysical 2402 Research-Solid Earth, 103, 30117-30129.
- Royden, L. (1996), Coupling and decoupling of crust and mantle in convergent orogens:

 Implications for strain partitioning in the crust, Journal of Geophysical Research: Solid
 Earth, 101, 17679-17705.
- Rudnick, R. L., and D. M. Fountain (1995), Nature and composition of the continental crust:
 A lower crustal perspective, Rev. Geophys., 33, 267-309.
- Rutter, E. H., K. H. Brodie, and P. J. Evans (1993), Structural geometry, lower crustal magmatic underplating and lithospheric stretching in the Ivrea-Verbano zone, northern Italy, J. Str. Geol., 15, 647-662.
- Sallares, V., and P. Charvis (2003), Crustal thickness constraints on the geodynamic evolution of hte Galápagos volcanic province, Earth planet. Sci. Lett., 214, 545-559.
- Sandwell, D. T., R. D. Müller, W. H. F. Smith, E. Garcia, and R. Francis (2014), New global marine gravity model from CryoSat-2 and Jason-1 reveals buried tectonic structure, Science, 346, 65.
- Santos Ventura, R., C. E. Ganade, C. M. Lacasse, I. S. L. Costa, I. Pessanha, E. P. Frazão, E. L. Dantas, and J. A. Cavalcante (2019), Dating Gondwanan continental crust at the Rio
- 2418 Grande Rise, South Atlantic, Terra Nova, 0.

- Sarafian, E., G. A. Gaetani, E. H. Hauri, and A. R. Sarafian (2017), Experimental constraints on the damp peridotite solidus and oceanic mantle potential temperature, Science, 355, 942-945.
- Sato, H., I. S. Sacks, T. Murase, G. Muncill, and H. Fukuyama (1989), Qp-melting temperature relation in peridotite at high pressure and temperature: Attenuation mechanism and implications for the mechanical properties of the upper mantle, J. Geophys. Res., 94, 10647-10661.
- Schaltegger, U., H. E. F. Amundsen, B. Jamtveit, M. Frank, W. L. Griffin, K. Gronvold, R.
 G. Tronnes, and T. Torsvik (2002), Contamination of OIB by underlying ancient
 continental lithosphere: U-Pb and Hf isotopes in zircons question EM1 and EM2 mantle
 components, Geochim. Cosmochim. Acta, 66, A673.
- Schiffer, C., N. Balling, B. H. Jacobsen, R. A. Stephenson, and S. B. (2014), Seismological evidence for a fossil subduction zone in the East Greenland Caledonides, Geology, 42, 311-314.
- Schiffer, C., N. Balling, J. Ebbing, B. H. Jacobsen, and S. B. Nielsen (2016), Geophysical-petrological modelling of the East Greenland Caledonides Isostatic support from crust and upper mantle, Tectonophysics, 692, 44-57.
- Schiffer, C., C. Tegner, A. J. Schaeffer, V. Pease, and S. B. Nielsen (2017), High Arctic geopotential stress field and implications for geodynamic evolution, Geological Society, London, Special Publications, 460.
- Schiffer, C., R. A. Stephenson, K. D. Petersen, S. B. Nielsen, B. H. Jacobsen, N. Balling, and
 D. I. M. Macdonald (2015), A sub-crustal piercing point for North Atlantic
 reconstructions and tectonic implications, Geology, 43, 1087-1090.
- Schiffer, C., A. Peace, J. Phethean, K. McCaffrey, L. Gernigon, K. D. Petersen, and G.
 Foulger (2018), The Jan Mayen Microplate Complex and the Wilson Cycle, *in* Tectonic
 Evolution: 50 Years of the Wilson Cycle Concept, edited by G. Houseman, Geological
 Society of London
- Schiffer, C., A. G. Doré, G. R. Foulger, D. Franke, L. Geoffroy, L. Gernigon, B. Holdsworth,
 N. Kusznir, E. Lundin, K. McCaffrey, A. Peace, K. D. Petersen, R. Stephenson, M. S.
 Stoker, and K. Welford (this volume), The role of tectonic inheritance in the evolution of
 the North Atlantic, Earth-Science Reviews.
- Schlindwein, V., and W. Jokat (2000), Post-collisional extension of the East Greenland Caledonides: a geophysical perspective, Geophys. J. Int., 140, 550-567.
- Schmidt-Aursch, M. C., and W. Jokat (2005), The crustal structure of central East
 Greenland—II: From the Precambrian shield to the recent mid-oceanic ridges, Geophys.
 J. Int., 160, 753-760.
- Shen, F., L. H. Royden, and B. C. Burchfiel (2001), Large-scale crustal deformation of the Tibetan Plateau, Journal of Geophysical Research: Solid Earth, 106, 6793-6816.
- Shih, J., and P. Molnar (1975), Analysis and implications of the sequence of ridge jumps that eliminated the Surveyor Transform Fault, J. Geophys. Res., 80, 4815-4822.
- Shorttle, O., J. Maclennan, and A. M. Piotrowski (2013), Geochemical provincialism in the Iceland plume, Geochim. Cosmochim. Acta, 122, 363-397.
- Sigmundsson, F. (1991), Post-glacial rebound and asthenosphere viscosity in Iceland, Geophys. Res. Lett., 18, 1131-1134.
- Simon, K., R. S. Huismans, and C. Beaumont (2009), Dynamical modelling of lithospheric extension and small-scale convection: implications for magmatism during the formation of volcanic rifted margins, Geophys. J. Int., 176, 327–350.

- Skogseid, J., S. Planke, J. I. Faleide, T. Pedersen, O. Eldholm, and F. Neverdal (2000), NE
 Atlantic continental rifting and volcanic margin formation, *in* Dynamics of the
 Norwegian Margin, edited by A. Nottvedt, pp. 295-326.
- Slagstad, T., Y. Maystrenko, V. Maupin, and S. Gradmann (2017), An extinct, Late Mesoproterozoic, Sveconorwegian mantle wedge beneath SW Fennoscandia, reflected in seismic tomography and assessed by thermal modelling, Terra Nova, 30, 72-77.
- Smith, W. H. F., and D. T. Sandwell (1997), Global Sea Floor Topography from Satellite Altimetry and Ship Depth Soundings, Science, 277, 1956.
- Smythe, D. K., A. Dobinson, R. McQuillin, J. A. Brewer, D. H. Matthews, D. J. Blundell,
 and B. Kelk (1982), Deep structure of the Scottish Caledonides revealed by the MOIST reflection profile, Nature, 299, 338-340.
- Soper, N. J., R. A. Strachan, R. E. Holdsworth, R. A. Gayer, and R. O. Greilung (1992), Sinistral transpression and the Silurian closure of Iapetus, Journal - Geological Society (London), 149, 871-880.
- Spice, H. E., J. G. Fitton, and L. A. Kirstein (2016), Temperature fluctuation of the Iceland mantle plume through time, Geochemistry, Geophysics, Geosystems, 17, 243-254.
- Srivastava, S., B. MacLean, R. Macnab, H. Jackson, A. Embry, and H. Balkwill (1982),
 Davis Strait: structure and evolution as obtained from a systematic geophysical survey,
 Proceedings of the Third International Symposium on Arctic Geology, Calgary, Alberta,
 pp. 267-278.
- Srivastava, S. P. (1978), Evolution of the Labrador Sea and its bearing on the early evolution of the North Atlantic, Geophys. J. Int., 52, 313-357.
- St-Onge, M. R., J. A. M. V. Gool, A. A. Garde, and D. J. Scott (2009), Correlation of Archaean and Palaeoproterozoic units between northeastern Canada and western Greenland: constraining the pre-collisional upper plate accretionary history of the Trans-Hudson orogen, *in* Earth Accretionary Systems in Space and Time, edited by P. A. Cawood and A. Kröner, pp. 193-235, Geological Society of London.
- Staples, R. K., R. S. White, B. Brandsdottir, W. Menke, P. K. H. Maguire, and J. H. McBride (1997), Faeroe-Iceland ridge experiment 1. Crustal structure of northeastern Iceland, JGR, 102, 7849-7866.
- Starkey, N. A., F. M. Stuart, R. M. Ellam, J. G. Fitton, S. Basu, and L. M. Larsen (2009), Helium isotopes in early Iceland plume picrites: constraints on the composition of high 3He/4He mantle, Earth planet. Sci. Lett., 277, 91–100.
- Steffen, R., G. Strykowski, and B. Lund (2017), High-resolution Moho model for Greenland from EIGEN-6C4 gravity data, Tectonophysics, 706-707, 206-220.

- Stixrude, L., and C. Lithgow-Bertelloni (2011), Thermodynamics of mantle minerals II. Phase equilibria, Geophys. J. Int., 184, 1180-1213.
- Stoker, M. S., A. B. Leslie, and K. Smith (2013), A record of Eocene (Stronsay Group)
 sedimentation in BGS borehole 99/3, offshore NW Britain: implications for early postrift development of the Faroe-Shetland Basin, Scottish Journal of Geology, 49, 133–148.
- Stoker, M. S., S. P. Holford, and R. R. Hillis (2018), A rift-to-drift record of vertical crustal motions in the Faroe–Shetland Basin, NW European margin: establishing constraints on NE Atlantic evolution, Journal of the Geological Society, 175, 263-274.
- Stoker, M. S., G. S. Kimbell, D. B. McInroy, and A. C. Morton (2012), Eocene post-rift tectonostratigraphy of the Rockall Plateau, Atlantic margin of NW Britain: Linking early spreading tectonics and passive margin response, Marine and Petroleum Geology, 30, 98–125.

- Stoker, M. S., D. Praeg, J. S. Hjelstuen, J. S. Laberg, T. Nielsen, and P. M. Shannon (2005a), Neogene stratigraphy and the sedimentary and oceanographic development of the NW
- European Atlantic margin, Marine and Petroleum Geology, 22, 977–1005.
- Stoker, M. S., D. Praeg, P. M. Shannon, B. O. Hjelstuen, J. S. Laberg, T. Nielsen, T. C. E.
- van Weering, H. P. Sejrup, and D. Evans (2005b), Neogene evolution of the Atlantic
- continental margin of NW Europe (Lofoten Islands to SW Ireland): anything but passive,
- *in* Petroleum Geology: North-West Europe and Global Perspectives–Proceedings of the
- 2520 6th Petroleum Geology Conference, edited by A. G. Doré and B. A. Vining, pp. 1057-
- 2521 1076, Geological Society, London.
- Stoker, M. S., R. J. Hoult, T. Nielsen, J. S. Hjelstuen, J. S. Laberg, P. M. Shannon, D. Praeg,
- A. Mathiesen, T. C. E. van Weering, and A. M. McDonnell (2005c), Sedimentary and
- oceanographic responses to early Neogene compression on the NW European margin,
- 2525 Marine and Petroleum Geology, 22, 1031–1044.
- Stoker, M. S., M. A. Stewart, P. M. Shannon, M. Bjerager, T. Nielsen, A. Blischke, B. O.
- 2527 Hjelstuen, C. Gaina, K. McDermott, and J. Ólavsdóttir (2017), An overview of the Upper
- 2528 Palaeozoic-Mesozoic stratigraphy of the NE Atlantic margin, in The NE Atlantic
- Region: A Reappraisal of Crustal Structure, Tectonostratigraphy and Magmatic
- Evolution, edited by G. Péron-Pinvidic, J. R. Hopper, M. S. Stoker, C. Gaina, J. C.
- Doornenbal, T. Funck and U. E. Árting, pp. 11-68, Geological Society, London, Special Publications.
- Stuart, F. M., S. Lass-Evans, J. G. Fitton, and R. M. Ellam (2003), High 3He/4He ratios in picritic basalts from Baffin Island and the role of a mixed reservoir in mantle plumes,
- 2535 Nature, 424, 57-59.
- Suckro, S. K., K. Gohl, T. Funck, I. Heyde, B. Schreckenberger, J. Gerlings, and V. Damm
- 2537 (2013), The Davis Strait crust—a transform margin between two oceanic basins,
- 2538 Geophys. J. Int., 193, 78-97.
- Suckro, S. K., K. Gohl, T. Funck, I. Heyde, A. Ehrhardt, B. Schreckenberger, J. Gerlings, V.
- Damm, and W. Jokat (2012), The crustal structure of southern Baffin Bay: implications from a seismic refraction experiment, Geophys. J. Int., 190, 37-58.
- Talwani, M., and O. Eldholm (1977), Evolution of the Norwegian-Greenland Sea, GSA Bull., 88, 969-999.
- Tapponnier, P., X. Zhiqin, F. Roger, B. Meyer, N. Arnaud, G. Wittlinger, and Y. Jingsui
- 2545 (2001), Oblique Stepwise Rise and Growth of the Tibet Plateau, Science, 294, 1671-2546 1677.
- Taylor, B., K. Crook, and J. Sinton (1994), Extensional transform zones and oblique spreading centers, Journal of Geophysical Research: Solid Earth, 99, 19707-19718.
- Theissen-Krah, S., D. Zastrozhnov, M. M. Abdelmalak, D. W. Schmid, J. I. Faleide, and L.
- Gernigon (2017), Tectonic evolution and extension at the Møre Margin Offshore mid-Norway, Tectonophysics, 721, 227-238.
- Thorbergsson, G., I. T. Magnusson, and G. Palmason (1990), Gravity data and gravity map of IcelandOS-90001/JHD-01, National Energy Authority Reykjavik.
- 2554 Thybo, H., and I. M. Artemieva (2013), Moho and magmatic underplating in continental lithosphere, Tectonophysics, 609, 605-619.
- 2556 Trela, J., E. Gazel, A. V. Sobolev, L. Moore, M. Bizimis, B. Jicha, and V. G. Batanova
- 2557 (2017), The hottest lavas of the Phanerozoic and the survival of deep Archaean reservoirs, Nature Geoscience, 10, 451.
- Tryggvason, E. (1962), Crustal structure of the Iceland region from dispersion of surface waves, Bull. seismol. Soc. Am., 52, 359-388.

- Tuttle, O. F., and N. L. Bowen (1958), Origin of granite in the light of experimental studies in the system NaAlSi3O8–KAlSi3O8–SiO2–H2O, *in* Origin of Granite in the Light of Experimental Studies in the System NaAlSi3O8–KAlSi3O8–SiO2–H2O, edited by O. F. Tuttle and N. L. Bowen, Geological Society of America.
- Ulmer, P., and V. Trommsdorff (1995), Serpentine Stability to Mantle Depths and Subduction-Related Magmatism, Science, 268, 858.

25772578

2579

2580

2581

2582

2583

2584

2585

- van Gool, J. A. M., J. N. Connelly, M. Marker, and F. C. Mengel (2002), The
 Nagssugtoqidian Orogen of West Greenland: tectonic evolution and regional correlations
 from a West Greenland perspective, Canadian Journal of Earth Sciences, 39, 665-686.
- Vauchez, A., G. Barruol, and A. Tommasi (1997), Why do continents break-up parallel to ancient orogenic belts?, Terra Nova, 9, 62-66.
- Vogt, P. R. (1971), Asthenosphere motion recorded by the ocean floor south of Iceland, Earth planet. Sci. Lett., 13, 153-160.
- Vogt, P. R., G. L. Johnson, and L. Kristjansson (1980), Morphology and magnetic anomalies north of Iceland, Journal of Geophysics-Zeitschrift Fur Geophysik, 47, 67-80.
 - Voppel, D., S. R. Srivastava, and U. Fleischer (1979), Detailed magnetic measurements south of the Iceland-Faroe Ridge, Deutsche Hydrographische Zeitschrift, 32, 154-172.
 - Walker, R. J., R. E. Holdsworth, J. Imber, and D. Ellis (2011), Onshore evidence for progressive changes in rifting directions during continental break-up in the NE Atlantic, Journal of the Geological Society, 168, 27.
 - Wegener, A. (1915), Die Entstehung der Kontinente und Ozeane, Friedrich Vieweg und Sohn, Braunschweig.
 - Welford, J. K., A. L. Peace, M. Geng, S. A. Dehler, and K. Dickie (2018), Crustal structure of Baffin Bay from constrained 3-D gravity inversion and deformable plate tectonic models, Geophys. J. Int., 214, 1281–1300.
- Wilkinson, C. M., M. Ganerød, B. W. H. Hendriks, and E. A. Eide (2017), Compilation and appraisal of geochronological data from the North Atlantic Igneous Province (NAIP), Geological Society, London, Special Publications, 447, 69.
- Zastrozhnov, D., L. Gernigon, I. Gogin, M. M. Abdelmalak, S. Planke, J. I. Faleide, S. Eide, and R. Myklebust (2018), Cretaceous-Paleocene evolution and crustal structure of the northern Vøring Margin (offshore Mid-Norway): results from integrated geological and geophysical study, Tectonics, 37.
- Zhang, J., and H. W. Green (2007), Experimental Investigation of Eclogite Rheology and Its Fabrics at High Temperature and Pressure, Journal of Metamorphic Geology, 25, 97-115.
- Zhou, H., and H. J. B. Dick (2013), Thin crust as evidence for depleted mantle supporting the Marion Rise, Nature, 494, 195–200.